Copy No. 8

DEFENCE R&D DÉFENSE

DROP TOWER UPGRADE PROJECT

Volume 1: Instrumentation & Data Acquisition System

D. A. Hull

ENGINEERING MATERIAL RESEARCH

DEFENCE RESEARCH ESTABLISHMENT ATLANTIC

Contractor Report

DREA CR 1999-034

April 1999

Défense nationale National Defence

Canada

National Defence
Research and Development Branch

Défense nationale
Bureau de recherche et développement

DREA CR 1999-034

DROP TOWER UPGRADE PROJECT

Volume 1

Instrumentation and Data Acquisition System

D.A. HULL

ENGINEERING MATERIAL RESEARCH
35 Carl Hall Drive
Downsview ON M3K2B6

Scientific Authority
J. Morrison

W7708-4-1386
Contract Number

April1999

CONTRACTOR REPORT

Prepared for

Defence Research Establishment Atlantic

Centre de Recherches pour la Défense Atlantique

Canada

102-02760/

DREA CR 1999 034 - Dockyard Laboratory Drop Tower Upgrade

D.A. Hull

Engineering Material Research, Downsview, Ontario

Abstract

This report describes contract work to upgrade the capabilities of the drop tower at the DREA Dockyard Laboratory (Pacific). There was a need for improved fracture data acquisition and analysis software. In addition elastic-plastic fracture measurements at impact velocities and low temperatures required improved transducer performance.

The contract requirements included a review of high rate testing standards and developments in instrumentation and data acquisition, the development of customized software for routine data acquisition and display, and drop tower modifications to meet specified performance criteria. One of the main requirements was to identify and apply promising methods of measuring crack mouth opening and load line displacement, to increase manageable drop tower velocities for such tests from 2 $m.s^{-1}$ to 5 $m.s^{-1}$, and to improve the low temperature capability.

Résumé

Le présent rapport décrit un travail à forfait visant à accroître les capacités de la tour d'essai au choc du laboratoire de chantier naval (Pacifique) du CRDA. Il existait un besoin d'amélioration en matière d'acquisition de données de rupture et de logiciel d'analyse. De plus, les mesures de rupture élastique-plastique aux vitesses d'impact et aux basses températures nécessitaient une amélioration de la performance des transducteurs.

Les exigences du contrat comprenaient un examen des normes d'essai à haute vitesse et des perfectionnements des instruments et des techniques d'acquisition de données, le développement de logiciel personnalisé pour l'acquisition et l'affichage courants de données ainsi que des modifications de la tour d'essai au choc, afin de satisfaire aux critères de performance spécifiés. Une des principales exigences consistait à déterminer et à appliquer des méthodes prometteuses de mesure du déplacement de l'ouverture de fissure et de la ligne de charge, à faire passer de 2 $m.s^{-1}$ à 5 $m.s^{-1}$ les vitesses maniables en tour d'essai au choc pour ce type d'essais et à améliorer la capacité à basse température.

DREA CR 1999 034 - Dockyard Laboratory Drop Tower Upgrade

Volume 1 - Instrumentation and Data Acquisition

D.A. Hull

Engineering Material Research, Downsview, Ontario

Executive Summary

There is a requirement for improved fracture control procedures for ships' hulls in order to reduce structural maintenance costs. This implies the use of more rigorous damage assessment procedures, including the ability to determine tolerable crack sizes and specify inspection intervals in critical locations under service conditions. A sufficiently high material resistance to crack initiation and propagation is needed to ensure that cracks can be detected and repaired without compromising the operation of the ship or risking catastrophic failure. Unfortunately the data currently generated from specified quality control tests during material selection and ship construction provide only a qualitative indicator of toughness, and are inadequate to describe the fracture behaviour of large components. Quantitative assessment of resistance to crack initiation requires laboratory testing at the minimum service temperature and at loading rates equivalent to hull impact events such as wave slamming and minor collisions. Test temperatures typically may need to be in the -30°C range, and the corresponding loading rates are intermediate between those used in quasi-static laboratory tests with servo-hydraulic machines, and the high rates obtained during an explosion test. The standardized test procedures used to quantify toughness typically only cover ambient conditions and quasi-static loading rates. To complicate matters, a demonstration of adequate toughness usually also entails measurement of fracture resistance under elastic-plastic as well as linear-elastic loading conditions at the crack tip. In general these require an accurate measurement of force and displacement while a pre-cracked test specimen is being rapidly fractured, and result in some difficult instrumentation and data acquisition challenges.

The DREA Dockyard Laboratory (Pacific) drop tower allows samples to be subjected to displacement rates of several metres per second. However, deficiencies in instrumentation have limited the laboratory's ability to carry out dynamic elastic-plastic fracture measurements. There was also a need to incorporate state-of-the-art-data acquisition and analysis software. This first volume of the resulting contract report describes work to address these requirements. Volume 2, published simultaneously, provides a manual for operation of the upgraded apparatus.

TABLE OF CONTENTS

	Page
1. Introduction	1
2. Review	2
2.1 Standard Test Methods	2
2.2 Commercial Drop Towers	3
2.3 Force Instrumentation	3
2.4 Crack Mouth Opening Displacement	4
2.5 Load Line Displacement	5
2.6 Determination of Crack Extension	5
3. Software Development	6
3.1 Program Initialization and Setup	6
3.2 Temperature Monitoring	6
3.3 Oscilloscope Settings	7
3.4 Data Presentation	7
4. Drop Tower Modifications	7
4.1 Load	7
4.2 Crack Mouth Opening Displacement	8
4.3 Load Line Displacement	8
4.4 Crosshead Velocity	8
4.5 Impact Velocities	9
4.6 Low Temperature Capability	9
5. Validation Test Results	
6. References	10
Figures 1-17	
Annex A - Extended Blibliography on high rate fracture testing	

1. INTRODUCTION

There is an ongoing requirement to characterize fracture behaviour under conditions similar to those which may be encountered during ship impact events, typically within the temperature range +30°C to -30°C. The corresponding loading rates are intermediate between those used in quasi-static laboratory test with servo-hydraulic machines, and the high rates obtained during an explosion test.

During the late 1970's the DREA Dockyard Laboratory Pacific (DL(P)) DL(P) purchased a Dynatup 8100E drop tower with standard instrumentation to conduct dynamic fracture evaluation of marine and welds. This allowed a sample to be subjected to displacement rates of several metres per second. The original equipment had very basic instrumentation and data was obtained from a simple oscilloscope trace. Some modifications were undertaken in the late 1980's to increase the capability for fracture mechanics based toughness estimates. A digital storage oscilloscope, computer, and dynamic load conditioning instrumentation were added. At this time detailed investigations of drop tower compliance and inertial effects on test results were also carried out at impact velocities up to 2 $m.s^{-1}$ [1,2].

These studies revealed drop tower deficiencies that limited dynamic elastic-plastic fracture measurements at the higher impact velocities and lower temperatures within the regime which includes ship hull slamming incidents and minor collisions. There was also an increasing need for fracture data acquisition and analysis software to be adapted to the existing equipment. By the mid-90's it was recognized that a further upgrading would be required if state of the art capability was to be maintained. and contract work was initiated to address the above needs.

The contract requirements included:

a) a review of high rate testing standards and technical literature dealing with developments in instrumentation and data acquisition,

b) to develop customized software for routine data acquisition and the display of dynamic fracture data.

c) drop tower modifications to meet specified performance criteria. The main requirements were to identify and apply promising methods of measuring crack mouth opening and load line displacement, to increase manageable drop tower velocities for such tests from 2 $m.s^{-1}$ to 5 $m.s^{-1}$, and to improve the low temperature capability.

This report describes work undertaken by Engineering Material Research under research and development contract W7708-4-1386/01-XSA. Volume 1 describes the features of both the hardware and software used on the drop tower, while the operating instructions for the upgraded tower are included in Volume 2 ("Operator Manual for the DL(P) Drop Tower and Application Software").

2. REVIEW

Dynamic fracture tests require the coincident measurement of force, length, and time to characterize material behaviour [3]. Accurate measurement of abrupt changes in force and length on time scales of a millisec or less poses formidable challenges. The length (displacement) parameters required for fracture toughness and J-Integral tests are crack mouth opening displacement, (CMOD), load line displacement (LLD) and crack extension. Technical standards, descriptions of the capabilities of existing drop towers, and reports of published research represent the consolidated knowledge gained in developing procedures and equipment for obtaining accurate and repeatable test results. Knowledge of test method and equipment limitations also determines directions for future research.

2.1 Standard Test Methods

In 1974 an ASTM task group was established to develop a rapid loading plane-strain fracture toughness test specification for inclusion in ASTM E399 "Standard Test For Plane-Strain Fracture Toughness Testing of Metallic Materials" [4]. Test results from two collaborative test programs were used to prepare Annex A7 "Special Requirements for Rapid-Load Plane-Strain Fracture Toughness $K_{Ic}(t)$ Testing". The A7 Annex is intended for test results that are obtained using conventional servo-hydraulic load frames. It covers a defined range of displacement velocity (fracture times greater than 1 ms) above the quasi-static ceiling. It also does not attempt to deal rigorously with the more severe impact events which occur in a drop tower. For a valid test result, and an unambiguous determination of the fracture load, P_Q, the load versus crack mouth opening record must lie within a defined linear envelope above $0.5P_Q$. These restrictions limit inaccuracies in the P_Q determination that are introduced by inertial effects and transducer response times.

A rapid load J-Integral fracture toughness annex has been proposed for the ASTM Standard Test Method for Measurement of Fracture Toughness, (ASTM E1820). Test results obtained from rapid loading servo-hydraulic machines or drop towers will be included. Load is obtained from strain gauges mounted on each specimen. Crack length is determined using load line displacement or the potential drop method. Alternately, a normalization procedure can be used to derive crack extension from the load-displacement record. Specimen effective mass and load line stiffness are used to determine a minimum fracture time that must be greater than 1 ms. Currently collaborative tests are being conducted in several participating laboratories on a draft version of this annex.

In 1972 the United Kingdom Working Party on Dynamic Fracture (UKWP) was established and developed the British Standard Method for the Determination of the Dynamic Fracture Toughness of Metallic Materials (BS 6729:1987)[5]. This standard is intended for the determination of crack tip opening displacement (CTOD) and K_{Ic} on conventional load frames using maximum cross head speeds of 100 $mm.s^{-1}$ sec and stress intensity rates of 10 000 $MPa\sqrt{m}.s^{-1}$. Tests are conducted under displacement control and the unfiltered dynamic response of the load cell, clip gauge, etc., is specified. BS 6729 has many elements in common with Annex 7 of ASTM E399. The UKWP is now part of the European Structural Integrity Society (ESIS). A Subcommittee on Dynamic Testing at Intermediate Strain (TC5)

recently revised BS 6729 for inclusion as Part 3 of the 4-part British Fracture Standard BS 7448. However Part 3 of the new standard is not yet available. Other ESIS dynamic fracture draft standards being reviewed include a high-rate tensile test method and an instrumented Charpy V notch test method. A Dynamic J_{Ic} and J-R Curve standard is in the early stages of development with round-robin tests recently completed.

2.2 Commercial Drop Towers

Four manufacturers of gravity driven drop towers were identified in the North American market. The manufacturers' literature was reviewed to assess the capability of these machines. One manufacturer [6] provides drop towers with maximum impact energies and velocities of 18 kJ and 7 $m.s^{-1}$ respectively. Drop towers available from the other manufacturers [7-9] had impact energies of 0.5 kJ and 6 $m.s^{-1}$. The latter drop towers are designed for the lower impact energies required in plastics, packaging and structural testing. Pneumatic assists are available to extend a drop tower's impact energy and velocity.

Impact load is measured using strain gauge or piezo-electric strikers and velocity is measured using a photo detector and flag arrangement. A computer using Windows or DOS based software and a high rate data acquisition card are used to display load, energy, velocity, and time or deflection. All manufacturers indicated that custom drop towers can be developed to meet specific requirements. Transducers to measure CMOD and LLD accurately over ms times are not off-the-shelf components. A survey was also made to find techniques developed by independent researchers to measure force, CMOD, LLD and crack extension.

2.3 Force Instrumentation

There was early recognition that the specimen crack tip experiences different forces than measured by the drop tower load cell [10-12]. These differences are attributed to specimen bounce on the support anvils, loss of contact between the striker and specimen, and elastic waves within the specimen. Mechanical damping of the specimen to attentuate the inertial force component has been investigated. A triangular pad of compliant material, e.g., aluminum, lead, or plastic, eliminates separation between the striker and specimen by allowing the impact force to increase gradually [2,13,14]. Attachment of a compliant material to the back face of three-point bend bars reduces bending away from the anvils that occurs during striker separation from the specimen. Pre-loading the specimen against the striker to enable both to move as an assembly prevents separation but specimen alignment to insure uniform loading at the anvils becomes more important.

Strain gauges mounted directly to the specimen circumvent striker load cell limitations and treat the specimen itself as the force transducer [15-16]. Force is obtained at one or two strain gauge locations on the single edge notch bend (SE(B)) specimens that have been optimized using a 2-D elastodynamic finite element method [5]. The W/2 position on SE(B) side face level with the crack tip gives the best results but W/4 location should be considered if plasticity is not expected. Strain gauges can be arranged on the front and rear faces of SE(B) specimens at the quarter span position, S/4, to form a Wheatstone bridge [14].The full bridge accounts for shifting of the neutral axis during fracture. Constantin/polymide gauges

with large copper tabs and epoxy glue are recommended for ease of attachment. The thin glue line obtained with hot-cured epoxy yields more consistent results in comparison to cyano adhesive [5]. After strain gauge installation, individual specimens are calibrated statically up to a finishing pre-cracking force that should be less than 70% of the final K_{Ic}. The effects of variations in strain gauge position, specimen geometry, crack length, etc. are included in the calibration using this procedure. The impact force at fracture is then substituted into the appropriate stress intensity equation.

Strain gauges have also been used to determine the stress profile across a specimen during fracture. Four or more strain gauges are distributed parallel to the crack path at the quarter span position. Integration of the fracture strains across the specimen width gives the stress profile [17]. One disadvantage is that each strain gauge requires a dedicated channel of high speed data acquisition.

The Westergaard stress equations have been used to develop an expression for K that makes direct use of strain measurements [18,19]. Six gauges were installed equally spaced along a line offset from the crack path to limit strain non-linearities introduced by yielding and stress state at the crack tip. Gauges were installed at an angle to the crack path to simplify the number of terms that must be considered in the K expression.

2.4 Crack Mouth Opening Displacement (CMOD)

The double cantilever beam clip gauges used to measure CMOD suffer from frequency response limitations. An open ring 10 mm diameter clip gauge formed in an Omega shape, exhibits increased stiffness that makes it suitable for minimum failure times of 0.2 ms [13,20]. Strain gauges are installed on the inside and outside diameter to form a Wheatstone bridge. Calibration procedures are similar to those for conventional clip gauges. The ESIS committee employs a low inertia extensometer for high rate tensile testing at strain rates of 1 to 100 s^{-1} that may be suitable for CMOD measurement [21].

A pair of parallel plate capacitance gauges have been employed to measure CMOD at outer and inner crack notch locations in the SE(B) specimen [22]. The outer gauge is aligned with the specimen crack mouth edge and the inner is located 16 mm into a 24 mm deep notch. The other plate of the capacitor consists of a block that is attached to the opposite side of the crack notch. The change in capacitance is limited to a short working distance and consequently two measurement positions along the crack notch are required for a 5 mm CMOD measuring range.

An interferometric strain-displacement technique [23-28] was developed for crack tip opening displacement (CTOD) measurements. The relative displacement of two reflecting indentations on a specimen surface are measured by counting diffraction pattern fringes as they move past a fixed detector in space. A laser, two photomultiplier tubes, and high speed data acquisition system are required. This technique has been applied to static and dynamic measurements of fracture toughness crack tip opening displacement (CTOD), and errors of $\pm$3% were reported. It is expected that this technique will be most useful for dynamic loading tests at high temperatures where foil strain gauges cannot survive.

COD was measured using a Moiré technique [29] where two grids of 33 lines/mm are mounted on either side of the specimen. As the crack opens, the relative displacement of the grids is determined from the changing interference pattern that is detected using a photo diode. A crack opening displacement as small as 3.8 microns was determined using this method.

Another non-contact measuring method used a light source and photoelectric detector arranged on opposite sides of the crack notch in a double edge notch specimen [30]. A rectangular slit produces a light speckle 4.0 mm long and 0.5 mm wide on the specimen. The light flux impinging on the detector increases as the crack opens. The recording system limited the response time to 0.1 μs. Application of this technique to the SEB specimen would require compensation for load line displacement.

2.5 Load Line Displacement (LLD)

LLD has been measured using a strain gauged transducer called a flex bar [17, 31-33]. Strain gauges are arranged for form a Wheatstone bridge at the center span of a slender flat strip of spring steel. The flex bar signal is calibrated against center span deflection using a micrometer. The flex bar forms a catenary when it rests on support screws that are attached to specimen side. As fracture occurs the LLD signal changes as the flex bar's center span deflection diminishes.

A non-contact method of LLD measurement utilized a fiber optic light probe assembly to measure the intensity of light that is reflected from a polished surface of a piston. The fiber optic probe assembly consists of an optoelectronic amplifier, fiber optic cable bundle with transmit and receiving fibers, and a sensor tip. The use of a reflectance compensated sensor is necessary because this type of sensor is not dependent on the reflectivity of the piston surface [31]. The piston moves toward the detector within a cylindrical guide to prevent measurement errors that would occur if the piston rotated with the specimen arm during fracture. A linkage connecting the piston to the specimen is required.

A set of eddy current probes were used to measure LLD at 5 $m.s^{-1}$ [17]. Four probes were located beneath the specimen at equally spaced intervals from the load line position to measure the bend angle. Equations relating LLD to bend angle were derived by assuming rigid rotation of the specimen arms and correcting for elastic beam curvature.

An electro-optical extensometer was used to measure LLD at impact velocities of 2 $m.s^{-1}$ [34] and 10 $m.s^{-1}$ [35]. The distance between two target edges on a specimen surface is measured and a signal of good quality was obtained that satisfied E399 Annex 7 requirements.

2.6 Determination of Crack Extension

The time at which the crack begins to propagate during a test is of interest. Frequently a change in CMOD or LLD slope is used to identify when crack extension begins. The direct current potential drop method has been studied but a magneto-elastic spike is generated in ferrous materials that makes identification of the time of initial crack propagation problematic

[36]. The alternating current potential drop [36] and acoustic emission techniques [38] show promise but sophisticated analytical methods must be used to separate the effects of the loading and plastic deformation from crack nucleation and propagation. A magnetic coil placed near the fatigue pre-crack tip has been used to detect the onset of crack extension [39]. Crack displacement and velocity up to 600 $m.s^{-1}$ have been measured using a grid of insulated wires that were deposited onto the specimen side [40]. Crack extension severs the wires to produce step changes in voltage. Foil crack gauges are commercially available and have been successfully used to measure crack propagation at 10 $m.s^{-1}$ impact velocities [35]. Crack gauge installation time and labour are comparable to a single strain gauge.

In summary, this brief review has indicated that standard test methods for conducting dynamic fracture toughness and J-Integral tests are still being developed. Commercially available drop tower equipment provides the necessary speeds and impact forces to simulate ship hull slamming events. However accurate measurement of force, CMOD and LLD requires additional transducer development. Published research has revealed different measurement schemes that may be explored and adapted to the existing DL(P) drop tower facility.

3. SOFTWARE DEVELOPMENT

A Windows based Graphical User Interface (GUI) was developed to enable routine operator acquisition of dynamic loading data using the high sampling rates of the Nicolet oscilloscope. The software is a menu driven program that offers flexibility in data acquisition, plotting and analysis of results. Software features are illustrated in Figure 1. The Labwindows CVI software code was structured using a main and hardware driver program. Commands that were hardware independent, or for data analysis, plotting, exporting of data and library functions were collected in the main program. The hardware driver program included oscilloscope specific instructions that used a RS232 communication link.

3.1 Program Initialization and Setup

Default or custom configuration files for specifying oscilloscope settings, specimen geometry and material properties must be selected after the program is started. Oscilloscope settings may be changed rapidly to suit different test requirements or user preferences by reading the appropriate configuration file. Test data acquired from past sessions may be re-analyzed and plotted or exported for external program use. Default file selection causes the oscilloscope to be set to standard operating parameters and the user must define specimen and material properties in a Setup menu.

The setup menu allows each of the oscilloscope's four input channels to be tagged with 7 different physical names that include, "LOAD, COD, VEL , DISP, LLD, STRAIN, SIGNAL or SPARE". Linear calibration equations require slope and y intercepts to be specified to convert voltage to engineering units. SEB or Compact Tension (CT) specimen geometry and the relevant material properties can be specified.

3.2 Temperature Monitoring

A readout function allows monitoring of the specimen until the desired test temperature is reached. Up to six channels of K type thermocouples and a cold junction sensor temperature can be displayed.

3.3 Oscilloscope Settings

The oscilloscope settings are specified by the selections made in the configuration file. The voltage range setting for each channel can be adjusted over discrete intervals from 30 mV to 120 V. The scope time base and number of samples can be varied in discrete intervals from 100 ns - 10 s and 1000 to 30,000 samples respectively. Scope triggering is set by the user to any one of the 4 signal channels or by an external signal input on the scope's front panel. Errors in oscilloscope operation or RS232 communication errors are available for inspection. Text information is presented in a message box to indicate operation status e.g., Waiting for Trigger, Acquiring Data, Displaying Waveform, etc.

3.4 Data Presentation

Test data can be presented in the following formats:

a) Y versus T - engineering units as a function of time.
b) Y versus X - three signals as Y and one signal as X in engineering units.
c) K versus Displacement and K versus T - Stress intensity vs. Displacement and Time.
d) J versus R - J integral versus crack length, or
e) Max-Min Table - maximum and minimum values.

A maximum of four individual plots and one summary plot of the acquired data can be viewed. Each plot has three mouse controlled cursors that are used to give individual data points in engineering units and to select part of the plot for viewing on expanded scales.

Test data is saved in an ASCII format for importing into other programs. Each file may be tagged with a 255 character line description of the data. The file creation date, time, configuration file directory path, name, date, and time are listed for tracking purposes. Calibration factors for each channel, numbers of samples and the sample rate are listed before the channel data is presented sequentially in a comma separated format.

4. DROP TOWER MODIFICATIONS

The DL(P) Dynatup 8100E drop tower components are identified in Figure 2. The drop tower consists of a base plate, guide and support posts, 300 kg crosshead, instrumented tup, electric hoist, air release valves, rubber rebound springs, brake, anvils, safety cage and specimen fixtures. Operation of the drop tower is controlled manually from the drop tower control panel illustrated in Figure 3.

4.1 Load

The DT utilizes semi-conductor strain gauges to measure the dynamic compression forces applied at the tup over a temperature range of -54°C to +149°C. The tup calibration was checked statically in a servo-hydraulic load frame at room temperature.

4.2 Crack Mouth Opening Displacement

The literature review identified several different methods of measuring the crack opening displacement. Replacement of a conventional cantilever arm gauge with the Omega ring gauge was attractive because existing transducer conditioners and calibration methods could be used. A 25 mm outside diameter x 12.5 mm wide gauge was fabricated from titanium, and it is illustrated in Figure 4. Strain gauges were installed on the ring surfaces to form a Wheatstone bridge. Omega gauge calibration and mounting was identical to a conventional clip gauge. The Omega gauge free arm natural frequency was determined experimentally to be 1,250 Hz. The comparable cantilever beam clip gauge frequency of 850 Hz was determined using an ASTM E399 equation. Gauges that exhibit free arm natural frequencies greater than 750 Hz are acceptable for ASTM E399 test durations greater than 1 ms.

4.3 Load Line Displacement

A flex bar was constructed to measure SEB specimen LLD and is illustrated in Figure 5. The flex bar stiffness was increased by including upper and lower elements in a leaf spring arrangement. The bar is shown initially preloaded between screws located on the specimen side. As the specimen fractures, the LLD gauge relaxes and is released from the specimen. LLD calibration and signal amplification are similar to that of the Omega gauge.

4.4 Crosshead Velocity

The drop tower was supplied with a light source, detector and flag to generate a trigger signal to initiate data acquisition or measure velocity. The fixed source and detector are mounted on the side of the DT, and can be adjusted in the vertical direction. A trigger signal is generated when light is blocked from the detector by the metal flag that is attached to the falling crosshead. Replacing the metal flag with a 25 mm long strip of film that contains a set of evenly spaced dark lines allows crosshead velocity to be measured. Passage of the film between the source and detector generates a series of pulses that are acquired on an oscilloscope channel. Determination of the velocity at discrete points in time is possible because the distance between the lines and the period of the pulses is known. This non-contact measurement of velocity was intended to determine the crosshead velocity immediately prior to impact.

During specimen fracture the crosshead velocity changes rapidly. Measurement of the velocity continuously over a longer distance than afforded by a light flag/detector unit is necessary because it allows direct comparison of velocity with load, CMOD, LLD, etc. A Linear Variable Displacement Transducer (LVDT) was considered for this extended

measurement because displacement and velocity are available from the same signal. However, the transducer frequency response at DT impact velocities of 2 - 5 $m.s^{-1}$ was a concern. Instead a Linear Velocity Transducer, (LVT), was selected that was rated to measure velocity up to 25 m.s-1 over a 76 mm distance. The DT's maximum impact velocity of 6.8 $m.s^{-1}$ was well within the LVT's operating range. The LVT produces a continuous voltage proportional to the time rate of change of a magnetic core. The LVT coil body is fixed to the side of the DT and the core moves with the falling drop tower crosshead.

4.5 Impact Velocity

Crosshead displacement control during fracture is required for crack arrest or multi-specimen J integral tests where crack extension must be halted before specimen fracture. Rudimentary control is possible by modification of the drop tower's compression spring rebound and friction brake system. Aluminum compression blocks are bolted to the base plate on the outside of the front guide posts and they are faced with sheets of natural gum rubber. This composite compression spring absorbs the kinetic energy of the falling crosshead and causes it to rebound during drop events. Pneumatically actuated air brakes are applied during the crosshead's rebound from the rubber pads.

During previous DT studies at DL(A), the aluminum/rubber springs were replaced with steel stop blocks that virtually eliminated cross head rebound at impact velocities up to 2 $m.s^{-1}$. These blocks were located between the guide posts to reduce the crosshead bending stresses. Control over crack extension was demonstrated using this arrest method but installation and removal of the heavy steel blocks was a difficult process.

A review of EDRD future testing needs revealed the DT would be used for tests requiring both the aluminum/rubber and the steel stop block arrest systems at impact velocities up to 5 $m.s^{-1}$. The aluminum/rubber blocks and friction brake arrest system was designed for 5 $m.s^{-1}$ impact velocities and consequently equipment problems were not anticipated. However crosshead bending stresses developed during impact with the steel stop blocks was a concern at 2 - 5 m $m.s^{-1}$.

Bending stresses were determined by considering the crosshead as a simply supported beam. The effect of the slender guide posts was neglected. Compression spring deflection and reaction forces were determined by equating the crosshead kinetic energy to the spring energy. Analysis revealed that substitution of aluminum for steel would increase the compression spring deflection from 0.5 mm to 0.8 mm at 5 $m.s^{-1}$, but the crosshead maximum bending stress would be reduced from 122 MPa to 58.6 MPa. Consequently the ends of two Al 6061-T6 cylinders, 200 mm diameter by 325 mm long were machined flat. A 12.5 mm thick steel plate was attached to the top of each cylinder for wear resistance. Steel plates were attached to the bottom of the cylinder to allow attachment to the drop tower base plate or existing steel blocks. The aluminum cylinders were supplied with removable eye hooks at the front and back to allow the cross head crane to lift the cylinders and speed installation or removal.

4.6 Low Temperature Capability

Cooling of specimens to -50°C is frequently required to determine material properties. A cold box was constructed that allows in situ cooling of the specimen while it is mounted against the tup using the EDRD pre-load fixture. Alternately the specimen may be cooled externally to the DT in the cold box and then installed. Stainless steel hoses conduct liquid nitrogren from a dewar to the cold box. Copper pipes drilled with a series of small diameter holes are arranged in the cold box interior to direct a uniform liquid nitrogen mist onto the sides of the specimen. Teflon and styrofoam were used for cold box insulation.

Routine testing at low temperatures requires a fast specimen turnaround time. Test time is reduced if thermocouples and other instrumentation are mounted prior to specimen installation in the DT. A thermocouple junction box that is connected to a computer was added to the DT. The thermocouple junction box accepts up to six K type thermocouples to allow specimen temperature gradients to be measured.

5. VALIDATION TEST RESULTS.

Validation tests were conducted to demonstrate the upgraded DT performance. Two sizes of single edge notch bend (SE(B)) specimens, 25 mm x 50 mm x 250 mm, and 15 mm x 30 mm x 125 mm, were pre-cracked to a nominal crack lengths of a/W = 0.5 in a three point bend fixture using a 100 kN servo-hydraulic load frame. The ASTM Standard Practice for Verification and Classification of Extensometers was used to calibrate the strain gauge specimen, omega gauge and flex bar. Three sets of measurements were recorded for each range of interest. One of the larger specimens was strain gauged to compare DT tup and specimen load signals. The strain gauges were arranged on the specimen to form a wheatstone bridge that was statically calibrated up to the final pre-cracking load.

The strain gauged specimen was evaluated using an impact velocity of 2 m/sec at ambient temperature. The tup and specimen loads during fracture are shown in Figures 6 and 7. Comparison of the two figures shows the effect of inertial loads and transducer ringing is reduced when the load signal is obtained from specimen mounted strain gauges. This result is consistent with the findings of other researchers. The specimen undergoes an initial 4 kN compressive load during the first 0.1 msec of the test before the load increases to a maximum and then decreases with decaying load oscillation. The tup and specimen peak loads were 39 kN and 22 KN respectively. This difference in load is attributed to ringing in the tup.

CMOD measured by the omega gauge for a displacement range of 3 mm is presented in Figure 8. The signal quality obtained from the omega gauge is linear in nature. Vibration of the omega gauge at its natural frequency after release from the specimen is illustrated at the top of the figure. At first glance the LLD signal shown in Figure 9 exhibits significant departures from linearity over the full displcaement range of 0 to 19 mm. However, the specimens used in this study limited the working displacement range to 0-8 mm before the gauge was released from the mounting screws. Figure 10 illustrates the working displacement

range and the LLD now appears linear. It is believed that the gauge was released from the mounting screws at a displacement of 7.5 mm.

At an impact velocity of 2m/sec, CMOD and LLD versus time are shown in Figures 11 and 12 respectively for the same measuring range and time period. Both results are linear, but the LLD lags behind CMOD by 30 msec. Additional improvement in the LLD gauge signal could be achieved by using a stiffer flex bar with an improved mounting arrangement.

Test results obtained at 4 m/sec impact velocities are presented in Figures 13-17. The load-time history that was measured at the tup with the specimen mounted in the DL(P) fixture is shown in Figure 13. The change from zero to peak load during a 0.2 msec time period is illustrated in Figure 14. Figures 15 and 16 demonstrate that the CMOD and LLD signal quality has not changed appreciably at the higher impact velocity for similar displacement ranges and time periods. LLD for the working displacement range is shown in Figure 17. It is believed that the LLD gauge separated from the specimen after 6 mm of displacement.

6. REFERENCES

[1] KarisAllen, K.J., Morrison, J., "The Determination of Instrumented Impact Machine Compliance Using Unloading Displacement Analysis", Experimental Mechanics, June 1989, pp. 152-156.

[2] KarisAllen, K.J., Morrison, J., "Mechanical Reduction of Inertially Generated Effects in Single-Edge Notched Bend (SENB) Specimens Subjected to Impact Loading", Rapid Load Fracturing Testing, ASTM STP 1130, R. Chona and W.R. Corwin, Eds., American Society for Testing and Materials, Philadelphia, 1991, pp. 76-91.

[3] Kalthoff, J.F., "On the Measurement of Dynamic Fracture Toughnesses - A Review of Recent Work", International Journal of Fracture, Vol. 27, 1985, pp. 277-298.

[4] Shoemaker, A.K., Seeley, R.R., "Summary Report of Round Robin Testing by the ASTM Task Group E24.01.06 on Rapid Loading Plane-Strain Fracture Toughness K_{Ic} Testing", Journal of Testing and Evaluation, JTEVA, Vol. 11, No. 4, July 1983, pp. 261-272.

[5] MacGillivray, J.H., Cannon, D.F., "The Development of Standard Methods for Determining the Dynamic Fracture Toughness of Metallic Materials", Rapid Load Fracture Testing, ASTM STP1130, R. Chona and W.R. Corwin, Eds., American Society of Testing and Materials, Philadelphia, 1992, pp. 161-179.

[6] Dynatup, "Innovative Solutions In Impact Testing Equipment", Product Literature, Santa Barbara, California.

[7] ATM, "Specifications for Model ITP200C Impact Testing Machine", Product Literature, Toronto, Ontario.

[8] Ceast, "Fractovis - Instrumented Falling Weight Tester", Product Literature, Fort Mill, South Carolina.

[9] Lansmount, "Precision Drop Tester", Product Literature, Monterey California.

[10] Cotterell, B., "Fracture Toughness and the Charpy V-Notch Impact Test", British Welding Journal, Vol. 9, 1962, pp. 83-89.

[11] Saxton, H.J., Ireland, D.R., Server, W.L., "Analysis and Control of Inertial Effects During Instrumented Impact Testing", Instrumented Impact Testing, ASTM STP 563, American Society for Testing and Materials, 1974, pp. 50-73.

[12] Venzi, S., Priest, A.H., May, M.J., "Influence of Inertial Load in Instrumented Impact Tests", Impact Testing of Metals, ASTM STP 466, American Society for Testing and Materials, Philadelphia, 1970, pp. 165-180.

[13] Thaulow, C., Gunleiksrud, A., Troset, J., "Dynamic Fracture Toughness Measurements Of Structural Steel", Fracture Toughness: Methods, Intrepretations and Application, The Welding Institute, Cambridge, June 1982, pp. 9 -20.

[14] Hackett, E.M., Joyce, J.A., Shih, C.F., "Measurement of Dynamic Fracture Toughness of Ductile Materials", Non-Linear Fracture Mechanics: Volume 1 - Time Dependent Fracture, ASTM STP 995, A. Saxena et al., Eds., American Society for Testing and Materials, Philadelphia, 1989, pp. 274-297.

[15] Dear, J.P., MacGillivray, J.H., "Strain Gauging for Accurate Determination of K and G in Impact Tests", Journal of Materials Science, Vol. 26, 1991, pp. 2124-2132.

[16] Kishi, T., "Dynamic Fracture Toughness in Ceramics and Ceramics Matrix Composites", Engineering Fracture Mechanics, Vol. 40, No. 4/5, 1991, pp. 785-790.

[17] Kirk, M.T., Waskey, J.P., Dodds, Jr., R.H., "A Procedure for Drop-Tower Testing of Shallow-Cracked Single-Edge Notched Bend Specimens", Rapid Load Fracture Testing, ASTM STP 1130, R. Chona and W. R. Corwin, Eds., American Society for Testing and Materials, Philadelphia, 1992, pp. 50-75.

[18] Dally, J.W., Sanford, R.J., "Measuring The Stress Intensity Factor For Propagating Cracks With Strain Gages", Journal of Testing and Evaluation, JTEVA, Vol 18, No.4., July 1990, pp. 240-249.

[19] Dally, J.W., Sanford, R.J., "Strain-Gage Methods For Measuring the Opening-Mode Stress-Intensity Factor, K_I", Experimental Mechanics, Dec. 1987, pp. 381-388.

[20] Pussegoda, L.N., Malik, L., "Final Report: Dynamic Toughness Of Ship Plate", Fleet Technology Ltd, Kanata, 1995, pp. 1- 40.

[21] Al-Mousawi, M.M., Deans, W.F., Strain, Vol 23, No. 2, 1987, pp. 71-74.

[22] Joyce, J.A., Hackett, E.M., "An Advanced Procedure for J-R Curve Testing Using a Drop Tower", Non-Linear Fracture Mechanics: Volume 1 - Time-Dependent Fracture, ASTM STP 995, A. Saxena et al., Eds., American Society for Testing and Materials, Philadelphia, 1989, pp. 298-317.

[23] Macha, D.E., Sharpe, Jr.,W.N., Grandt, Jr., A.F., "A Laser Interferometry Method for Experimental Stress Intensity Factor Calibration", Cracks and Fracture, ASTM STP 601, American Society for Testing and Materials, 1976, pp. 490-505.

[24] Sharpe, Jr., W.N., Waclawiw, Z., Douglas, A.S., "Dynamic Measurement of Crack-Tip Opening Displacement", Fracture Mechanics: Ninteenth Symposium, ASTM STP 969, T.A., Cruse, Ed., American Society for Testing and Materials, Philadelphia, 1988, pp. 406-481.

[25] Sharpe, Jr., W.N., Shapiro, J.M., "Dynamic K Measurements in Three-Point-bend Specimens", Journal of Testing and Evaluation, JTEVA, Vol. 18, No. 1, 1990, pp. 38-44.

[26] Tregoning, R.L., Shapiro, J.M., Sharpe, Jr., W.N., "Dynamic Crack-Tip Opening Displacement (CTOD) Measurements with Application to Fracture Toughness Testing", Rapid Load Fracture Testing, ASTM STP 1130, R. Chona and W. R. Corwin, Eds., American Society for Testing and Materials, Philadelphia, 1992, pp. 118-133.

[27] Premack, T., Douglas, A.S., "An Analysis of the Crack Tip Fields in a Ductile Three-Point Bend Specimen Subjected to Impact Loading", Engineering Fracture Mechanics, Vol. 45, No. 6, 1993, pp. 717-728.

[28] Sharpe, Jr., W.N., Bohme, W., "Dynamic Fracture Toughness Measurements on Small Charpy Specimens - A Preliminary Study", Journal of Testing and Evaluation, JTEVA, Vol. 22, No. 1, 1994, pp. 14-19.

[29] Couque, H., Asaro, R.J., Duffy, J., Lee, S.H., "Correlations of Microstructure with Dynamic and Quasi-Static Fracture in a Plain Carbon Steel," Metallurgical Transactions A, Vol. 19A, 1988, pp. 2179-2206.

[30] Yuanming, X., Shiguo, R., Baochang, Y., "A Novel Method For Measuring Plane Stress Dynamic Fracture Toughness", Engineering Fracture Mechanics, Vol. 48, No.1, 1994, pp. 17-24.

[31] Joyce, J.A., Hackett, E.M., "Dynamic J-R Curve Testing of a High Strength Steel Using the Key Curve and Multispecimen Techniques", Fracture Mechanics: Seventeenth Volume, ASTM STP 905, J.H. Underwood et al., Eds., American Society for Testing and Materials, Philadelphia, 1986, pp. 741-774.

[32] Kirk, M.T., Hackett, E.M., "An Evaluation of J-R Curve Testing Using Three-Point Bend Specimens", Fracture Mechanics: Eighteen Symposium, ASTM STP 945, D.T. Read and R.P. Read, Eds., American Society for Testing and Materials, Philadelphia, 1988, pp. 347-373.

[33] KarisAllen, K.J., Matthews, J.R., "The Determination of Single Edge-Notched Bend Specimen Load Line Displacement from Remotely Located Sensors in Elastic-Plastic Fracture Testing", Journal of Testing and Evaluation, JTEVA, Vol. 22, No. 6, November 1994, pp. 581-583.

[34] Fujii, E., Sakai, Y., Ando, Y., "An Evaluation of Dynamic Fracture Toughness of Type A508 Class 3 Steel", Journal of Testing and Evaluation, JTEVA, Vol. 14, No. 4, 1986, pp. 181-190.

[35] Jones, R.L., Davies, P.C., "Experimental Characterisation of Dynamic Tensile and Fracture Toughness Properties", Fatigue Fracture of Engineering Material and Structures, Vol. 12, No. 5, 1989, pp. 423-437.

[36] Hackett, E.M., Kirk, M.T., Hays, R. A., "An Evaluation of J-R Curve Testing of Nuclear Piping Materials Using the Direct Current Potential Drop Technique", NUREG/CR-4540, U.S. Nuclear Regulatory Commission, Washington, DC, Aug. 1986.

[37] Joyce, J.A., "Application of Alternating Current Potential Difference to Drop Towr J-R Curve Measurement", NUREG/CR-4699, U.S. Nuclear Regulatory Commission, Washington, DC, Aug. 1986.

[38] Viehrig, H.-W., Popp, K., "Measurement of Dynamic Elastic-Plastic Fracture Toughness Parameters Using Various Methods", International Journal of Pressure Vessel and Piping, Vol. 55, 1993, pp. 233-241.

[39] ESIS, "Proposed Standard Methods for Instrumented Pre-cracked Charpy Impact Testing of Steels - Combined K_{Id}, J_{Id}, and CTOD Test Methods", Draft 8: October 1997.

[40] Kallivayalil, J.A., Zehnder, A. T., "Measurement Of The Temperature Field Induced By Dynamic Crack Growth in Beta-C Titanium", International Journal Of Fracture, Vol 66, 1994, pp. 99-120, 1974, pp. 3-29.

[41] Barnes, C.R., "A Measurement Technique for Determining Dynamic Crack Speeds in Engineering Materials Experimentation", Experimental Techniques, March 1985, pp. 33-37.

[42] Chang, C., "A Digital Dynamic-Crack Speed Measuring Device", Experimental Techniques, Vol. 17, 1989, pp. 16-17.

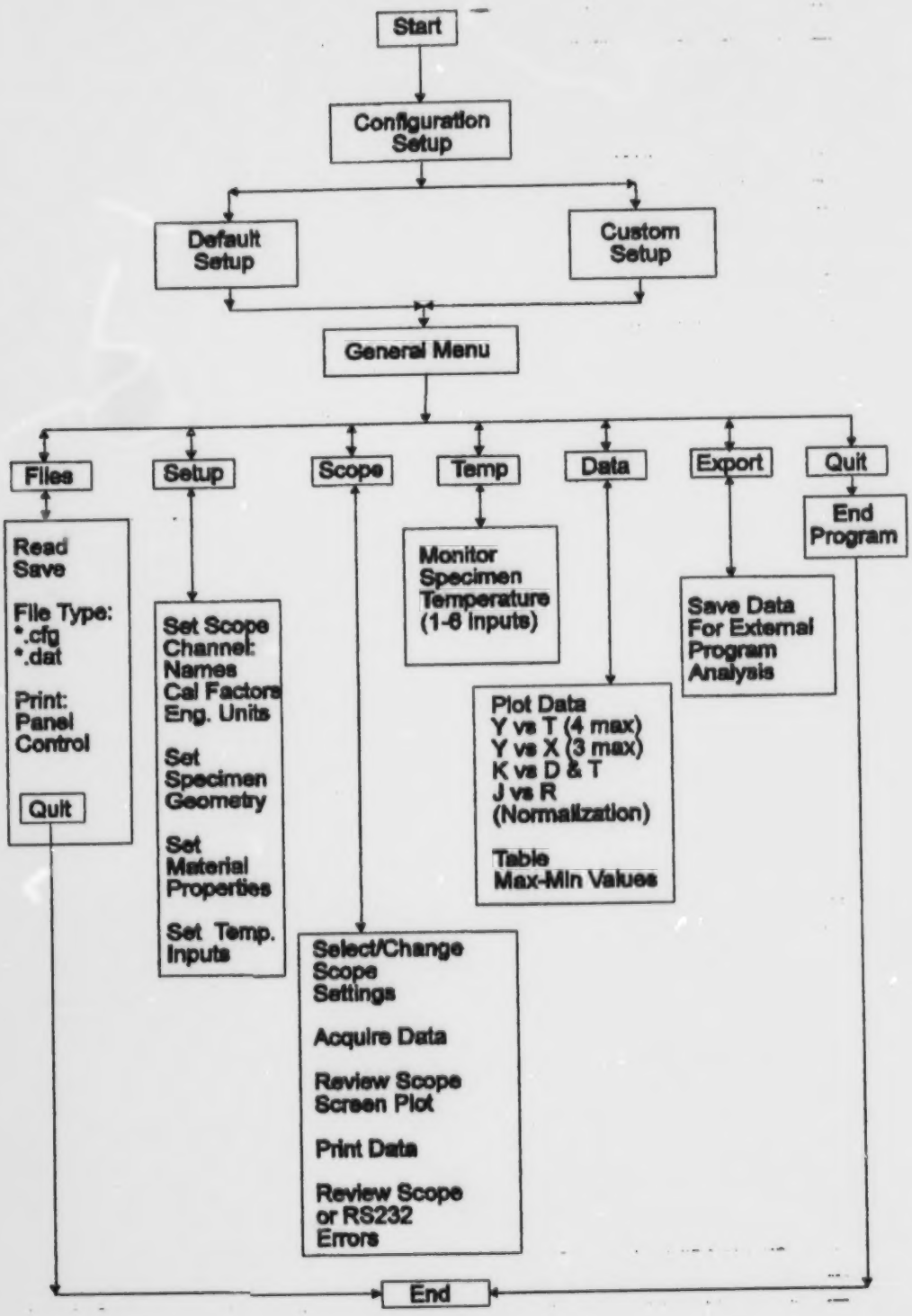

Figure 1.
Software Organization Flowchart.

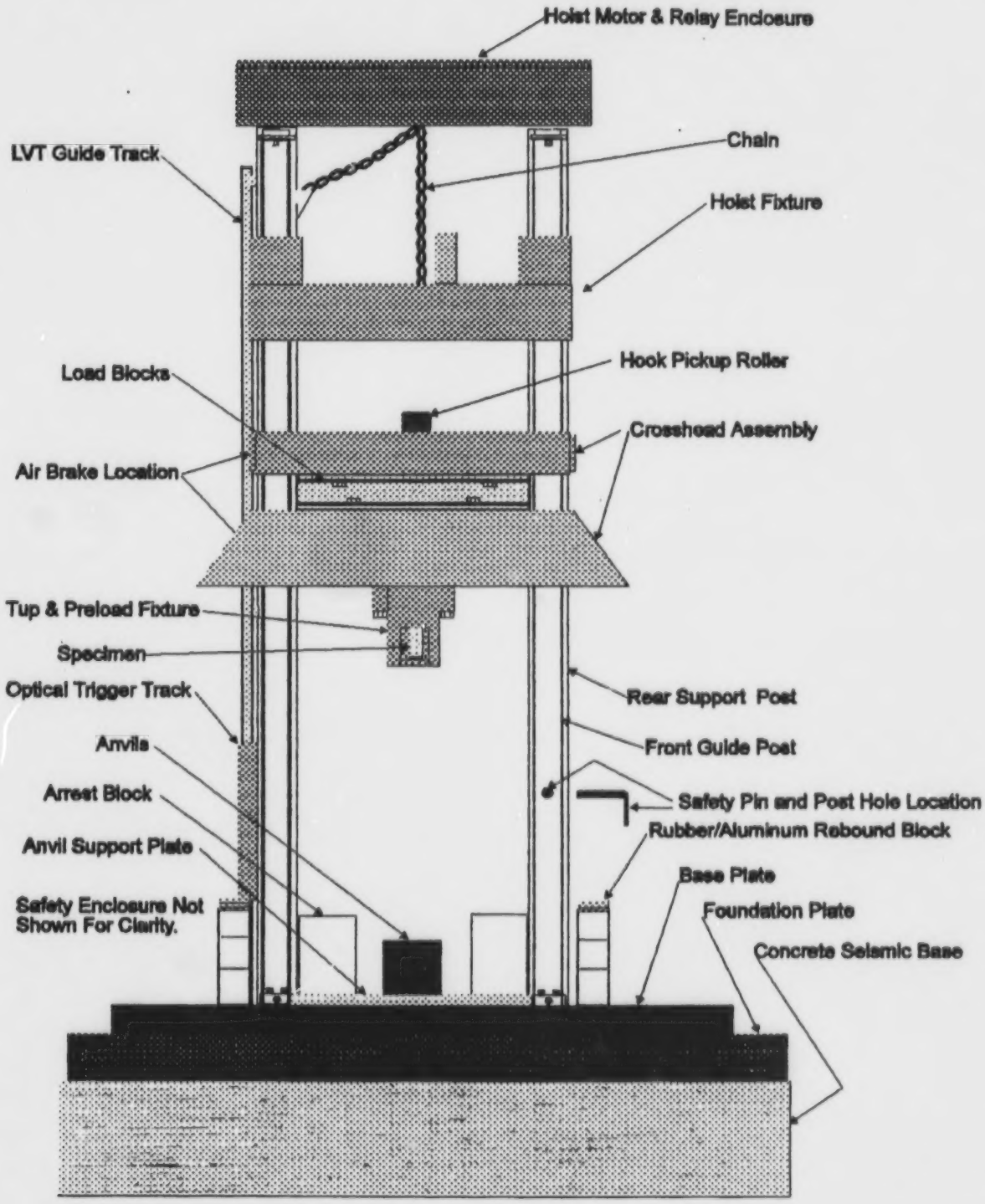

Figure 2.
Drop Tower Component Location.

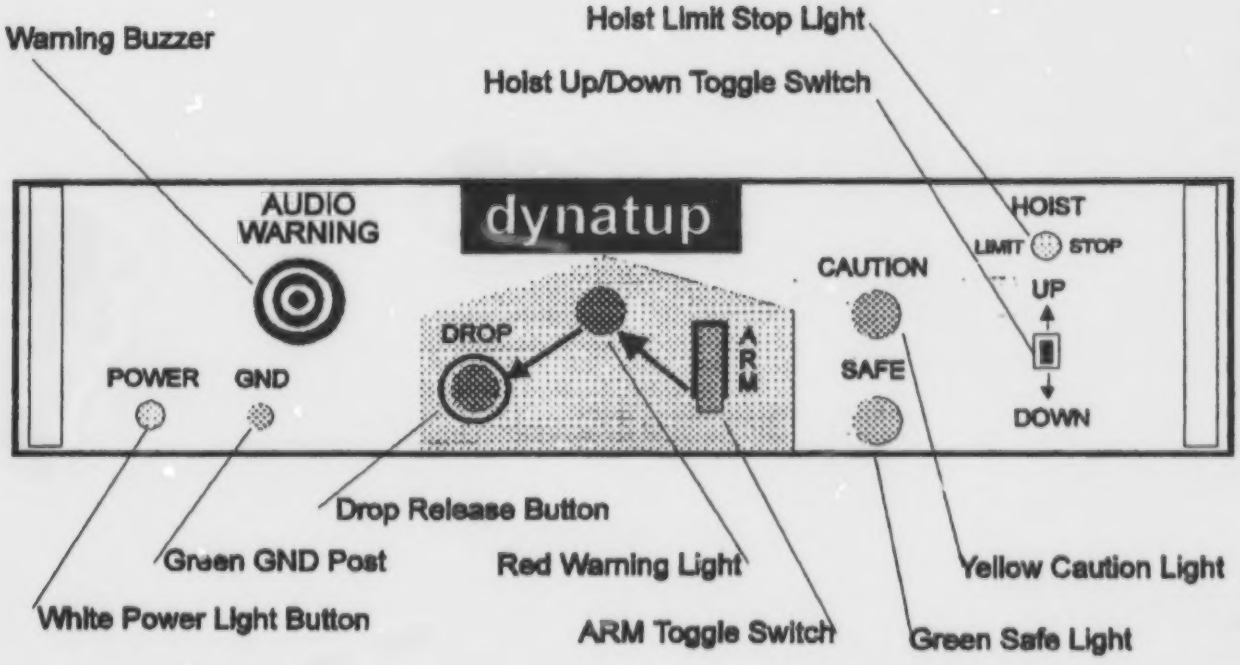

Figure 3.
Drop Tower Control Panel.

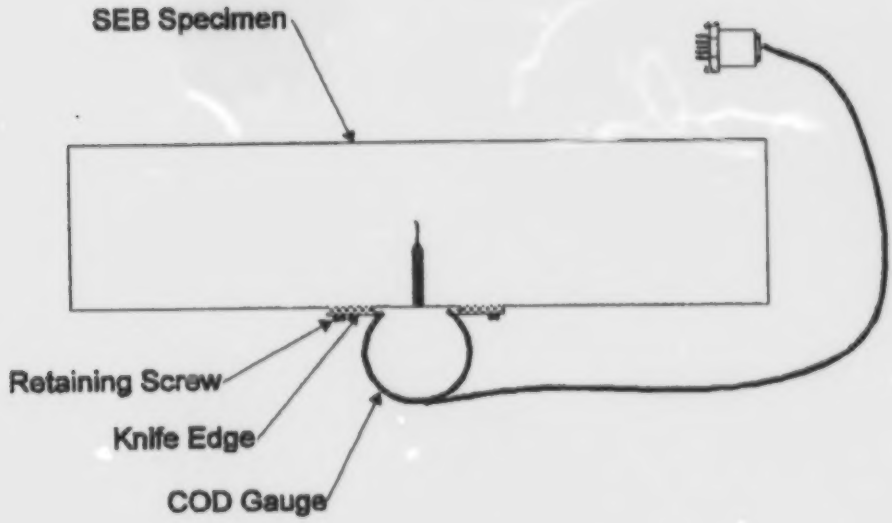

Figure 4.
Omega Shaped COD Gauge.

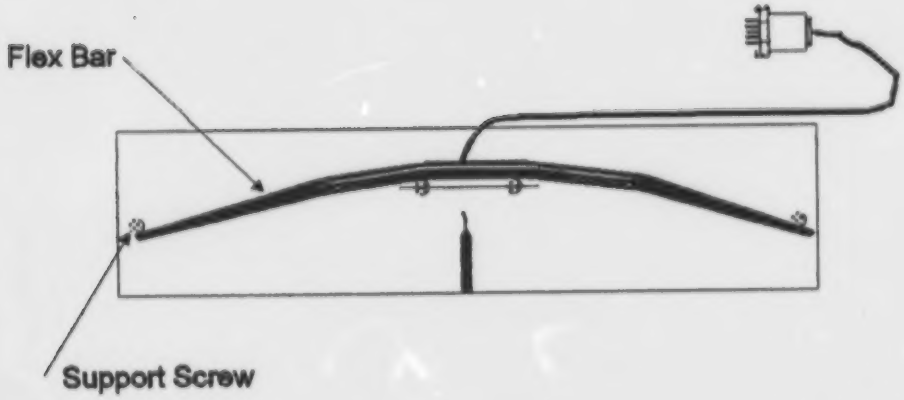

Figure 5.
Flex Bar LLD Gauge.

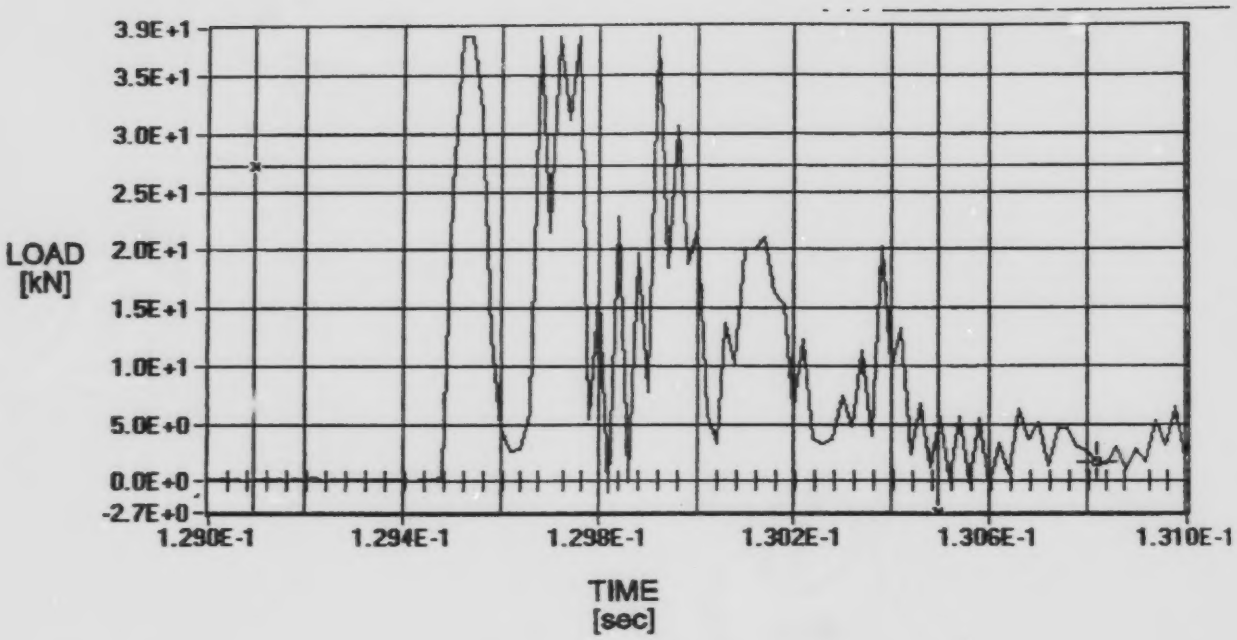

Figure 6.
Tup Load Versus Time.

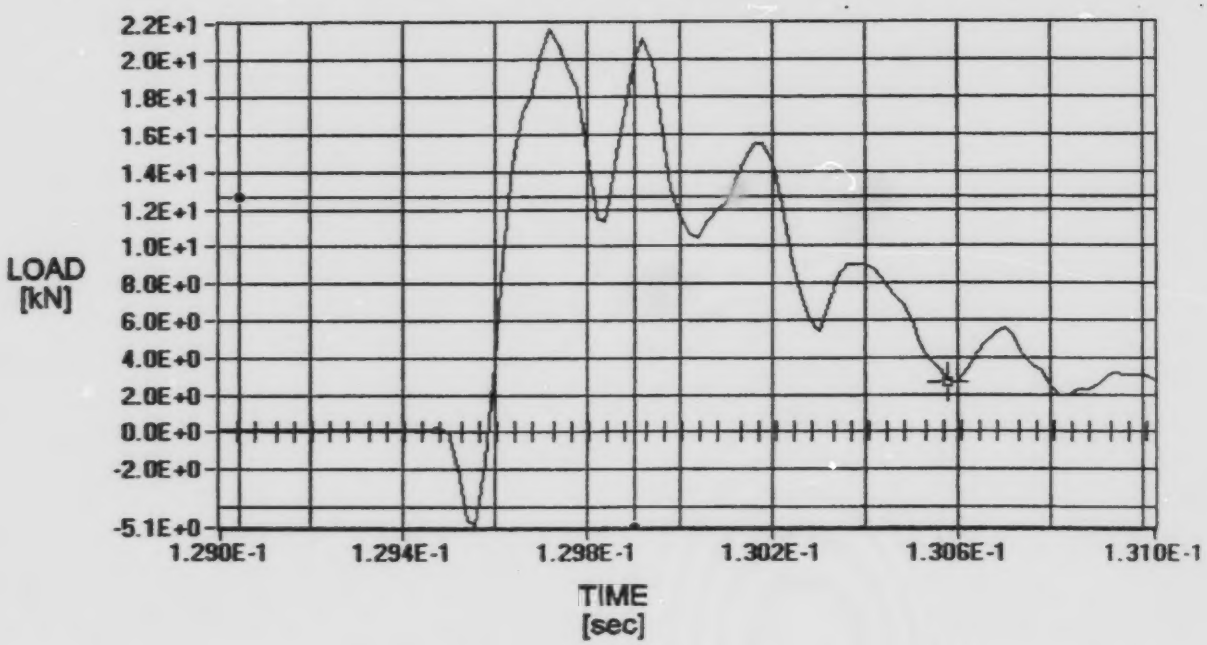

Figure 7.
Specimen Strain Gauge Load Versus Time.

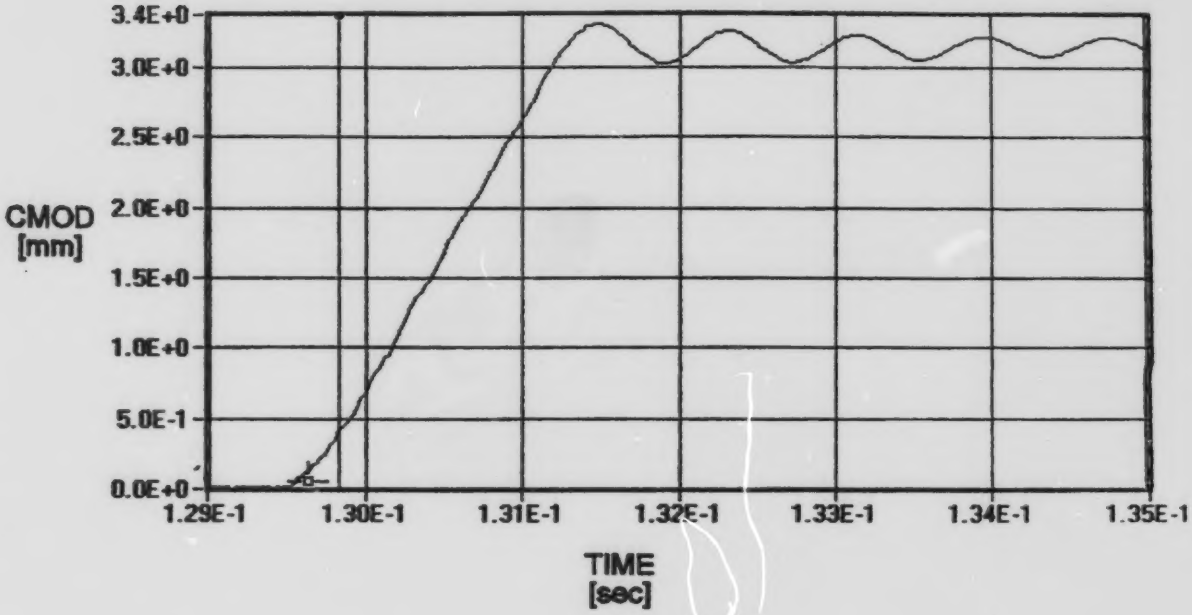

Figure 8.
CMOD Versus Time.

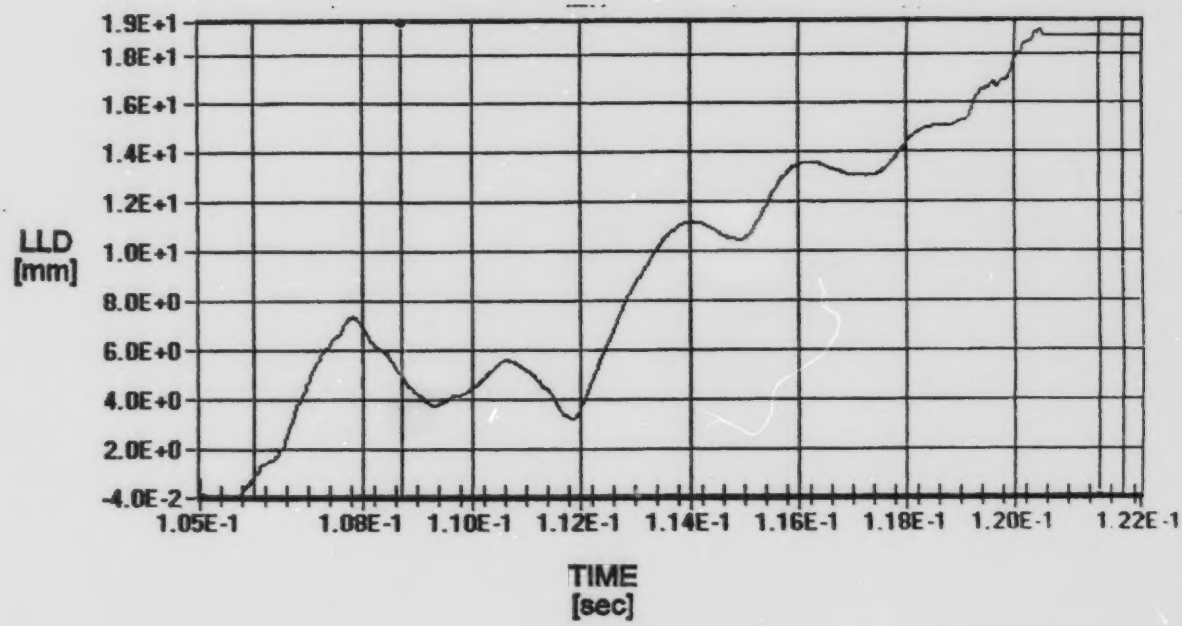

Figure 9.
LLD Versus Time.
(Full Displacement Range.)

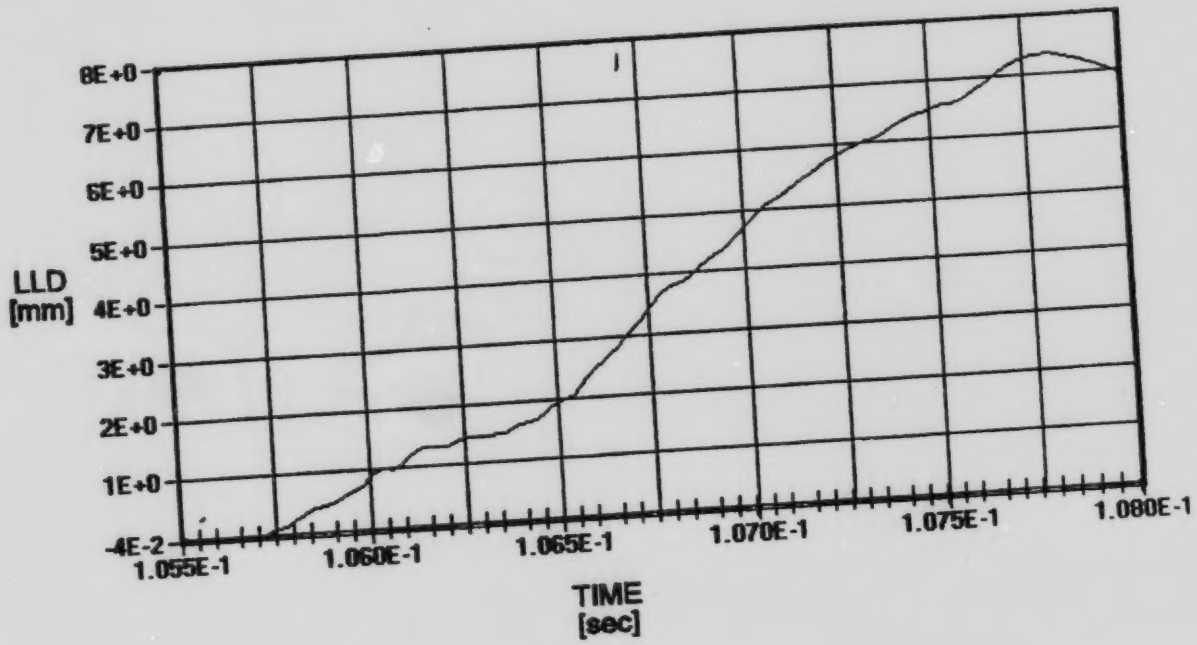

Figure 10.
LLD Versus Time.
(Working Displacement Range.)

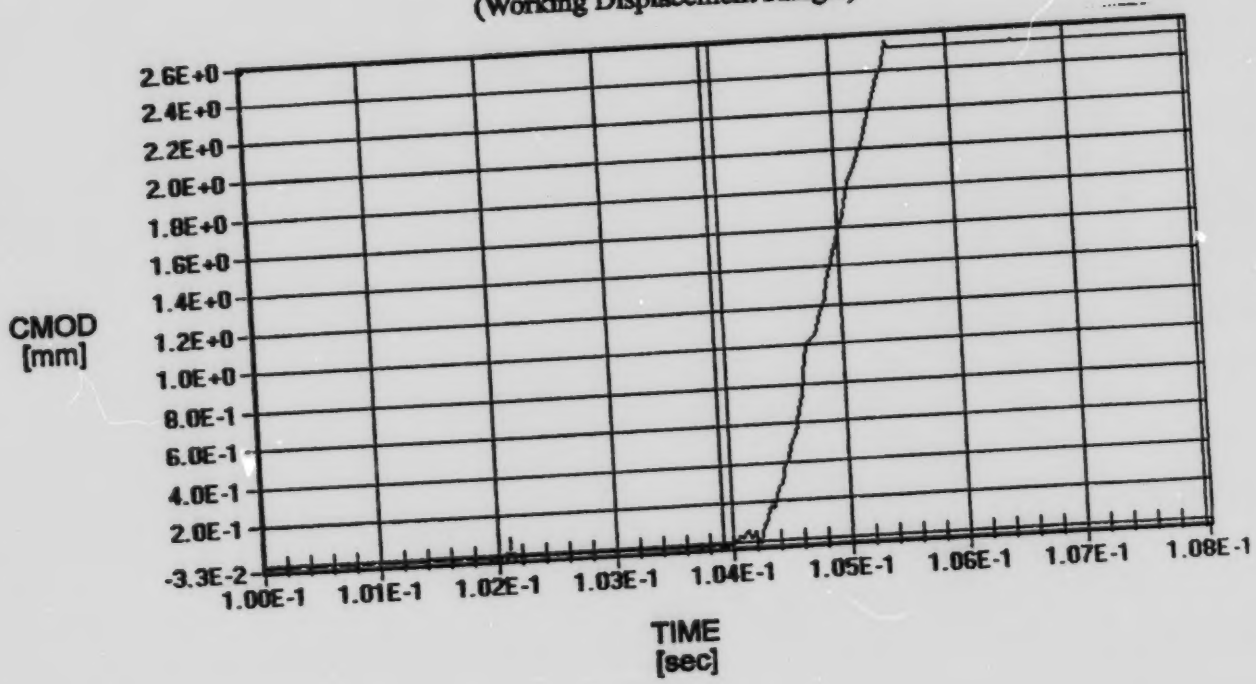

Figure 11.
CMOD Versus Time.
(2 m/sec Impact Velocity)

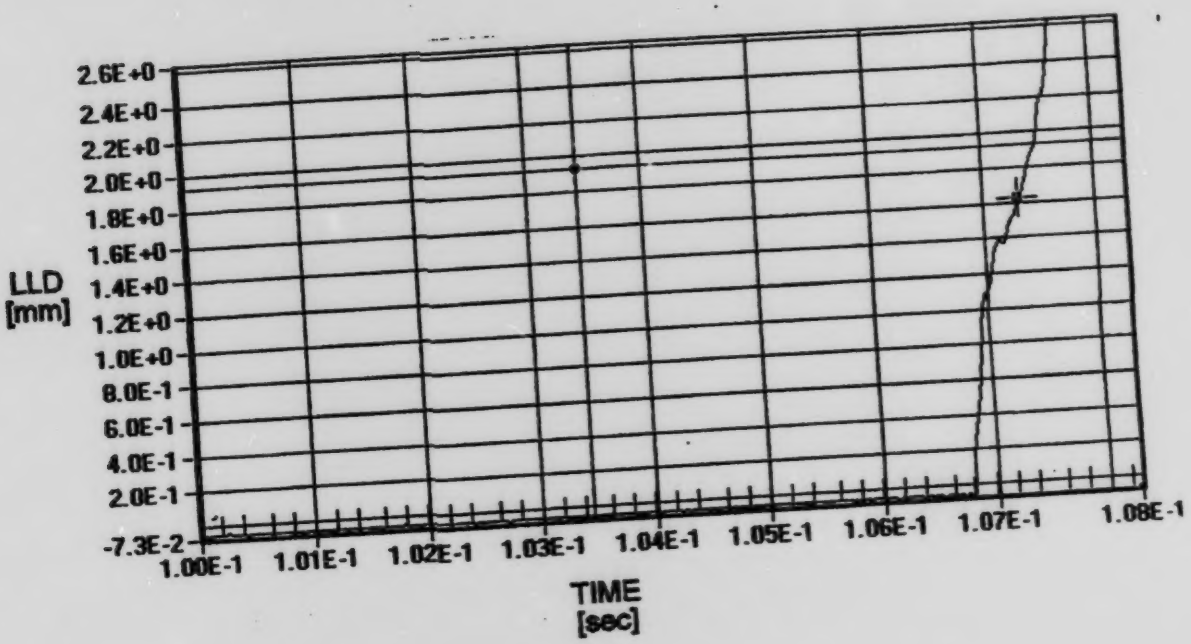

Figure 12.
LLD Versus Time.
(2 m/sec Impact Velocity.)

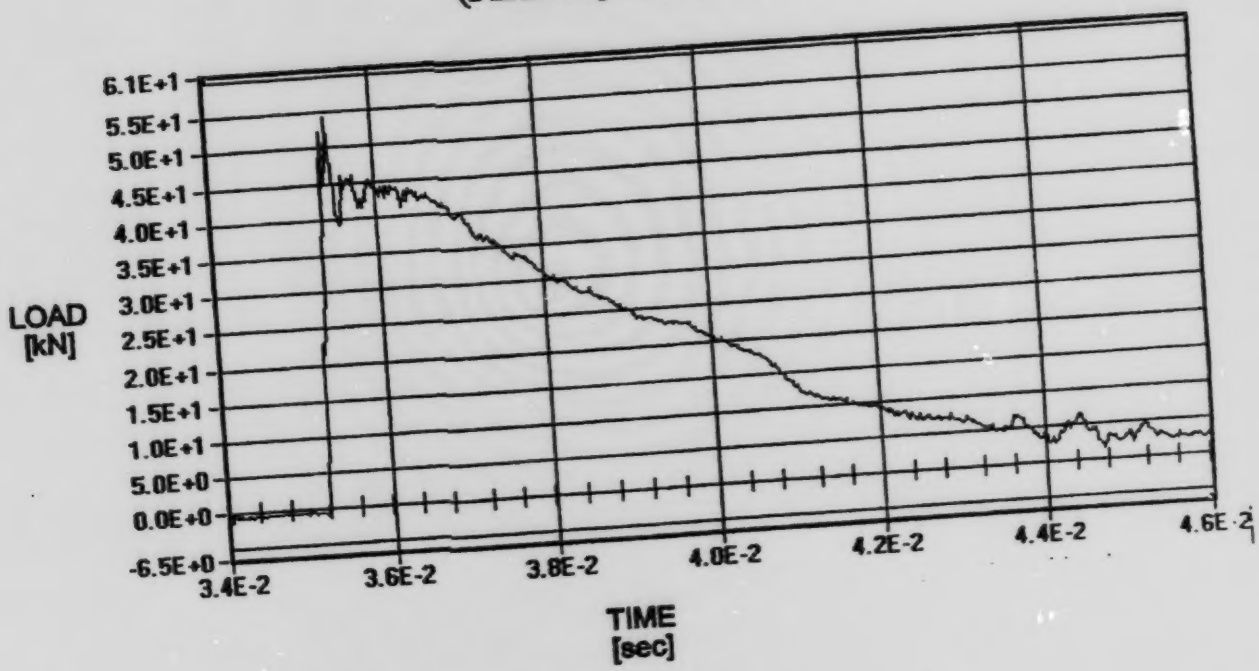

Figure 13.
Load Versus Time.
(4 m/sec Impact Velocity)

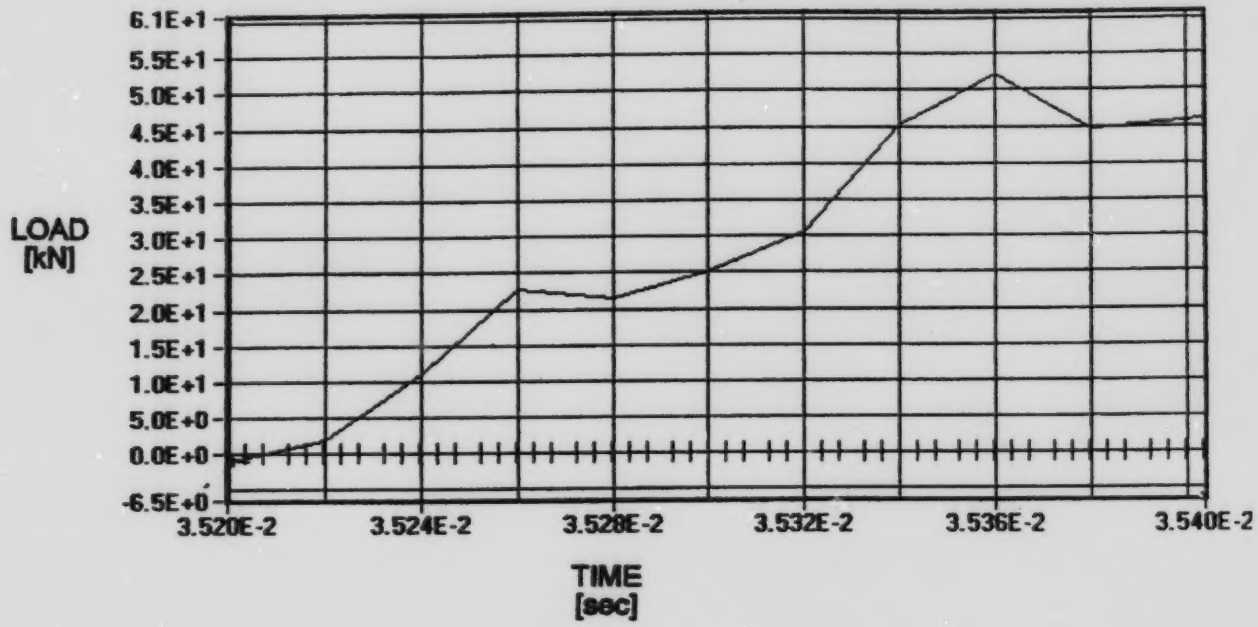

Figure 14.
Load Versus Time.
Expanded Time Scale.
(4 m/sec Impact Velocity.)

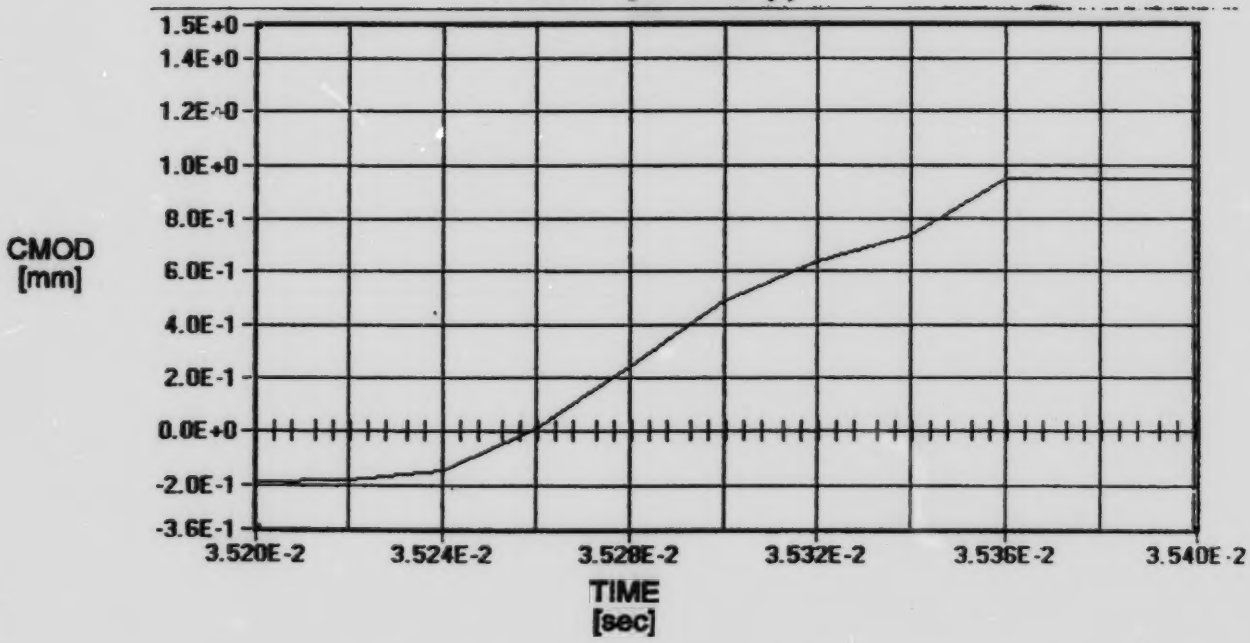

Figure 15.
CMOD Versus Time.
(4 m/sec Impact Velocity)

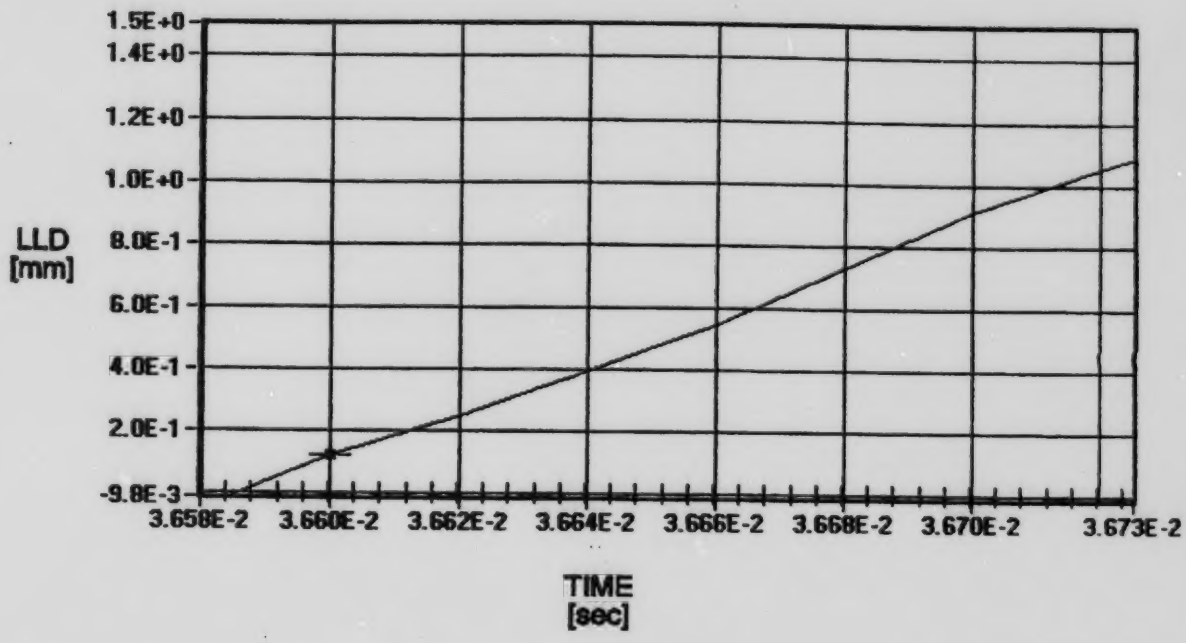

Figure 16.
LLD Versus Time
(4 m/sec Impact Velocity.)

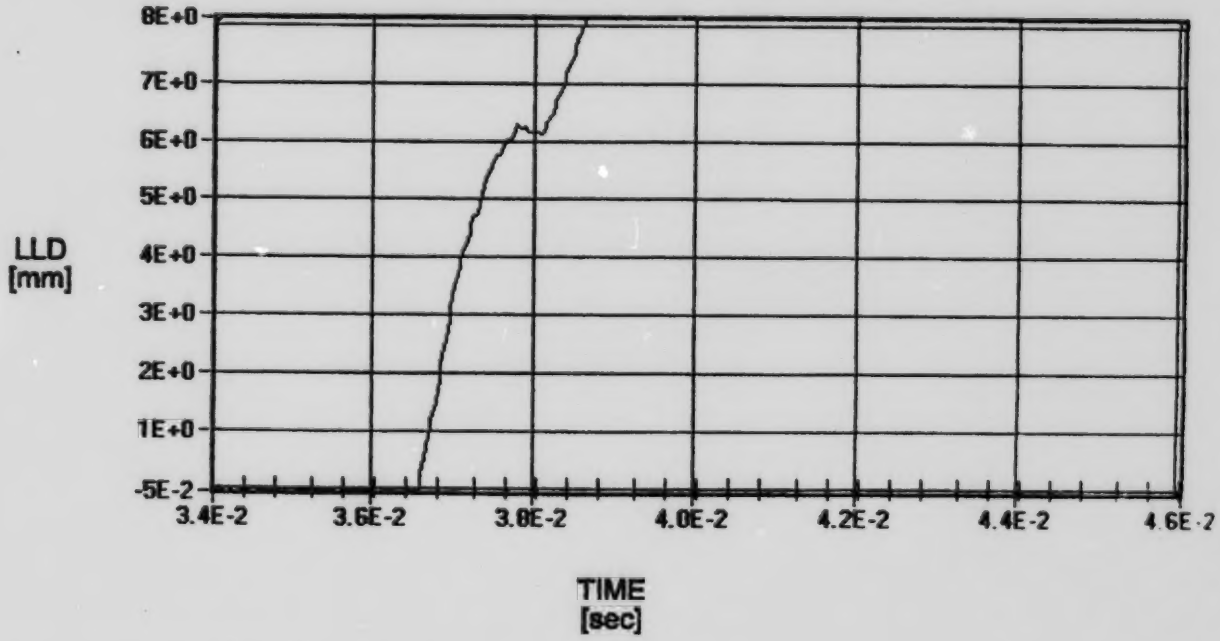

Figure 17.
LLD Working Displacment Range Versus Time.
(4 m/sec Impact Velocity)

ANNEX A

EXTENDED BIBLIOGRAPHY ON HIGH RATE FRACTURE TESTING

A1. Alexander, D.J., Nanstad, R.K., Corwin, W.R., Hutton, J.T., "A Semiautomated Computer-Interactive Dynamic Impact Testing System", Applications of Automation Technology to Fatigue and Fracture Testing, ASTM STP 1092, A.A. Braun et al., Eds., American Society for Testing and Materials, Philadelphia, 1990, pp. 83-94.

A2. Banerjee, M.M., Das, J.N., Sikdar, S., "On Dynamic Crack Propagation - A Literature Study", International Journal of Pressure Vessels and Piping, Vol. 55, 1993, pp. 495-509.

A3. Banthia, N., Mindess, S., Bentur, A., Pigeon, M., "Impact Testing of Concrete Using a Drop-Weight Impact Machine", Experimental Mechanics, March 1989, pp. 63-69.

A4. Bassim, M.N., Bayoumi, M.R., Hsu, T.R., Matthews, J.R., "Investigation of Dynamic JId for Alloy Steel Weldments Using the Split Hopkinson Bar", Journal of Testing and Evaluation, JTEVA, Vol. 14, No. 5., 1986, pp. 229-235.

A5. Bohme, W., "The Influence of Stress Waves on the Dynamic Crack Tip Loading in Three-Point Bend Impact Testing", Impact Loading and Dynamic Behaviour of Materials, International Conf.(Impact), C.Y. Chen et al., Eds., Vol. 1. pp. 305-311.

A6. Bohme, W., Kalthof, J.F., "The Behavior of Notched Bend Specimens in Impact Testing", International Journal of Fracture, Vol. 20, 1982, R139-R143.

A7. Bohme, W., "Dynamic Key-Curves for Brittle Fracture Impact Tests and Establishment of a Transition Time", Fracture Mechanics: Twenty-First Symposium, ASTM STP 1074, J.P. Gudas and E.M. Hackett, Eds., American Society for Testing and Materials, Philadelphia, 1990, pp. 144-156.

A8. Bohme, W., "Fracture Resistance of a Pressure Vessel Steel Under Impact Loading Conditions", Rapid Load Fracture Testing, ASTM STP 1130, R. Chona and W. R. Corwin, Eds., American Society for Testing and Materials, Philadelphia, 1992, pp. 92-103.

A9. Bowles, K.J., "The Correlation of Low-Velocity Impact Resistance of Graphite-Fiber-Reinforced Composites with Matrix Properties", Composite Materials: Testing and Design (Eighth Conference), ASTM STP 922, J.D. Whitcomb, Ed., American Society for Testing and Materials, Philadelphia, 1988, pp. 124-142.

A10. Bui, H.D., Maigre, H., Rittel, D., "A New Approach to the Experimental Determination of the Dynamic Stress Intensity Factor", International Journal of Solids and Structures, Vol. 29, No. 23, 1992, pp. 2881-2895.

A11. Bush, A.J., "Dynamic Fracture Toughness Tests on A302-B Steel", Impact Testing of Metals, ASTM STP 466, American Society for Testing and Materials, Philadelphia, 1970, pp. 259-280.

A12. Chen, B.Y., Shi, Y.W., "A Comparison of Various Dynamic Elastoplastic Fracture Toughness Evaluating Procedure by Instrumented Impact Test", Engineering Fracture Mechanics, Vol. 36, No. 1, 1990, pp. 17-26.

A13. Dally, J.W., Fourney, W.L., Irwin, G.R., "On the Uniqueness of the Stress Intensity Factor - Crack Velocity Relationship", International Journal of Fracture, Vol. 27, 1985, pp. 159-168.

A14. Fahey, N.H., "The Charpy Impact Test - Its Accuracy and Factors Affecting Tests Results", Impact Testing of Metals, ASTM STP 466, American Society for Testing and Metals, Philadelphia, 1970, pp. 76-92.

A15. Hoover, W.R., "Effect of Test System Response Time on Instrumented Charpy Impact Data", Instrumented Impact Testing, ASTM STP 563, American Society for Testing and Materials, Philadelphia, 1974, pp. 203-214.

A16. Ireland, D.R., "Procedures and Problems Associated with Reliable Control of the Instrumented Impact Test", Instrumented Impact Testing, ASTM STP 563, American Society for Testing and Materials, Philadelphia, 1974, pp. 3-29.

A17. Irwin, G.R., Dally, J.W., Zhang, X.-J., Boneberger, R.J., "Lower-Bound Initiation Toughness ofA533-B Reactor-Grade Steel", Rapid Load Fracture Testing, ASTM STP 1130, R. Chona and W.R. Corwin, Eds., American Society for Testing and Materials, Philadelphia, 1992, pp. 9-23.

A18. Kalaida, V.V., Naumov, A.V., "Calculation of the Current Value of Stress Intensity Factor Under Impact Testing", Engineering Fracture Mechanics, Vol. 45, No. 6, pp. 875-879.

A19. Knauss, W.G., Ravi-Chandar, K.,"Some Basic Problems in Stress Wave Dominated Fracture", International Journal of Fracture, Vol. 27, 1985, pp. 127-143.

A20. Kobayashi, A.S., Ramulu, M., Dadkhah, M.S., Yang, K.-H., Kang, B.S.J., "Dynamic Fracture Toughness", International Journal of Fracture, Vol. 30, 1986, pp. 275-285.

A21. Kobayashi, T., Yamamoto, H., Matsuo, K., "Evaluation of Dynamic Fracture Toughness on Heavy Ductile Cast Iron for Container", Engineering Fracture Mechanics, Vol. 30, No. 3, 1988 pp. 397-407.

A22. Kobayashi, T., Yamamoto, I., Nunomi, M.. "Introduction of a New Dynamic Fracture Toughness Evaluation System", Journal of Testing and Evaluation, JTEVA, Vol. 21, No. 3, 1993, pp. 145-153.

A23. Matthews, J.R., "On the Relationship Between Shear Index and Energy in Dynamic Tear Specimens", Engineering Fracture Mechanics, Vol. 39, No. 1, 1991, pp. 131-140.

A24. Matthews, W.T., "The Role of Impact Testing in Characterizing the Toughness of Materials", Impact Testing of Metals, ASTM STP 466, American Society for Testing and Materials, Philadelphia, 1970, pp. 3-20.

A25. Meyer, M.A., "Dynamic Behaviour of Materials", John Wiley & Sons, New York. 1994.

A26. Miyazaki, N., "Application of Line-Spring Model to Dynamic Stress Intensity Factor Analysis of Pre-Cracked Bending Specimen", Engineering Fracture Mechanics, Vol. 38, No. 4/5, 1991, pp. 321-326.

A27. Morland, E., "Fracture Toughness in the Transition Regime for A533B-1 Steel: The Effect of Specimen Sidegrooving", Fracture Mechanics: Twenty-first Symposium, ASTM STP 1074, J.P. Gudas and E.M. Hackett, Eds., American Society for Testing and Materials, Philadelphia, 1990, pp. 215-237.

A28. Nakano, Y., Sakai, Y.,Yagawa, G., Ando, K., Ando, Y., "Dynamic Fracture Toughness of LWR Pressure Vessel Steel A508 C1.3: A Japanese Round-Robin Study", International Journal of Pressure Vessels and Piping, Vol. 31, 1988, pp. 255-270.

A29. Nakano. M., Kishida. K., "Measurement of Dynamic Fracture Toughness by Longitudinal Impact of Precracked Round Bar", International Journal of Pressure Vessels and Piping, Vol. 44, 1990, pp. 3-15.

A30. Prakash, V., Clifton, R.J., "Experimental and Analytical Investigation of Dynamic Fracture Under Conditions of Plane Strain", Fracture Mechanics, Twenty-Second Symposium (Volume 1), ASTM STP 1131, E.A. Saxena et al., Eds., American Society for Testing and Materials, Philadelphia, 1992, pp. 412-444.

A31. Premack, T., Douglas, A.S., "An Analysis of the Crack Tip Fields in a Ductile Three-Point Bend Specimen Subjected to Impact Loading", Engineering Fracture Mechanics, Vol. 45, No. 6, 1993, pp. 717-728.

A31. Ravichandran, G., Clifton, R.J., "Dynamic Fracture Under Plane Wave Loading", International Journal of Fracture, Vol. 40, 1989, pp. 157-201.

A32. Rittel. D., Maigre, H., Bui, H.D., "A New Method for Dynamic Fracture Toughness Testing", Scripta Metallurgica et Materialia, Vol. 26, 1992, pp. 1593-1598.

A33. Rosakis, A.J., Zehnder, A.T., "On the Dynamic Fracture of Structural Metals", International Journal of Fracture, Vol. 27, 1985, pp. 169-186.

A34. Sahraoui, S., Lataillade, J.L., "Dynamic Effects During Instrumented Impact Testing", Engineering Fracture Mechanics, Vol. 36, No. 6, 1990, pp. 1013-1019.

A35. Saxton, H.J., Ireland, D.R., Server, W.L., Analysis and Control of Inertial Effects During Instrumented Impact Testing", Instrumented Impact Testing, ASTM STP 563, American Society for Testing and Materials, 1974, pp. 50-73.

A36. Schmitt, W., Sun, D.-Z., Bohme, W., Nagel, G., "Evaluation of Fracture Toughness Based onResults of Instrumented Charpy Tests", International Journal of Pressure Vessel and Piping, Vol. 59, 1994, p. 21-29.

A37. Server, W.L., Henderson, G.R., "The Measurment of Absorbed Charpy Impact Energy Using a Vertical Drop Tower", Journal of Testing and Evaluation, JTEVA, Vol. 9, No. 3, 1981, pp. 210-213.

A38. Server, W.L., Ireland, D.R., "Nonstandard Test Techniques Utilizing the Instrumented Charpy and Izod Tests", Instrumented Impact Testing, ASTM STP 563, American Society for Testing and Materials, 1974, pp. 74-91.

A39. Server, W.L., Mager, T.R., "Irradiated Dynamic and Arrest Fracture Toughness Compared to Lower-Bound Predictions", Rapid Load Fracture Testing, ASTM STP 1130, R. Chona and W. R. Corwin, Eds., American Society for Testing and Materials, Philadelphia, 1992, pp. 1-8.

A40. Shockey, D.A., Kalthoff, J.F., Erlich, D.C., "Evaluation of Dynamic Crack Instability Criteria", International Journal of Fracture, Vol. 22, 1983, pp. 217-229.

A41. Shockey, D.A., Seaman, L., Curran, D.R., "The Micro-Statistical Fracture Mechanics Approach to Dynamic Fracture Problems", International Journal of Fracture, Vol. 27, 1985, pp. 145-157.

A42. Shockey, D.A., Erlich, D.C., Kalthoff, J.F, Homma, H., "Short-Pulse Fracture Mechanics", Engineering Fracture Mechanics, Vol. 23, No. 1, 1986, pp. 311-319.

A43. Shum, D., Bassim, M.N., Bayoumi, M.R., "Dynamic Tensile Fracture Toughness Evaluation Using Compact Tension Specimens", International Journal of Fracture, Vol. 29, 1985, R3-R10.

A44. Tanaka, Y., Iwadate, T., Suzuki, K., "Small Specimen Meaasurements of Dynamic Fracture Toughness of Heavy Section Steels for Nuclear Reactor Pressure Vessels", InternationalJournal of Pressure Vessels and Piping, Vol. 31, 1988, pp. 221-236.

A45. Turner. C.E., "Measurement of Fracture Toughness by Instrumented Impact Test", Impact Testing of Metals, ASTM STP 466, American Society for Testing and Materials, Philadelphia, 1970, pp. 93-114.

A46. Tyler, W.R., "Discussion of "Correlations of Microstructure with Dynamic and Quasi-Static Fracture in a Plain Carbon Steel", Metallurgical Transactions A, Vol. 20A, 1989, pp. 2860-2862.

A47. Varga, T., Schneeweiss, G., "A New Method to Test Crack-Arrest Toughness by Using Three-Point Bend Specimens", Rapid Load Fracture Testing, ASTM STP 1130, R. Chona and W. R. Corwin, Eds.. American Society for Testing and Materials, Philadelphia, 1992, pp. 134-146.

A48. Wullaert, R.A., "Applications of the Instrumented Charpy Impact Test", Impact Testing of Metals, ASTM STP 466, American Society for Testing and Materials, Philadelphia, 1970, pp. 148-164.

A49. Yokoyama, T., Kishida, K.: "A Microcomputer-Based System for the High-Speed Compression Test by the Split Hopkinson Pressure Bar Technique", Journal of Testing and Evaluation, JTEVA, Vol. 14, No. 5, 1986, pp. 236-242.

A50. Zehnder, A.T., Rosakis, A.J., Krishnaswamy, S., "Dynamic Measurement of the J Integral in Ductile Metals: Comparison of Experimental and Numerical Techniques", International Journal of Fracture, Vol. 42, 1990, pp. 209-230.

A51. Zehnder, A.T., Rosakis, A.J., " Dynamic Fracture Initiation and Propagation in 4340 Steel UnderImpact Loading", International Journal of Fracture, Vol. 43, 1990, pp. 271-285.

UNCLASSIFIED
SECURITY CLASSIFICATION OF FORM
(highest classification of Title, Abstract, Keywords)

DOCUMENT CONTROL DATA

(Security classification of title, body of abstract and indexing annotation must be entered when the overall document is classified)

1. ORIGINATOR (the name and address of the organization preparing the document.. Organizations for whom the document was prepared. e.g. Establishment sponsoring a contractor's report. or tasking agency, are entered in section 8.)

Engineering Material Research

2. SECURITY CLASSIFICATION (overall security classification of the document including special warning terms if applicable).

UNCLASSIFIED

3. TITLE (the complete document title as indicated on the title page. Its classification should be indicated by the appropriate abbreviation (S,C,R or U) in parentheses after the title).

Drop Tower Upgrade Project (U) Volume 1 Instrumentation and Data Acquisition System
Volume 2 Operator Manual: Tower and Application Software

4. AUTHORS (Last name. first name, middle initial. If military, show rank, e.g. Doe, Maj. John E.)

D.A. Hull

5. DATE OF PUBLICATION (month and year of publication of document)

April1999

6a. NO .OF PAGES (total containing information Include Annexes, Appendices, etc).

Vol 1 33
Vol 2 30

6b. NO. OF REFS (total cited in document)

Vol1 42 refs
Vol 2 3 refs

7. DESCRIPTIVE NOTES (the category of the document. e.g. technical report, technical note or memorandum. If appropriate, enter the type of report, e.g. interim, progress, summary, annual or final. Give the inclusive dates when a specific reporting period is covered).

CONTRACT REPORT

8. SPONSORING ACTIVITY (the name of the department project office or laboratory sponsoring the research and development. Include address).

Defence Research Establishment Atlantic, PO Box 1012, Dartmouth NS B2Y 3Z7

9a. PROJECT OR GRANT NO. (if appropriate. the applicable research and development project or grant number under which the document was written. Please specify whether project or grant).

9b. CONTRACT NO. (if appropriate. the applicable number under which the document was written).

W7708-4-1386

10a ORIGINATOR'S DOCUMENT NUMBER (the official document number by which the document is identified by the originating activity. This number must be unique to this document.)

DREA CR 1999-034

10b OTHER DOCUMENT NOs. (Any other numbers which may be assigned this document either by the originator or by the sponsor.)

11. DOCUMENT AVAILABILITY (any limitations on further dissemination of the document, other than those imposed by security classification)

(X) Unlimited distribution
( ) Defence departments and defence contractors; further distribution only as approved
( ) Defence departments and Canadian defence contractors; further distribution only as approved
( ) Government departments and agencies; further distribution only as approved
( ) Defence departments; further distribution only as approved
( ) Other (please specify):

12. DOCUMENT ANNOUNCEMENT (any limitation to the bibliographic announcement of this document. This will normally correspond to the Document Availability (11). However, where further distribution (beyond the audience specified in (11) is possible, a wider announcement audience may be selected).

UNCLASSIFIED
SECURITY CLASSIFICATION OF FORM

13. ABSTRACT (a brief and factual summary of the document. It may also appear elsewhere in the body of the document itself. It is highly desirable that the abstract of classified documents be unclassified. Each paragraph of the abstract shall begin with an indication of the security classification of the information in the paragraph (unless the document itself is unclassified) represented as (S), (C), (R), or (U). It is not necessary to include here abstracts in both official languages unless the text is bilingual).

This report describes contract work to upgrade the capabilities of the drop tower at the DREA Dockyard Laboratory (Pacific). There was a need for improved fracture data acquisition and analysis software. In addition elastic-plastic fracture measurements at impact velocities and low temperatures required improved transducer performance.

The contract requirements included a review of high rate testing standards and developments in instrumentation and data acquisition, the development of customized software for routine data acquisition and display, and drop tower modifications to meet specified performance criteria. One of the main requirements was to identify and apply promising methods of measuring crack mouth opening and load line displacement, to increase manageable drop tower velocities for such tests from 2 m.s-1 to 5 m.s-1, and to improve the low temperature capability.

14. KEYWORDS, DESCRIPTORS or IDENTIFIERS (technically meaningful terms or short phrases that characterize a document and could be helpful in cataloguing the document. They should be selected so that no security classification is required. Identifiers, such as equipment model designation, trade name, military project code name, geographic location may also be included. If possible keywords should be selected from a published thesaurus. e.g. Thesaurus of Engineering and Scientific Terms (TEST) and that thesaurus-identified. If it not possible to select indexing terms which are Unclassified, the classification of each should be indicated as with the title).

Drop Tower
Toughness
Instrumentation
Lab Windows

DCD03 2/06/87-M/ DREA mod. 17 Dec 1997

Copy No. 11

DEFENCE R&D DÉFENSE

DROP TOWER UPGRADE PROJECT

Volume 2: Operator Manual: Tower & Application Software

D. A. Hull

ENGINEERING MATERIAL RESEARCH

DEFENCE RESEARCH ESTABLISHMENT ATLANTIC

Contractor Report

DREA CR 1999-034

April 1999

National Defence Défense nationale

Canada

National Defence
Research and Development Branch

Défense nationale
Bureau de recherche et développement

DREA CR 1999-034

DROP TOWER UPGRADE PROJECT

Volume 2

Operator Manual: Tower and Application Software

D.A. HULL

ENGINEERING MATERIAL RESEARCH
35 Carl Hall Drive
Downsview ON M3K2B6

Scientific Authority
J. Morrison

W7708-4-1386
Contract Number

April1999

CONTRACTOR REPORT

Prepared for

Defence Research Establishment Atlantic

Centre de Recherches pour la Défense Atlantique

Canada

DREA CR 1999 034 - Dockyard Laboratory Drop Tower Upgrade

D.A. Hull

Engineering Material Research, Downsview, Ontario

Abstract

This report describes contract work to upgrade the capabilities of the drop tower at the DREA Dockyard Laboratory (Pacific). There was a need for improved fracture data acquisition and analysis software. In addition elastic-plastic fracture measurements at impact velocities and low temperatures required improved transducer performance.

The contract requirements included a review of high rate testing standards and developments in instrumentation and data acquisition, the development of customized software for routine data acquisition and display, and drop tower modifications to meet specified performance criteria. One of the main requirements was to identify and apply promising methods of measuring crack mouth opening and load line displacement, to increase manageable drop tower velocities for such tests from 2 $m.s^{-1}$ to 5 $m.s^{-1}$, and to improve the low temperature capability.

Résumé

Le présent rapport décrit un travail à forfait visant à accroître les capacités de la tour d'essai au choc du laboratoire de chantier naval (Pacifique) du CRDA. Il existait un besoin d'amélioration en matière d'acquisition de données de rupture et de logiciel d'analyse. De plus, les mesures de rupture élastique-plastique aux vitesses d'impact et aux basses températures nécessitaient une amélioration de la performance des transducteurs.

Les exigences du contrat comprenaient un examen des normes d'essai à haute vitesse et des perfectionnements des instruments et des techniques d'acquisition de données, le développement de logiciel personnalisé pour l'acquisition et l'affichage courants de données ainsi que des modifications de la tour d'essai au choc, afin de satisfaire aux critères de performance spécifiés. Une des principales exigences consistait à déterminer et à appliquer des méthodes prometteuses de mesure du déplacement de l'ouverture de fissure et de la ligne de charge, à faire passer de 2 $m.s^{-1}$ à 5 $m.s^{-1}$ les vitesses maniables en tour d'essai au choc pour ce type d'essais et à améliorer la capacité à basse température.

DREA CR 1999 034 - Dockyard Laboratory Drop Tower Upgrade

Volume 2 - Operator Manual: Tower and Application Software

D.A. Hull

Engineering Material Research, Downsview, Ontario

Executive Summary

There is a requirement for improved fracture control procedures for ships' hulls in order to reduce structural maintenance costs. This implies the use of more rigorous damage assessment procedures, including the ability to determine tolerable crack sizes and specify inspection intervals in critical locations under service conditions. A sufficiently high material resistance to crack initiation and propagation is needed to ensure that cracks can be detected and repaired without compromising the operation of the ship or risking catastrophic failure. Unfortunately the data currently generated from specified quality control tests during material selection and ship construction provide only a qualitative indicator of toughness, and are inadequate to describe the fracture behaviour of large components. Quantitative assessment of resistance to crack initiation requires laboratory testing at the minimum service temperature and at loading rates equivalent to hull impact events such as wave slamming and minor collisions. Test temperatures typically may need to be in the -30°C range, and the corresponding loading rates are intermediate between those used in quasi-static laboratory tests with servo-hydraulic machines, and the high rates obtained during an explosion test. The standardized test procedures used to quantify toughness typically only cover ambient conditions and quasi-static loading rates. To complicate matters, a demonstration of adequate toughness usually also entails measurement of fracture resistance under elastic-plastic as well as linear-elastic loading conditions at the crack tip. In general these require an accurate measurement of force and displacement while a pre-cracked test specimen is being rapidly fractured, and result in some difficult instrumentation and data acquisition challenges.

The DREA Dockyard Laboratory (Pacific) drop tower allows samples to be subjected to displacement rates of several metres per second. However, deficiencies in instrumentation have limited the laboratory's ability to carry out dynamic elastic-plastic fracture measurements. There was also a need to incorporate state-of-the-art-data acquisition and analysis software. Volume 1 of this report described contract work to address these requirements, while this volume provides an Operator Manual for the upgraded system.

TABLE OF CONTENTS

	Page
1. System Overview	1
2. Drop Tower	1
3. Control Panel	2
4. Signal Amplifiers	3
5. Oscilloscope	3
6. Transducers	4
6.1. Load Cell	4
6.2. Specimen Load	4
6.3. COD Gauge	4
6.4. LLD Gauge	5
6.5. LVT Gauge	5
6.6. Optical Trigger and Velocity Flag	5
7. Low Temperature Evaluation	6
8. Software Description.	7
8.1. Program Initialization	7
8.2. Files	7
8.3. Setup	8
8.4. Scope	9
8.4.1 Scope Channel Selection	9
8.4.2 Scope Time and Trigger	9
8.5. Data	10
8.5.1 Y versus T Plots	10
8.5.2 Channel Waveform Plot	10
8.5.3 Zoom and Restore	10
8.5.4 Window Data	11
8.5.5 File Data Box	11
8.5.6 Summary Waveform Plot	11
8.5.7 Y versus X Plots.	11
8.5.8 K vs. Disp. and K vs. Time plots	11
8.5.9 Normalization Plot	11
8.5.10 Max-Min Table	12
8.6. Temperature	12
8.7. Export	12
8.8. Quit	13
9. Guidelines for Evaluating Specimens	13
10. References	14

Figures 1-35

Appendix A - Dynatup Tup Specification
Appendix B - LVT Specification
Appendix C - Pinout/wire Designation for Thermocouple Inputs

1. SYSTEM OVERVIEW

At the Dockyard Laboratory Pacific (DL(P)) rapid loading fracture events are studied using an instrumented Dynatup Model 8100E Drop Tower, Nicolet 440 Digital Storage Oscilloscope and an IBM compatible computer. Load, crack opening displacement, load line displacement, and velocity transducers are mounted on the drop tower as shown schematically in Figure 1. The transducer analog signals are amplified by signal conditioners and digitized by the oscilloscope at sampling rates up to 2M samples/sec. The waveform data is transferred to the computer using an RS232 link. A LabWindows CVI graphical user interface allows the oscilloscope to be user controlled from the computer. The software is written in the C programming language and converts raw data into engineering units and provides analysis, plotting and export functions.

Drop tower hardware details are presented in Sections 2 - 7 and the software is described in Section 8. Guidelines for evaluating specimens at ambient and cold temperatures are described in Section 9.

2. DROP TOWER

The Dynatup 8100E drop tower components are identified in Figure 2. The tower consists of base plate, guide and support posts, 300 kg crosshead, instrumented tup, electric hoist, air release valves, rubber rebound springs, brake, anvils, safety cage and specimen fixtures. Proper operation of the drop tower requires regulated air pressure in the range of 80 -100 psig. The air supply to the drop tower must be turned on before each test.

The 1016 x 813 mm aluminum base plate is fastened to a steel support plate that has been bolted and epoxied to an isolated concrete base. Two chrome plated steel posts are set 610 mm apart on the base plate and guide the cross head during hoisting or dropping operations. A T-slot plate or an anvil support plate are bolted to the base plate between the guide posts to accommodate different anvil sizes and shapes. A Lexan plastic enclosure around the support plate perimeter was installed to contain specimen fragments.

The electric chain hoist, relays, and solenoid valves are located in a steel box at the top of the drop tower. Electric power and air supply connections are made to the rear of this box. The hoist enclosure is supported by the guide posts at the front and two hollow square posts at the back. The left rear post acts as a chain fall for the electric hoist and the right post serves as a conduit for electric power, air lines and system interlock cables. Slotted rails are attached to both rear posts. The right rail allows vertical height adjustment of the hoist travel and brake rebound switches. The light trigger for oscilloscope and velocity transducers is moved vertically on the left rail to allow different specimen heights.

The crosshead assembly consists of two 200 mm thick aluminum blocks that are bolted to steel load plates. Currently this assembly mass is nominally 300 kg, although different load plate masses may be used to suit the test requirements. A pickup roller is attached to the top block to allow attachment of the hoist hook. The solid block at the

bottom of the crosshead is faced with a 25.4 mm thick steel plate. The drop tower load cell is attached to this plate. The tup or indenter that impacts the specimen is bolted to the end of the load cell. Tups with different radius of curvature are available. In some test configurations, a DL(P) designed preload fixture seats the specimen firmly against the tup.

An aluminum hoist fixture is raised or lowered by the electric hoist to position the crosshead assembly. The hook action is pneumatically controlled to lock onto or release the pickup roller. The hook is retracted and held open by a pneumatic actuator that operates when the drop button on the operator panel is pressed. The front panel will be described in the next section. When the crosshead is released the hoist's upward motion is disabled until the crosshead is again supported by the hook. Three proximity switches must be set properly to prevent operator injury and hoist damage. Two switches are mounted at the rear of the hoist fixture. These switches close when the clearance between the bottom of the hoist fixture and top of the crosshead will enable the hook to engage the pickup roller. The third proximity switch is mounted on the hook itself and is closed when the roller is firmly lodged in the hook. When this switch operates the pneumatic brakes that may be supporting the crosshead are released and upward travel of the hoist is again possible. These switches are designed to minimize danger to the operator. However, the operator should never work beneath the crosshead while it is supported only by the hoist. Physical support beneath the crosshead to make it impossible for downward movement is the only recommended practice when working below the crosshead. Aluminum compression blocks are bolted to the base plate on the outside of the front guide posts and they are faced with sheets of natural gum rubber. This composite compression spring absorbs the kinetic energy of the falling crosshead and causes it to rebound during drop events. Pneumatically actuated air brakes are applied during the crosshead's rebound from the rubber pads. A crosshead mounted magnet closes a reed switch mounted on the right support rail. This switch energizes a solenoid to admit air to the pneumatic brakes that are an integral part of the crosshead assembly. Large aluminum pistons press phenolic pads firmly against the guide post to arrest the crosshead's upward motion.

3. CONTROL PANEL

Operation of the drop tower is controlled manually from the control panel illustrated in Figure 3. The illuminated power switch is located on the left side of the panel. The SAFE light is illuminated when a black safety pin is engaged in the right front post hole shown in Figure 2. A magnet on the safety pin end engages a reed switch located on the rear square post. Proper seating of the safety pin disables operation of the hoist and drop release mechanism to provide a measure of operator safety. However, the crosshead should always be physically supported such that it cannot fall when the operator is working around or underneath the crosshead. It is a safe practice to leave the crosshead on the rubber rebound blocks when the drop tower is not in use.

When the safety pin is removed from the post hole, the CAUTION light is illuminated. The crosshead is raised or lowered by pressing the hoist switch located on the right side of the panel. The hoist LIMIT STOP light illuminates when a magnet on the

crosshead closes the maximum height switch located on the right side rail. Operation of this switch disables further upward motion of the hoist. The switch position is adjusted to suit the operator. It may be set as a stop for repetitive tests requiring the same drop height or to the maximum height to prevent damage to the hoist enclosure box by the hoist fixture. When the operator is ready to release the cross head/tup assembly, a plastic safety cover is raised and the ARM toggle switch is raised. Actuating the ARM switch illuminates the red warning light, disables the hoist motion, and sounds the front panel mounted audio warning buzzer. This alerts personnel in the immediate area to the imminent drop. Pressing the DROP button retracts the hoist lifting hook allowing the crosshead/tup assembly to fall. Operation of the red, yellow and green lights may be tested by pressing on the indicator bezel to illuminate the bulb. Burned out bulbs should be replaced at once.

4. SIGNAL AMPLIFIERS

Two signal amplifiers are mounted above the drop tower control panel and they are depicted in Figure 4. The unit on the left provides 5 volt excitation to the tup load cell and amplifies the tup load signal using a wide band amplifier. An Error knob on its panel allows the load signal to be zeroed. A null condition is set when the light from the two LEDs mounted above this knob are extinguished. The low level light flag detector signal uses the same conditioner. The optical detector signal is input to a comparator circuit to generate a 5 Volt trigger signal for the oscilloscope. Noise transients occurring during operation of the air solenoids are suppressed by gating circuits if these transients are less than 100 μs. A power light and toggle switch are located on the right. A complete description and wiring diagrams for this unit are contained in [1].

A half-bridge strain gauge amplifier is located at the right of Figure 4. Signal gains of 100 or 1000 are selected by a toggle switch. A half bridge strain gauge wiring diagram is affixed to the unit's front panel. Currently this unit is not dedicated to a transducer and it may be used for additional transducers.

Two MTS Model 440.21 DC transducer conditioners or Measurements Group Model 2310 strain gauge conditioners are used to amplify crack opening displacement and load line displacement transducer signals. These two transducers are described in section 6.0. The user is referred to Section 440.21 DC Transducer Conditioner of the MTS 442 Controller Manual or the Measurements Group 2310 Operator's Manual for instructions.

5. OSCILLOSCOPE

The Nicolet 440 Oscilloscope is used to acquire up to 4 channels of data at maximum sampling rates of 2M samples/sec for each channel. An RS232 link provides communication between the oscilloscope and the computer. The computer uses the oscilloscope's remote command set to control scope functions. The user is referred to the Nicolet 440 Operation and Remote Command Sets manuals for a full description.

6. TRANSDUCERS

6.1. Load Cell.

The tup load cell uses semi-conductor strain gauges to measure impact loads. The load cell excitation and signal amplification is performed by the amplifier described in Section 4. The load cell output is sensitive to temperature and changes approximately 0.3% per °C. Consequently, the tup should be calibrated at the test temperature if it will be cooled significantly below ambient temperature during an experiment. For tup specifications see Appendix A. Calibration is suggested every 6 months or 5,000 impacts.

The ASTM Standard Practices for Force Verification of Testing Machines (E4-96) contains guidelines for static load cell calibration. Calibration can be performed in a servo-hydraulic load frame at room temperature or at the temperature of interest. It is suggested that a static and dynamic calibration of the drop tower load cell be carried out. The static calibration will require manually setting the load frame applied load and comparing the drop tower load cell output. The closed loop response of the load frame's actuator, load cell and signal conditioners will determine its suitability for dynamic calibration of the drop tower load cell. Ireland [1] suggested methods of determining transducer/signal amplifier dynamic response that may be used for evaluating a load frame's dynamic capabilities. Dynamic loads of short duration may be applied by the load frame's actuator using a ramp waveform to reach a pre-determined load. The load signals from the load frame and drop tower load cells are then compared on two channels of the Nicolet oscilloscope. Alternate methods of calibration are described in [2].

6.2. Specimen Load.

Tup load cell signals exhibit noise and ringing during impact when the specimen is supported on anvils. While alternate methods of supporting the specimen [2] have been shown to improve the tup load signal response, one solution is to measure load directly from the specimen. Load signals are derived from strain gauges mounted on the specimen surface, and these signals exhibit less noise and ringing than is measured by the tup load cell. Joyce [3] recommends the strain gauges be located at the positions shown in Figure 5 for the Single Edge Bend (SEB) and Compact Tension (CT) specimens. The gauges are applied and wired to form a Wheatstone bridge on the specimen surface. The specimen strain gauge output is statically calibrated in a load frame. The maximum applied load should not exceed the final pre-cracking load. Alternately, load can be applied to an uncracked specimen to calibrate strain versus load. The resulting function is assumed valid for specimens of the same geometry.

6.3. COD Gauge.

Crack Opening Displacement (COD) is measured using a Wheatstone bridge of strain gauges mounted on the clip gauge in Figure 6. In order to increase the ringing frequency and consequently improves the signal response relative to cantilever arm clip gauge designs, the gauge was made from titanium, and has an omega shape. This COD

gauge is mounted on knive edges that span the specimen's crack mouth. The gauge output is amplified by one of the standard signal conditioners described in Section 4. COD gauge output is calibrated using a commercially available displacement reference. The ASTM Standard Practice for Verification and Classification of Extensometers (E83) provides instructions for gauge calibration.

6.4. LLD Gauge.

Load Line Displacement (LLD), is measured using strain gauges mounted on a flex bar. Figure 7 shows the LLD gauge is initially preloaded between screws located on the specimen side. As the specimen fractures, the LLD gauge unbends and is released from the specimen. The stiffness of the heat treated tool steel has been increased by including upper and lower spring elements to create a leaf spring arrangement. LLD signal amplication and calibration are the same as described for the COD gauge.

6.5. LVT Gauge.

The Linear Velocity Transducer (LVT) induces a voltage proportional to the time rate of change of a magnetic core. The LVT measures velocity over a 76 mm interval. The LVT is composed of a fixed coil body and a core that moves with the falling drop tower crosshead that is illustrated in Figure 8. The core is supported by a bracket that is attached to the side of the crosshead. A track to guide the entry of the core in the coil is attached to the side of the drop tower. Different specimens sizes may require adjustment of the core relative to the fixed coil body. A dummy specimen having the same dimension as the test coupon is placed on the anvils. The cross head is lowered until it rests on the dummy specimen. Vertical adjustment of the core is made by loosening the two Allen head cap screws and moving the bracket in the slot. The core should be positioned midway in the coil and the screws re- tightened. The crosshead is raised slightly to allow removal of the dummy specimen. A product data sheet and wiring diagram for the LVT are provided in Appendix B.

6.6. Optical Trigger and Velocity Flag.

A light source and detector are used to generate a trigger signal to initiate data acquisition by the oscilloscope. The source and detector are mounted on the left rear support rail in Figure 8, and they can be adjusted in the vertical direction. A trigger signal is generated when the light is removed from the detector. A metal flag is attached to the crosshead and blocks the source light from the detector as the crosshead falls.

Velocity is measured using a masked square of film that is composed of evenly spaced dark and light lines. This flag's passage between the source and detector generates a series of pulses that is acquired on one of the oscilloscope's channels. Determination of the velocity is possible because the distance between lines and the period of the pulses is known. This method of velocity measurement may be used as a check on the LVT output.

7. LOW TEMPERATURE EVALUATIONS

Cooling of specimens is a frequent test requirement, and the use of liquid nitrogen or dry ice as the cooling agent is sufficient for most drop tower tests. Specimens can be cooled while supported by the anvils, pre-loaded against the tup or detached from the drop tower. One of the drop tower's cold boxes may be used for both remote or insitu cooling of specimens while the other is used for remote cooling only. Undercooling below the test temperature is required when the specimen is cooled remotely prior to installation in the drop tower. Liquid nitrogen is used in both cold boxes for cooling. The cold box is connected to a liquid nitrogen dewar by two insulated flexible stainless steel hoses. Nozzles in the cold box provide a uniform spray of nitrogen vapour/liquid on the specimen sides. The flow of liquid nitrogen is controlled by the dewar ball valve. A needle valve may be added between the dewar and cold box for improved liquid nitogen flow control. A pressure relief valve must be added between an additional valve and the dewar ball valve to prevent hose failure by expanding liquid nitrogen when both valves are closed.

Thermocouples are attached to the specimen surface to ensure the test temperature is reached prior to releasing the drop tower crosshead. Two thermocouples placed at the crack tip on both specimen sides should be the minimum number considered. Additional thermocouples enable temperature gradients at the crack tip or along the specimen body to be measured. Spot welding the thermocouples to the specimen is one method of obtaining a rugged attachment point. A thermocouple connection box is installed on the rear face of the drop tower crosshead. It allows the computer to monitor up to six type K (chromel-alumel) thermocouples. A barrier terminal block or plug-in jacks are used to connect the specimen thermocouple wires to the computer. The terminal block uses thermally compensated lugs that are designated CR or AL.

Two temperature transducers are used to measure the ambient temperature between -25 °C and 105 °C and the error is within ±0.5 °C degree over this temperature range. The transducers are temperature dependent current sources that are not affected by voltage noise pickup or IR drops in the signal leads. One transducer is mounted on the inside of the aluminum connection box lid where it provides cold junction compensation for the K type thermocouples. The other transducer is mounted inside the blue screw terminal box located next to the computer. A jumper wire in the box allows the user to select the transducer sampled by the computer and the setup in the blue screw terminal box is shown schematically in Figure 9. A variable resistor is used to trim the transducer error. Calibration of the remote unit requires the aluminum box lid temperature to be measured with a reference temperature sensor and the variable resistor is adjusted to give:

$$T_{cjc} = 1\text{mV/K}$$

Where K is the measured reference temperature in °K. A similar procedure is used to calibrate the temperature transducer in the screw terminal box.

A National Instruments Data Acquisition card, model AT-MIO-16E-10, is used to sample the thermocouple inputs. The analogue/digital channels are configured for bipolar,

differential input mode on the ± 50 mV range. Channels 0 - 5 measure the thermocouple voltage inputs from the drop tower. Channel 6 is dedicated to sampling the reference temperature transducer output. Channel 7 is used to determine the voltage offset of the data acquisition card's instrumentation amplifier. Pinout/wire designation for the thermocouple inputs are shown in Appendix C.

8. SOFTWARE DESCRIPTION.

A graphical user interface (GUI) was developed using the LabWindows CVI development package. The GUI allows the user to acquire rapid loading data using the high sampling rates of the Nicolet 440 oscilloscope. A software flowchart is shown in Figure 10. This menu driven program offers flexibility in data acquisition, plotting and analysis. The software code was structured using a main and hardware driver program. A software driver for the oscilloscope using a RS232 communication link was developed. Machine specific instructions were included in this part of the software. Commands that were independent of the hardware plaform and specific to data analysis and plotting were collected in the main program listing. Supporting library functions from the LabWindows package were included as required. Reference is frequently made to buttons or labels that appear in the GUI. In the following text, reference to GUI label will be indicated by printing the label in upper case letters, e.g., ZOOM.

8.1. Program Initialization.

Upon starting the program, the user must select default or custom configuration files for specifying oscilloscope settings, specimen geometry and material properties. The decision panel is illustrated in Figure 11. Custom configuration files are defined during previous sessions by the user. The default file causes the oscilloscope to be set to standard operating parameters; the user selects specimen and material properties later in the program. After the configuration file is selected the user is presented with a general pull down menu screen that is shown in Figure 12. Different operations may be performed depending on the selection from the menu bar that includes, FILES, SETUP, SCOPE!, TEMP!, DATA, EXPORT!, and QUIT Functions. These functions are described below.

8.2. Files.

File reading and saving of configuration and data files are done using the menu shown in Figure 13. File extensions for configuration and data files are *.cfg and *.dat respectively. Oscilloscope settings may be rapidly changed to suit different test requirements or user preferences by reading the appropriate configuration file. In addition, data acquired from past sessions may be re-analyzed, plotted within the application or exported for external program use. Selecting the open command enables the user to inspect all directory file contents prior to making a file selection through a pop-up window. It is important to note that each data file created by this program writes the channel calibration factors and units at the beginning of the file. Consequently opening a data file changes the calibration factors and the user should inspect the configuration setup before proceeding.

Configuration files created before November 97 did not include material property data. The user is notified when an old configuration file is used and it is suggested the configuration table be inspected. The configuration setup table is described in section 8.3. A PRINT PANEL option allows the currently selected panel to be printed. A PRINT CONTROL option lets the currently selected control be printed. This print feature is intended to allow individual plots to be printed without including other control buttons on the currently selected panel. The user would move the mouse to click on a plot and then select the PRINT CONTROL option.

8.3. Setup.

The setup menu allows Calibration-General and Temperature Input selections to be made. The Calibration-General panel is shown in Figure 14. This panel allows each of the oscilloscope's four input channels to be tagged with 7 different physical names that include, "LOAD, COD, VEL , DISP, LLD, STRAIN, SIGNAL or SPARE". Linear calibration equations require slope and y intercepts to be specified to convert voltage to engineering units. A total of 12 different physical units may be selected for each channel.

Specimen geometry may be selected for the Single Edge Bend (SEB) or the Compact Tension (CT) specimen geometry. Specimen dimensions to be specified include:

W - width.
B - thickness.
B_n - net thickness for side grooved specimens.
S - span for SEB specimens
a - initial crack length
a_f - final crack length.

Compact tension specimen, crack opening compliance measurements are corrected using:

H* - initial half-span of the load points (center of pin holes)
D - half the original distance between the displacement measurement points.

Material property selections include:

E - Young's Modulus,
YS - yield strength,
UTS - ultimate strength, and
ν - Poisson's ratio.

The name of the currently selected configuration file and data file are shown at the bottom of the screen. After all selections have been made, pressing the DONE button removes the setup screen. The configuration file is designed to allow scope calibration factors defined in previous sessions to be set quickly without operator intervention. However, it is important to note that if a data file is opened, the channel calibration factors will be changed to the settings that existed at the time the data was originally acquired.

Consequently, it is important to check the channel calibration factors whenever an existing data file is opened.

The Temperature Input panel is shown in Figure 15. The mouse is used to select the input channels that will be sampled. The number of samples acquired per channel and the sampling rate can be selected by the user.

8.4. Scope.

The scope panel that appears after selecting SCOPE! on the general menu bar is depicted in Figure 16. The scope panel appears with the channel names that were selected using the Setup menu. Initially the scope's signal display screen appears dimmed and this condition indicates communication and setup of the scope have not been established. Selecting the POWER button at the top right of the screen starts the setup process. Communication with the scope is established over the RS232 communication link and the scope configuration is determined by the default or custom configuration file that was selected by the user.

8.4.1. Scope Channel Selection. The oscilloscope's channel selection block is the same for each channel and is presented in Figure 17. The channel number is shown at the top left next to the colour that is used for the channel's signal trace. Blue, Red, Dark Blue, and Black are used for channels 1-4. The channel's name, e.g., LOAD, as selected by the user, is shown below the channel number. The next box shows the channel's current voltage range setting that can be adjusted by the user over discrete intervals from 30 mV to 120 V. The coupling polarity for the channel's two signal inputs (BNC jacks on the scope front panel) may be selected as AC, DC or GND. The ACQUIRE button's state of ON or OFF determines if data from a particular signal is sampled by the oscilloscope and presented on the scope's signal display screen.

8.4.2. Scope Time and Trigger. Beneath the four channels on the scope panel are the TIME and TRIGGER selection boxes. The scope time base may be adjusted in discrete intervals from 100nS to 10S as shown in Figure 18. The SWEEP LENGTH box allows the number of data points acquired per signal to be varied in discrete intervals from 1000 to 30,000 samples per channel. The TRIGGER box allows scope data acquisition to be initiated by any one of the 4 signal channels or by an external signal input (E) on the scope's front panel. The triggering slope can be selected as POS, NEG, DUAL or OFF. The trigger is disabled if OFF is chosen. The trigger level and sensitivity are specified as a percentage of the maximum voltage range. Triggering occurs automatically by the oscilloscope's onboard clock (auto mode) or by waiting for a signal to exceed a preset voltage threshold (normal mode).

Oscilloscope operation errors or RS232 communication errors are inspected by pressing the NIC440 STATUS or COM STATUS buttons that are shown on Figure 16. Selecting the Full Screen Display Popup button gives individual plots of the channel signals that have been acquired. The message box prints text information to identify

software operations that are being performed e.g., Waiting for Trigger, Acquiring Data, Displaying Waveform, etc.

Initiating scope data acquisition occurs when the LIVE or HOLD NEXT buttons are selected. The LIVE button causes the scope to continuously trigger and record data on its own screen. The HOLD NEXT button causes the scope to wait for the next trigger signal before recording data that is transferred to the computer for plotting and further analysis.

8.5. Data.

Selecting DATA on the general menu bar allows data to be plotted in different formats as shown in the pull-down menu at the top of Figure 19. The data can be presented several ways:

a) Y versus T, engineering units as a function of time.
b) Y versus X, three signals as Y and one signal as X in engineering units.
c) K versus Disp and K versus T, Stress intensity vs. Displacement and Time.
d) J versus R, J integral versus crack length.
e) Max-Min Table, maximum and minimum values.

The plotting functions available to the user are similar for each of the options listed above. Consequently the Y versus T plots will be discussed in depth while differences for the other options will be mentioned.

8.5.1. Y versus T Plots. A maximum of four individual plots and one summary plot of the acquired data are printed in a tiled format upon a background panel. Control buttons for operations that are common to all plots are located on the background screen shown in Figure 19. The VIEW SELECT buttons numbered 1-4 and the SUM button at the top left allow a selected plot to be inspected. The SAVE ALL DATA button causes a file window to appear that is depicted at the bottom of Figure 19. In this window the user specifies a file name for all of the recorded data. The DONE button clears the plot panel and returns to the general menu panel.

8.5.2. Channel Waveform Plot. An example of an individual plot is depicted in Figure 20. Each of four plots has three cursors, text and number boxes associated with it. All of the cursors may be moved by clicking on them with the mouse and dragging the cursor to a new position. The purpose of the short red cross is to give the x and y co-ordinate in engineering and time units in the boxes at the bottom left of the plot. The red and yellow cursors are used in conjunction with the zoom and data window buttons shown at the bottom right.

8.5.3. Zoom and Restore. The ZOOM button enables a segment of the data to be replotted on the screen using expanded scales. To zoom on the plot, the long red and yellow crosses are positioned on the boundaries of the area of interest. To operate properly, the red cursor should always be to the left of the yellow cursor. Then the ZOOM button is selected by

clicking on with the mouse and the data is replotted on an expanded scale. The user may zoom as many time as needed. To restore the graph to its original scale, the RESTORE button is selected by clicking on with the mouse.

8.5.4. Window Data. Frequently after inspecting a waveform, the user wishes to save only a portion of the plotted data in a file. The user moves the short red cursor with the mouse to the beginning of the data to be saved. Next click on the WINDOW DATA button and use the mouse to drag the red cursor to the end of the data segment. After releasing the cursor, a save file pop-up window appears. The user must specify a file name and the selected data is saved to a file. The saved file may then be opened and plotted as required.

8.5.5. File Data Box. Numbers preceding and following the current position of the red cursor are printed in a number box when the Y versus T plots have been selected. The user can inspect the raw data being used in the plot.

8.5.6. Summary Waveform Plot. The summary plot has the same features as the Channel Waveform plot except that up to 4 channels of data are plotted and this plot is shown in Figure 21. To accommodate 4 waveforms on one plot, each waveform is normalized by its maximum value and plotted as a percentage on the Y axis. However, the actual value of a data point can be determined by moving the short red cross and inspecting the appropriate number box at the bottom left of the screen. The ON/OFF and ZERO SEL buttons allow the user to independently select each waveform's zero. This function appears only in the Summary Waveform plot. The user moves the red cursor to the data point that will act as a waveform's new zero. At the bottom of the plot panel, ON/OFF boxes are located next to the channel number boxes. The user selects ON for the channel to be zeroed and then clicks on the ZERO SEL button with the mouse. The data is replotted and presented to the user.

8.5.7. Y versus X Plots. After selecting the Y versus X option on the DATA menu, the user must specify the data to be plotted as Y and X. The selection box is shown in Figure 22. Pressing the DONE button clears the screen and the data is presented in a format similar to the Y versus T plots.

8.5.8. K vs. Disp. and K vs. Time plots. After selecting K versus Displacement on the DATA menu, the user must specify the channels to be plotted. Then the DONE button is pressed with the mouse and the data is plotted. The user should check the SETUP menu to verify that the correct specimen type, specimen dimensions and material properties have been chosen.

8.5.9. J-R Normalization Plot. Normalization of J-R data is following a method outlined by Joyce [3] and it is carried out in a sequence of steps that require operator input. After selecting J-R Normalization, the user specifies the load and displacement waveforms that are to be analyzed using the selection box shown in Figure 22. The selected data is plotted and the user selects all or only a portion of the data that is to be analyzed. The plastic area beneath the load versus displacement curve is determined using a regression line and Simpson rule integration method. Pop-up panels provide instructions to guide the user. For

example in Figure 23, the user must select the elastic portion of the load versus displacement plot by moving the red cursor to the lower and upper elastic limits and clicking on the WINDOW DATA button. Linear regression of the selected data is performed and the resulting line is plotted for inspection by the user. The user accepts the plotted line or iterates by changing the elastic limits that were chosen earlier. After the user is satisfied with the regression line, the normalized values of load and plastic displacement are calculated and plotted. The user must select the fitting function for interpolating the crack length data. The available functions include: the exponential, polynomial and that provided in [3]. The user must specify the polynomial order or the initial coefficient values from [3] on the panel shown in Figure 24. The selected function is plotted with the data and the user may make alternate selections before crack length data is calculated. Selected data points may be deleted at the user's discretion and the fitting function is then recalculated using the remaining data. An example of this prompt panel is shown in Figure 25. Values of crack length are determined and the J-R data is plotted in Figure 26. Then the user may perform previously described plotting operations, export the data, or start at the beginning of the J-R normalization menu.

8.5.10. Max-Min Table. Figure 27 depicts the table of maximum and minimum values for each channel of acquired data that appears after the user selects the Max-Min Table option. This table should be selected after the user has viewed one of the plots described in sections 8.5.1, 8.5.7 and 8.5.8.

8.6. Temperature.

Selection of Temp! displays a readout panel that is shown in Figure 28. This panel is intended to allow the user to monitor specimen temperature until the test temperature is reached. After the specimen has dwelled at the test temperature, the user can acquire and evaluated data from the specimen in the drop tower. Up to six channels of K type thermocouple data are displayed based on selections made in the Setup:Temperature Input Section of 8.3. The cold junction temperature is displayed for reference purposes. The user can start and stop the temperature measurement process by toggling the On/Off button at the bottom of the panel.

8.7. Export.

The EXPORT function saves program data in an ASCII format for importing into other programs. After selecting EXPORT, a text box appears where a 255 character line description of the data may be entered. Pressing "OK" with the mouse, removes the text box. It is followed by SAVE FILE directory box where the file name is entered. Choosing the SAVE button completes the Export operation. The format used for DL(P) export files is shown in Figure 29. The NICOLET440/DYNATUP DATA FILE header appears first. The specimen description entered by the user appears beneath the header. The file creation date and time appear next. The configuration file directory path, name, date, and time are listed next for tracking purposes. Calibration factors for each channel, numbers of samples and the sample rate are listed before the channel data is presented sequentially in a comma separated format.

8.8. Quit.

Selection of the QUIT button on the general menu bar causes the program to terminate. A decision panel allows the user to save the current program configuration or exit directly from the program. It is recommended that all setup table. scope and plot windows be closed before the user selects the QUIT button to ensure the program terminates properly.

9. GUIDELINES FOR EVALUATING SPECIMENS

The drop tower has been modified to allow two different test methods of evaluation to be employed. In the first setup, the specimen rests on the fixed anvils and it is fractured by contact with the falling cross head. The second setup uses a fixture to preload the specimen against the tup. In this case the specimen and tup fall as an assembly and the specimen fractures when it contacts the fixed anvils. Additional details are presented in [2].

Flowcharts to conduct tests at Ambient and Cold Temperatures are presented in Figures 30 to 32. Cold tests may be performed insitu or using external specimen cooling. Each flowchart has been divided into three categories: Test Setup, Conduct Test and Review Test Results. An estimated time for each activity is shown at the right of the flowchart.

External cooling of the specimen illustrated in Figure 32 will be used to highlight requirements indicated in the other flowcharts. Conditions that may not require attention during every test are described first. Anvils or other specimen support fixtures require alignment and periodic verification to ensure they provide repeatable results. The vertical position of the LVT core or optical trigger at the left side of the drop tower may require adjustment to suit different specimen sizes. The LVT or optical trigger adjustment procedure is described in Section 6.5 and 6.6 respectively. The hoist's maximum height switch and the brake switch position on the right side of the drop tower should be adjusted as required. The cooling box with the liquid nitrogen dewar should be located conveniently close to the drop tower for rapid transfer from the box to the drop tower. Appropriate clothing, gloves and safety glasses should be worn while cooling the specimen. Other personnel in the lab area should be notified that drop tower experiments will be occurring. It is a good practice to always wear safety glasses and safety shoes while working around the drop tower.

Setting up the oscilloscope using the GUI is illustrated by the flowchart in Figure 33. To begin the program, click on the program icon. Selection of a default or custom configuration file is made next. SCOPE! is selected from the general menu and the power button is turned on with the mouse. Channel, time base, trigger settings should be reviewed and adjusted as required. The scope should now be ready to acquire data. If the default setup is selected, review of the Setup Menu is recommended to ensure operating conditions for the scope are correct. Select the temperature input panel on the screen. The program path for the default setup is illustrated in Figure 34.

A pre-cracked specimen with thermocouples attached is placed in a cold box. Monitor the temperature by setting the On button on the GUI temperature panel and undercool the specimen 15-25°C below the test temperature. The specimen should stay at this temperature for 30 minutes for each 25 mm of specimen thickness. Remove the specimen from the cold box using insulated gloves or tongs. COD and LLD gauges may be added to the specimen upon removal from the cold box. Install the specimen on the anvils or in the preload fixture against the tup. Attach the thermocouple plugs or wires to the thermocouple junction box. Ensure that cables will not be damaged by the falling crosshead. Remove the safety pin from the right front post of the drop tower. The safety light on the drop tower control panel should extinguish and the Caution light should illuminate. Install the safety enclosure door(s) at the front and rear of the drop tower. Raise the specimen to the required height using the hoist switch on the drop tower control panel.

Select the HOLD NEXT button on the scope panel of the GUI. When the specimen temperature approaches the test temperature, raise the cover on the ARM switch and turn it on. The audio buzzer sounds and the danger light will illuminate. Verify that it is safe to release the crosshead. Press the drop button when the test temperature is reached.

After the test is completed, lower the hoist to engage the lifting hook in the pickup roller. When the hook is properly seated the pneumatic brakes will be released. It may be necessary to raise the hoist support fixture relative to the top of the crosshead with a bar to fully seat the hook in the roller. When the hook is fully seated the pneumatic brakes will release if they were applied. Remove the safety enclosure door and retrieve the specimen. After specimen removal the crosshead should be lowered onto the rubber rebound pads or other support fixture while preparing the drop tower for the next specimen or at the conclusion of testing.

Review the acquired data by selecting the DATA menu and Y versus T option. Save the data in files for later analysis or exporting to different programs. Plotting of the data at a later date may not require use of the oscilloscope. The program path to plot existing data files is illustrated in Figure 35.

10. REFERENCES.

[1] Ireland,D.R., "Procedures and Problems Associated with Reliable Control of the Instrumented Impact Test", Instrumented Impact Testing, ASTM 563, American Society of Testing and Materials, 1974, pp. 3-29.

[2] KarisAllen, K.J., Morrison, J., "Mechanical Reduction of Inertially Generated Effects in Single-Edge Notched Bend (SENB) Specimens Subjected to Impact Loading", Rapid Load Fracture Testing, ASTM 1130, Ravinder Chona and William R. Corwin, Eds., American Society of Testing and Materials, 1991, pp. 76-91.

[3] Joyce, J., Private Communication, September 1996.

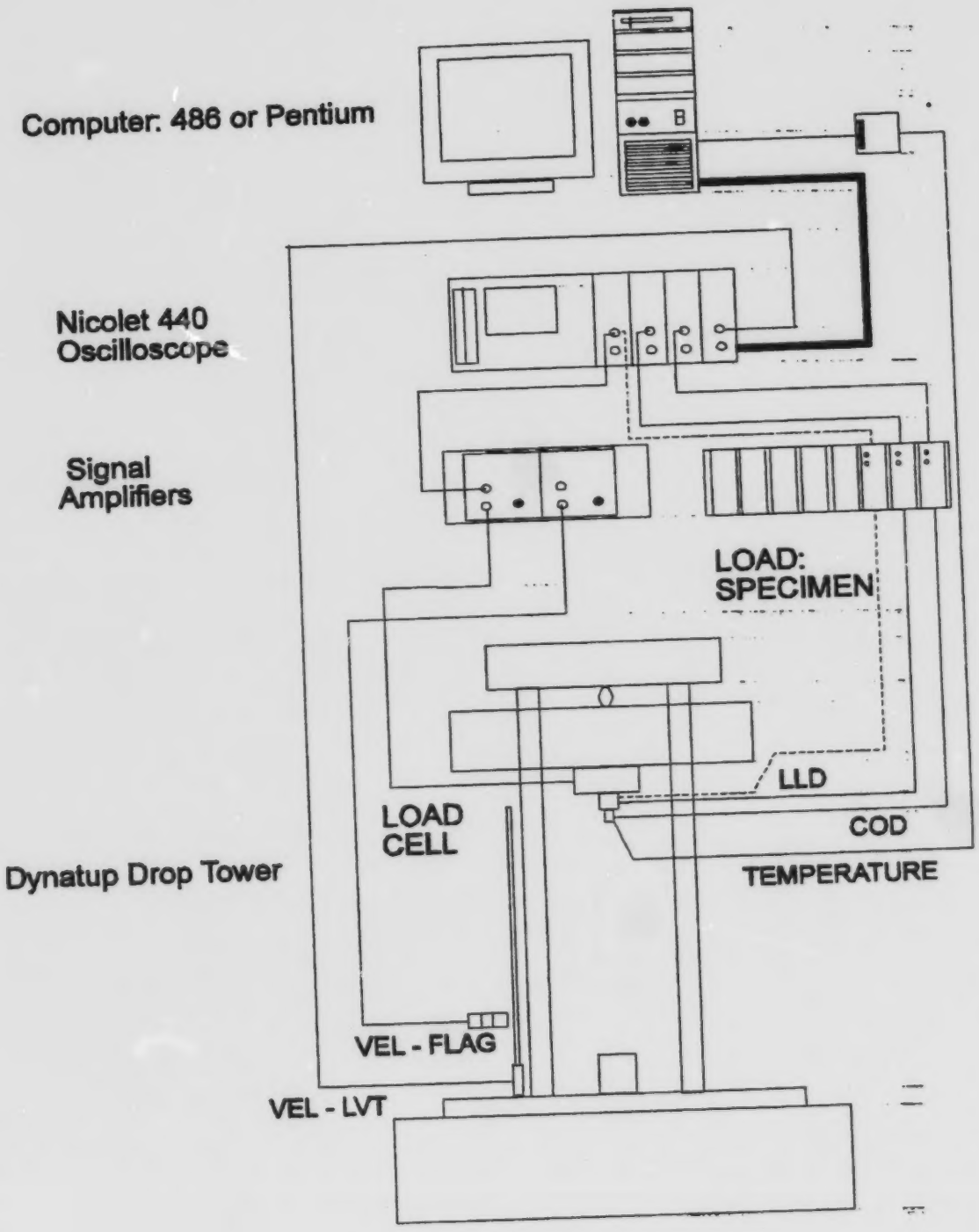

Figure 1.
Drop Tower and Data Acquisition System.

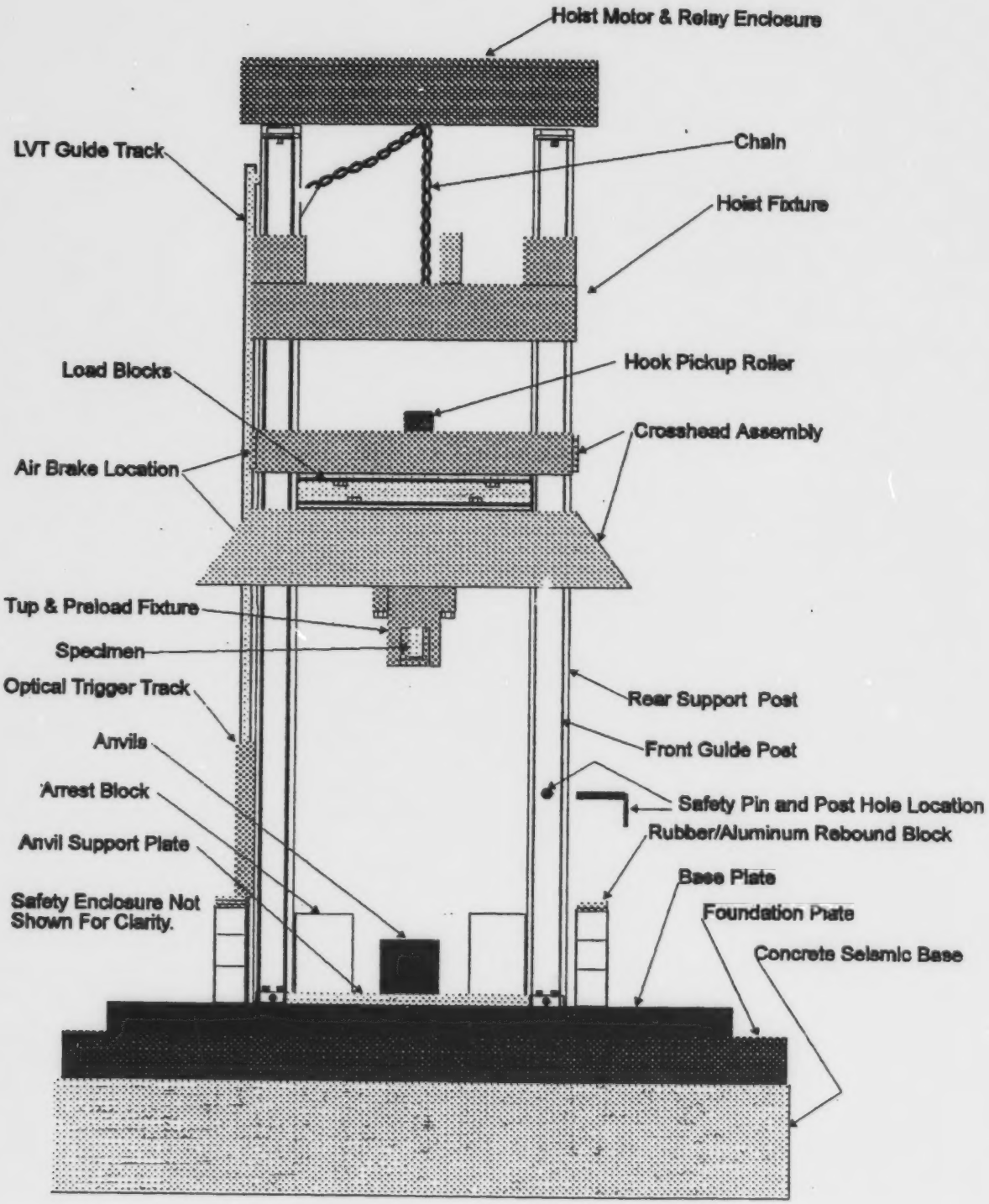

Figure 2.
Drop Tower Component Location.

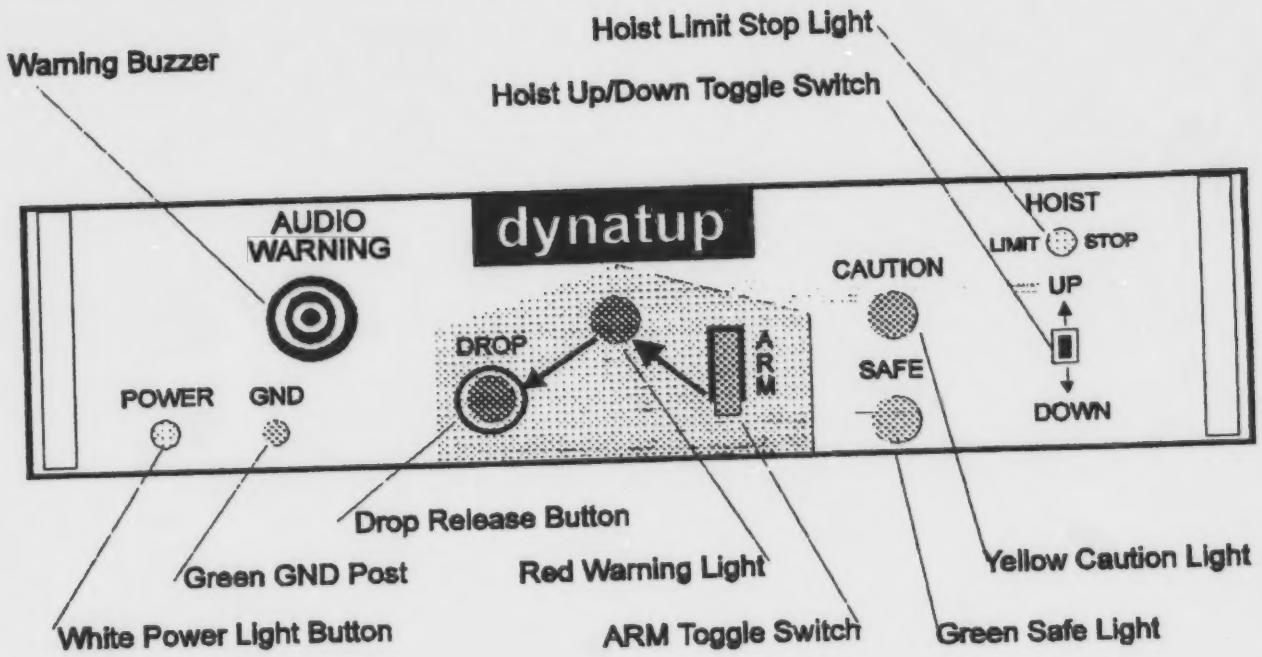

Figure 3.
Drop Tower Control Panel.

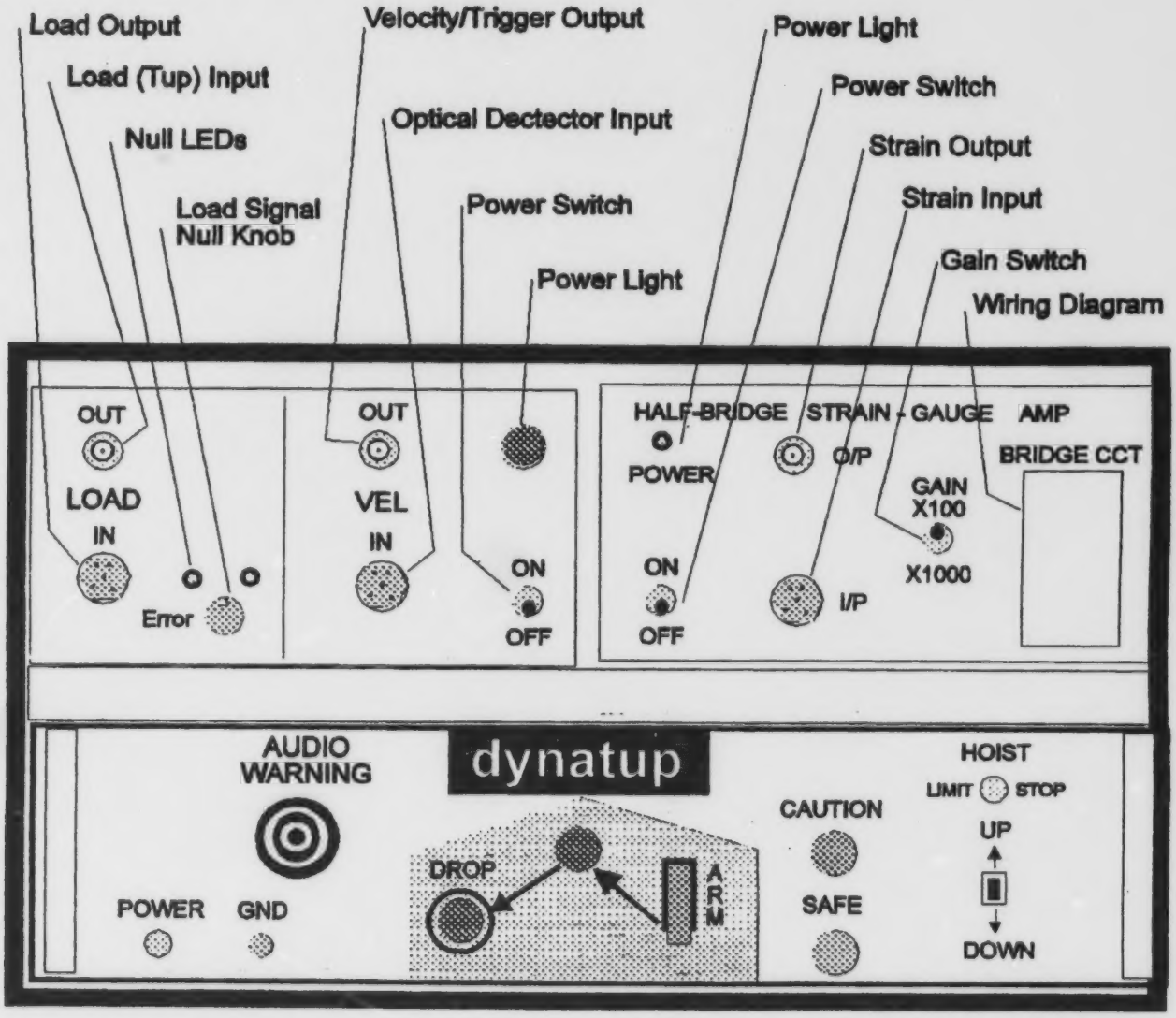

Figure 4.
Amplifier Front Panel Description.

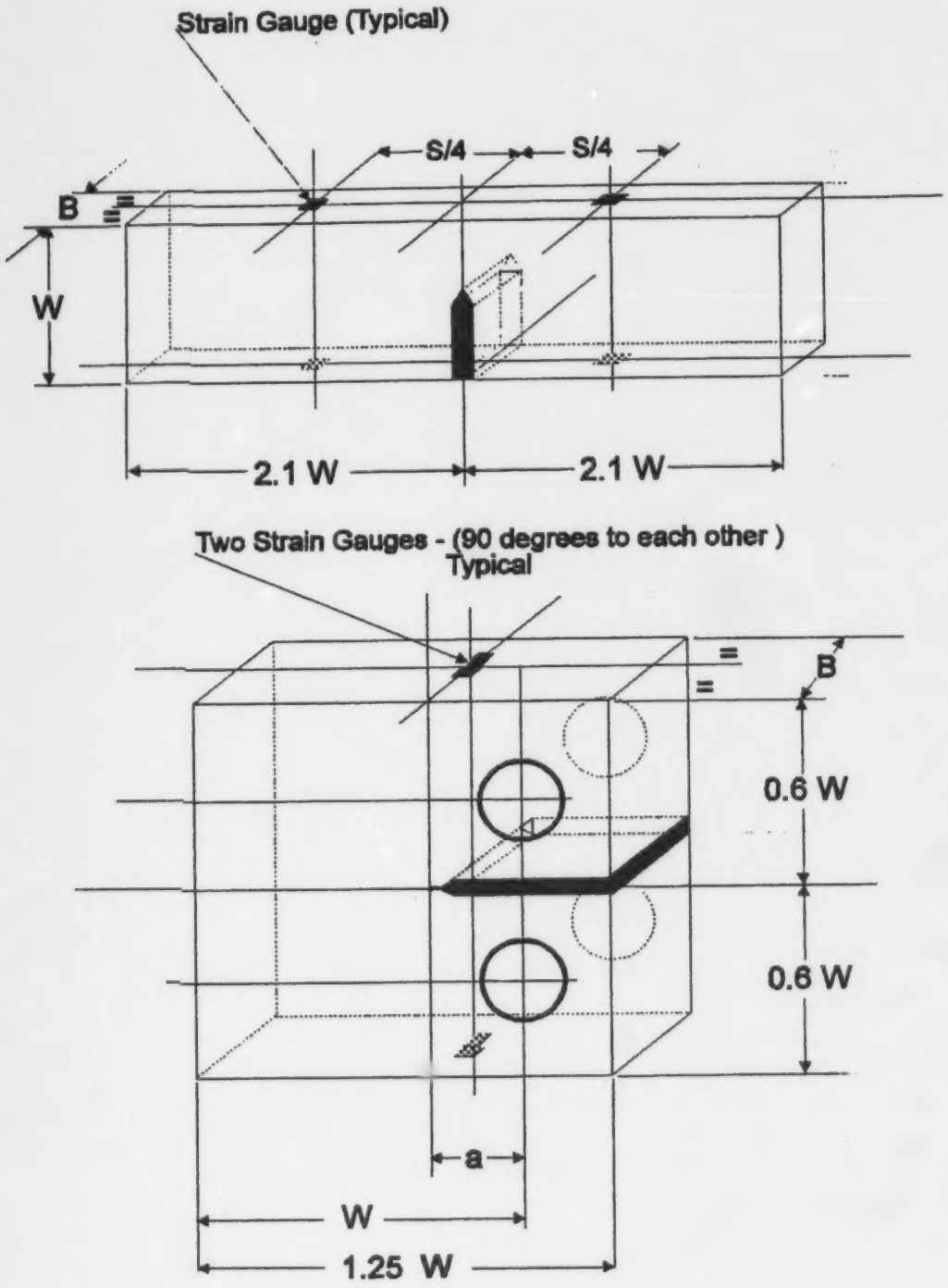

Figure 5.
Strain Gauge Location for SEB and CT Specimens.

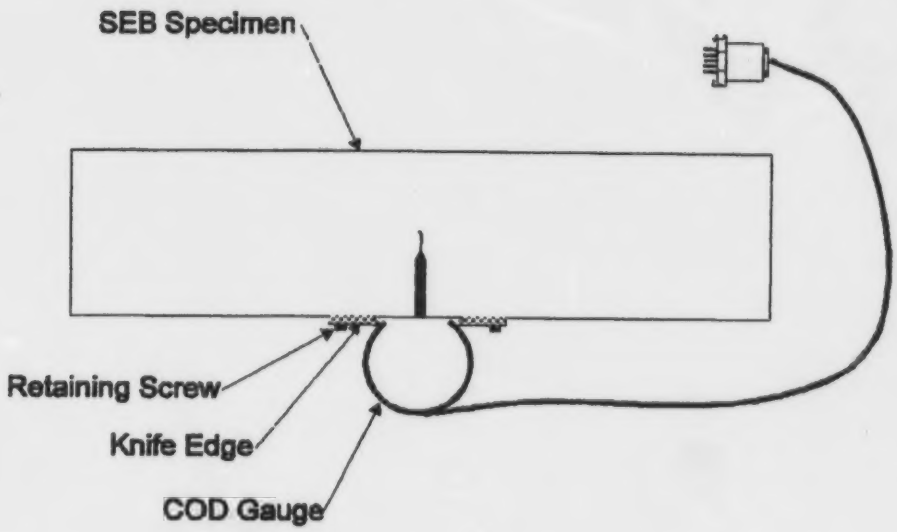

Figure 6.
Omega Shaped COD Gauge.

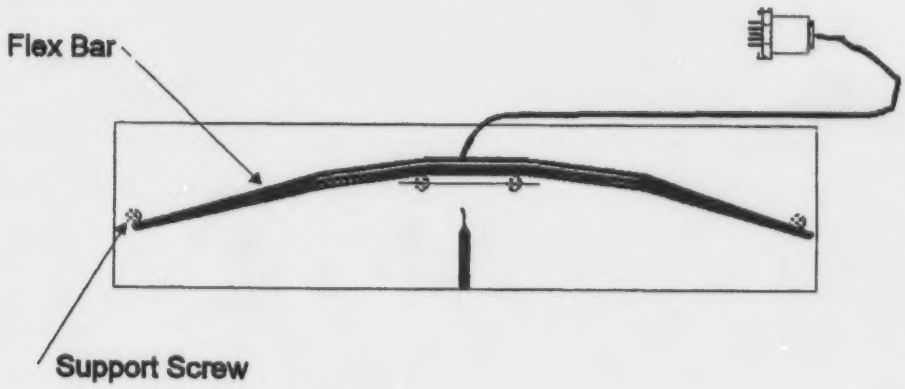

Figure 7.
Flex Bar LLD Gauge.

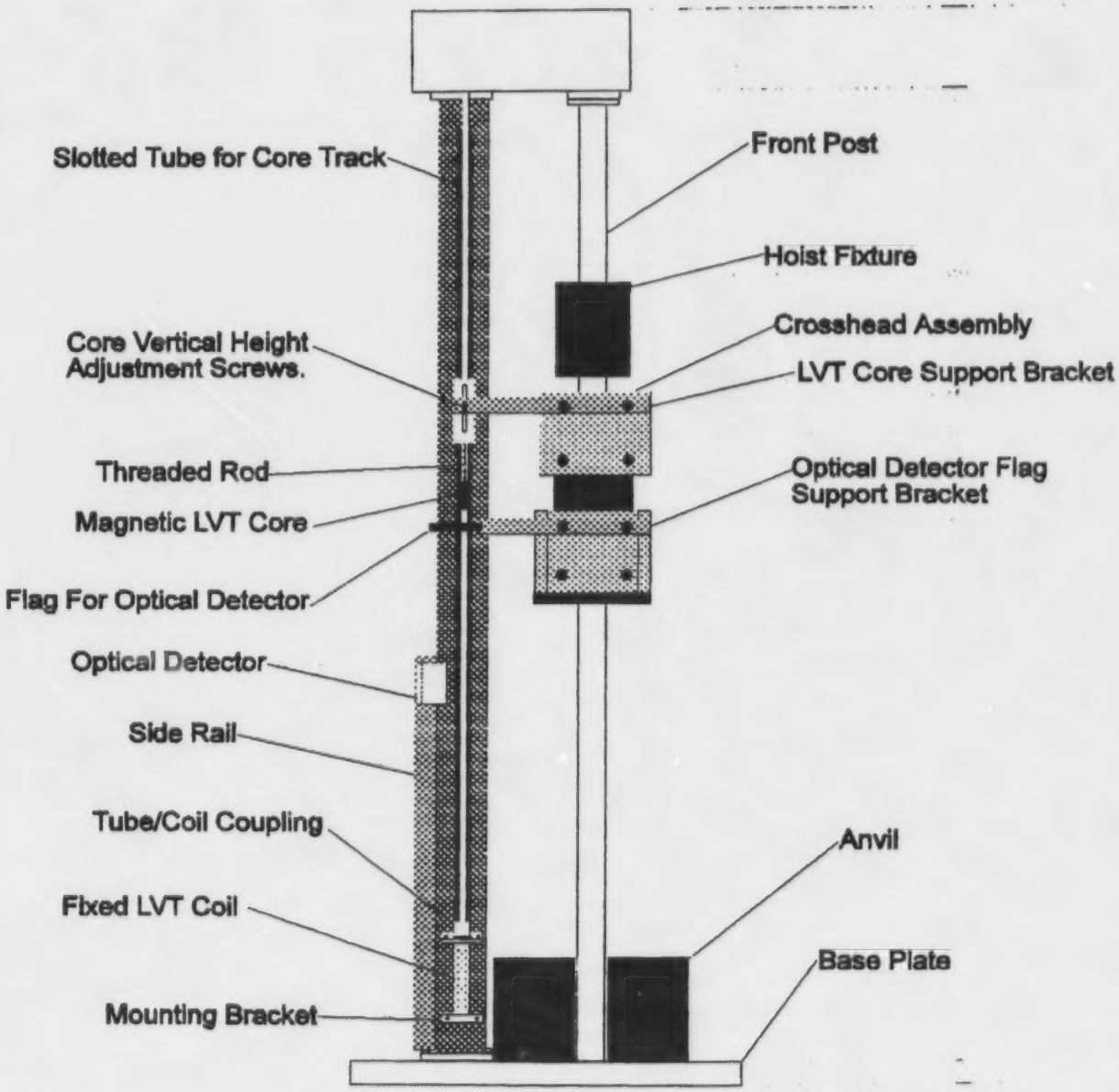

Figure 8.
Side View Of The Drop Tower
Showing The LVT And Optical Detector
Component Locations.

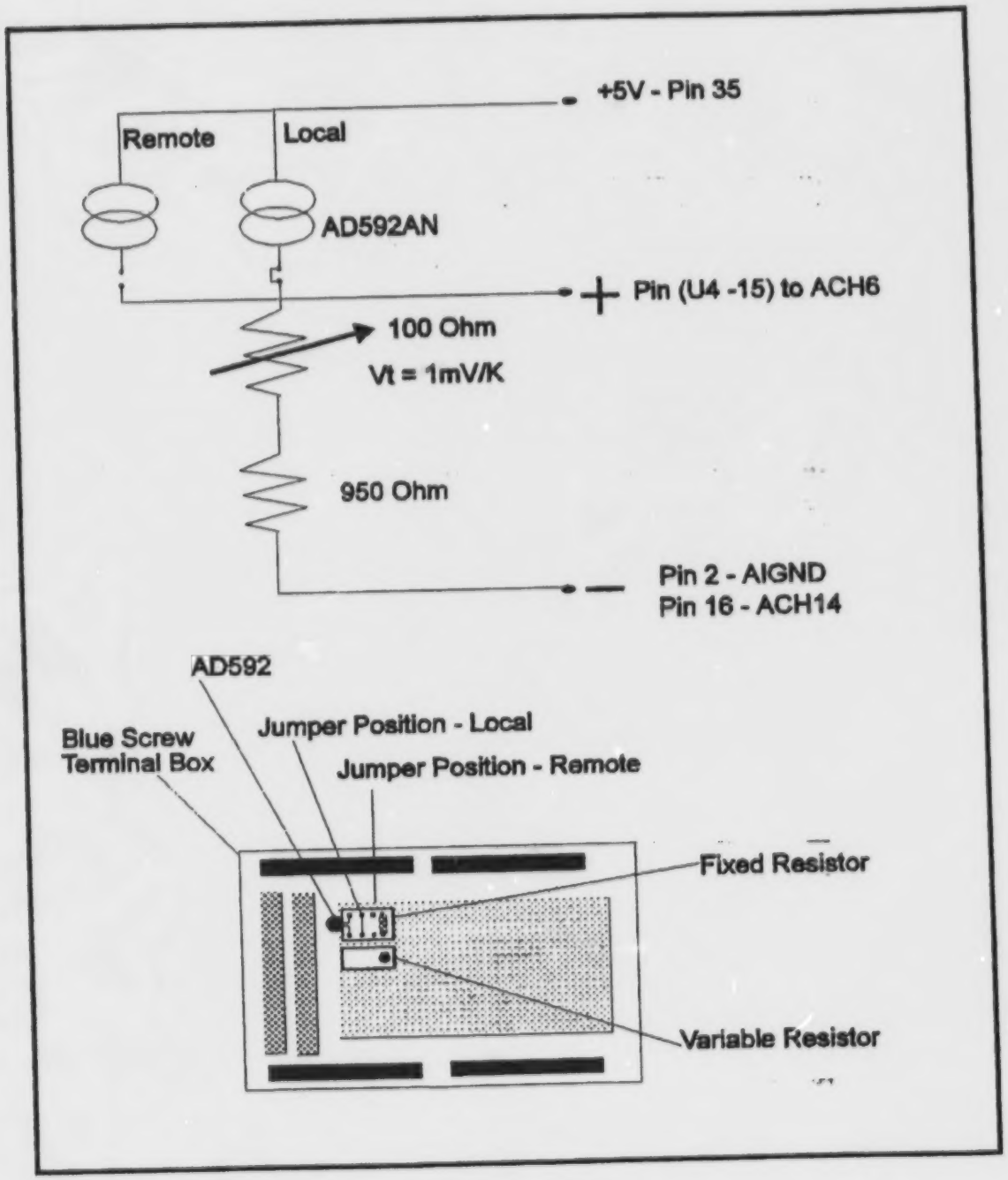

Figure 9.
Cold Junction Sensor Circuit And Component Location Diagram.

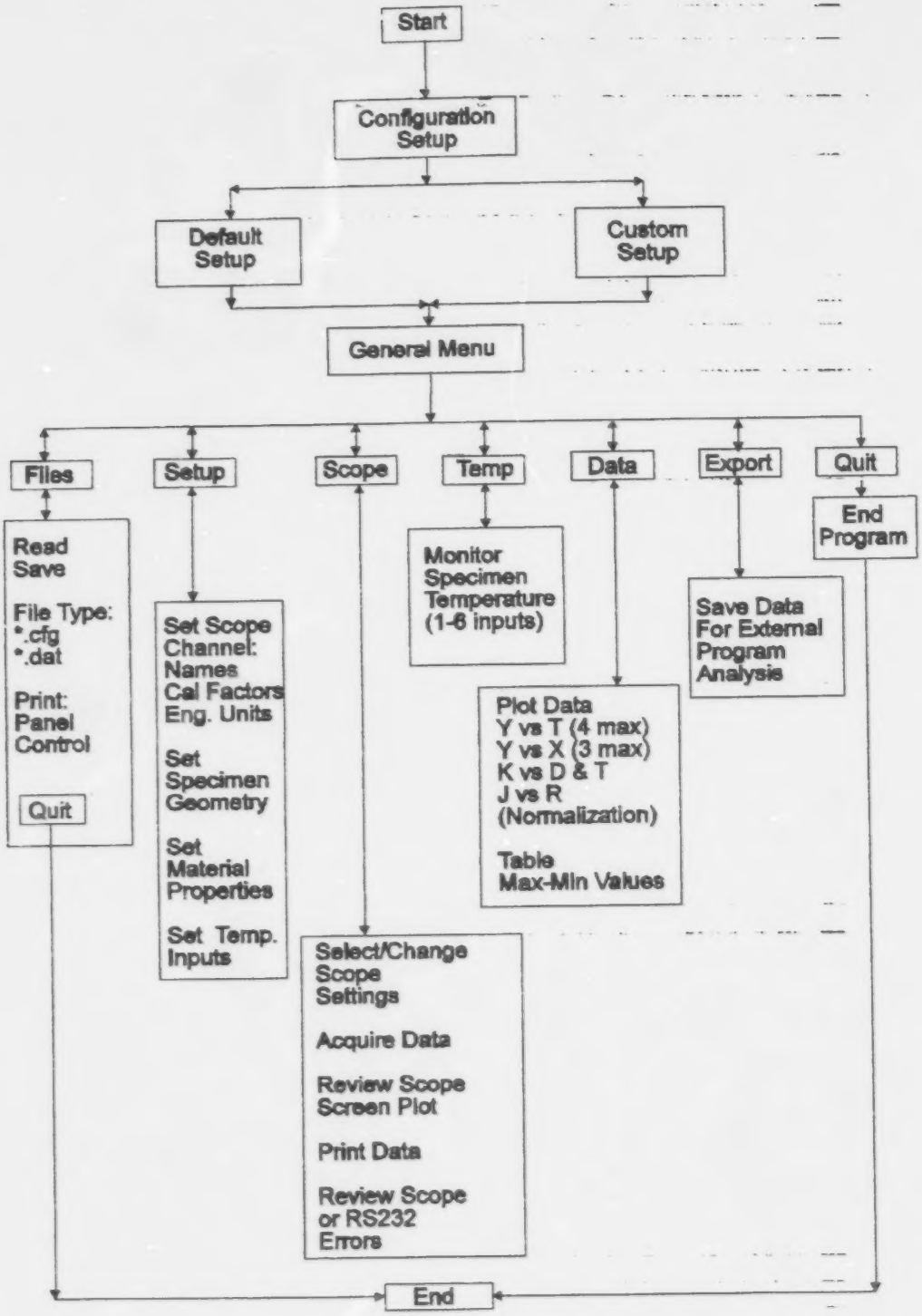

Figure 10.
Software Organization Flowchart.

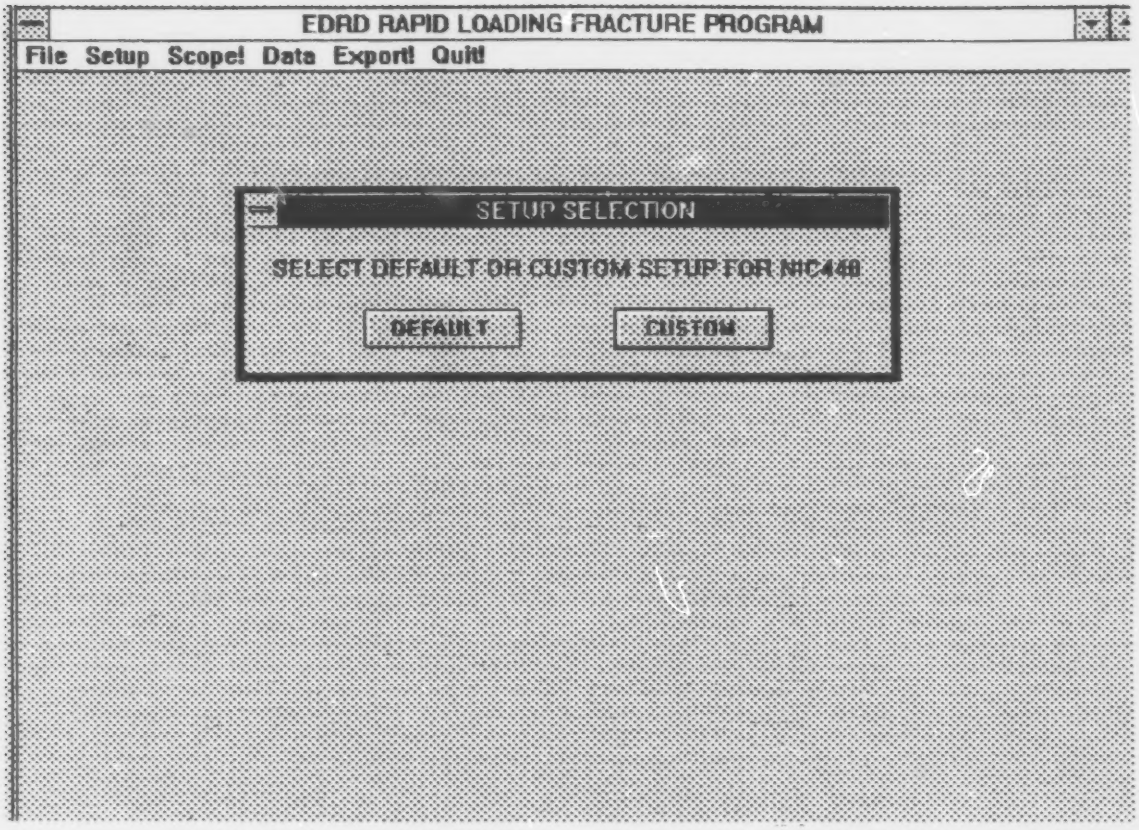

Figure 11.
Software Configuration Decision Panel.

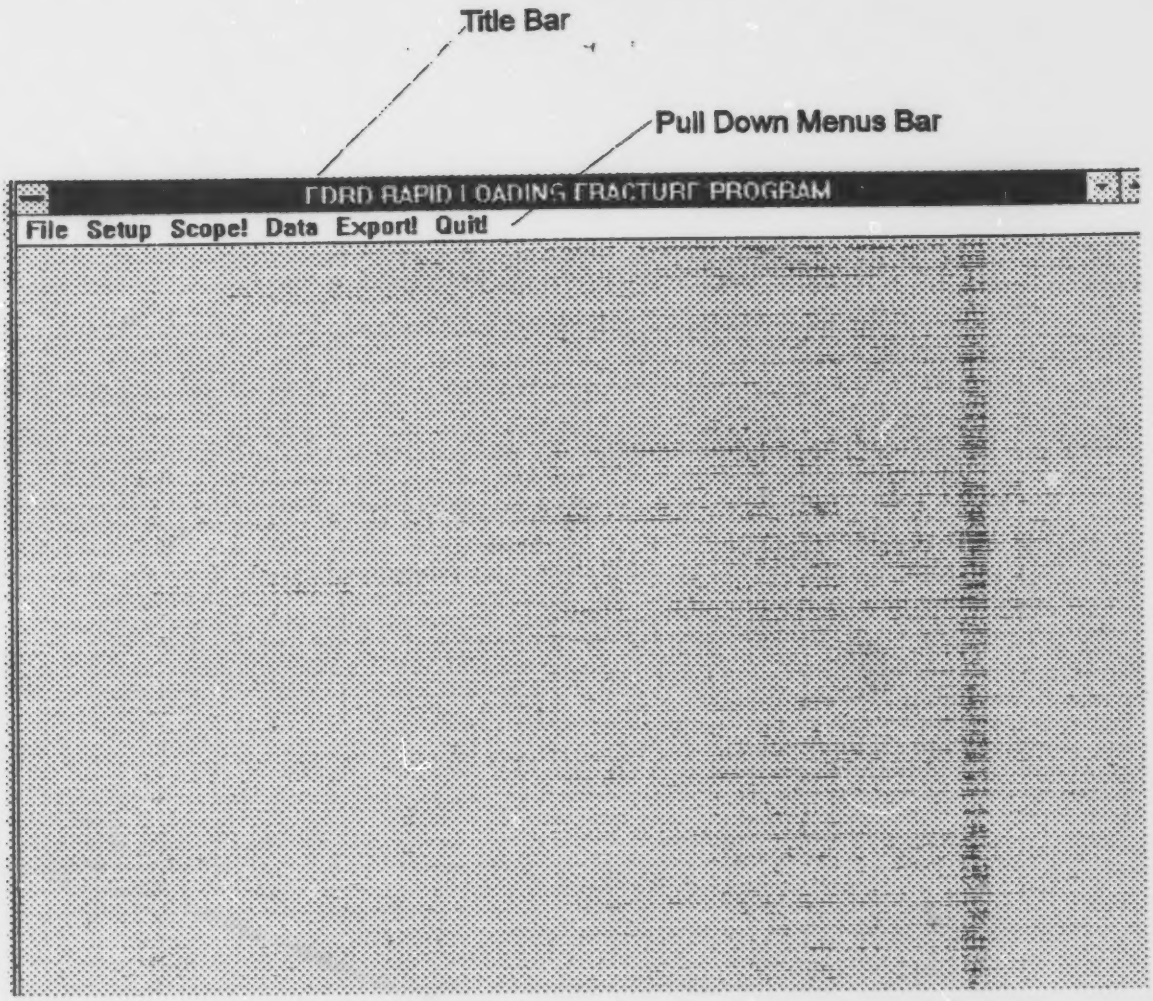

Figure 12.
General Menu.

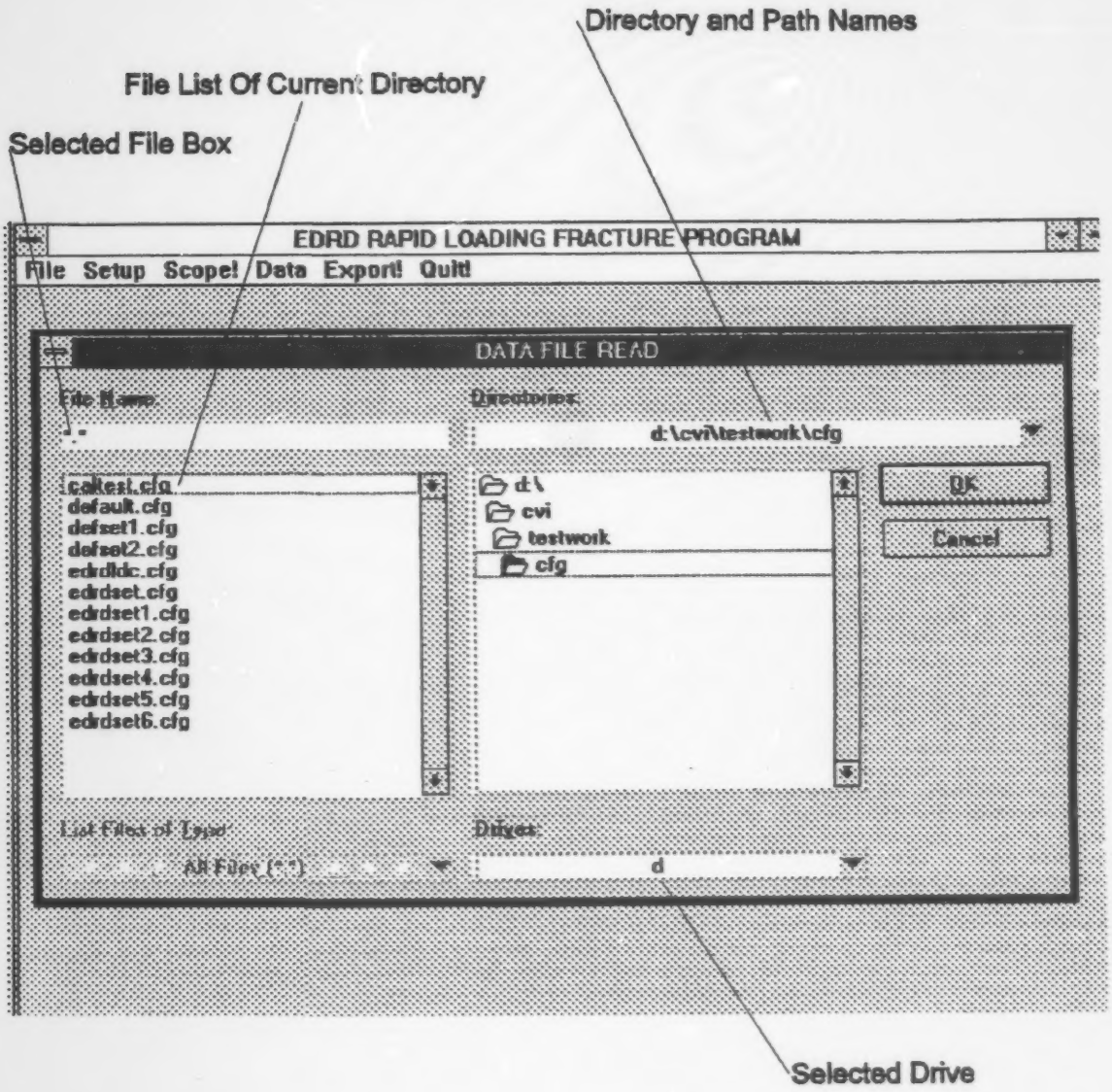

Figure 13.
Typical File Read Panel.

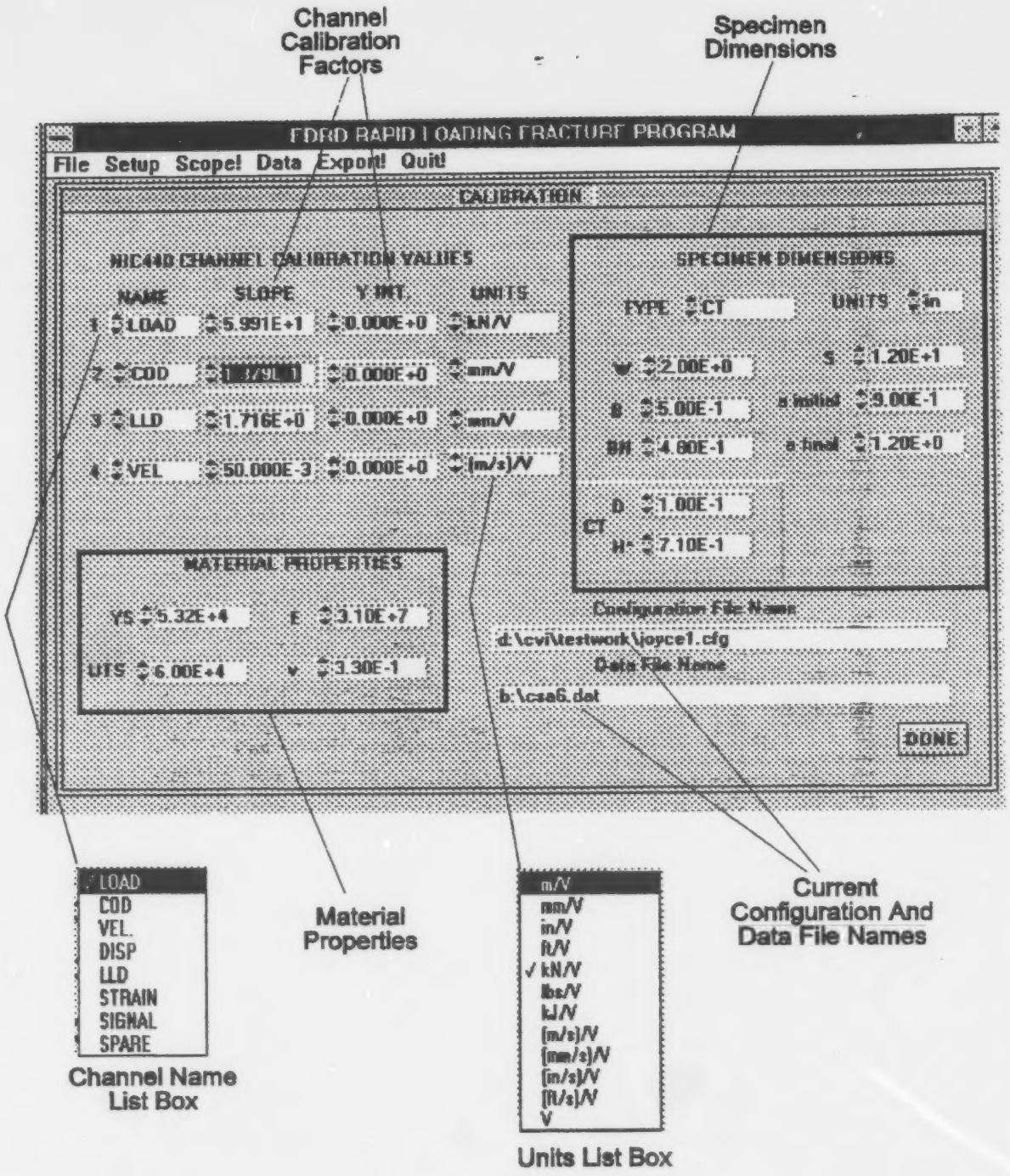

Figure 14.
Setup Panel.

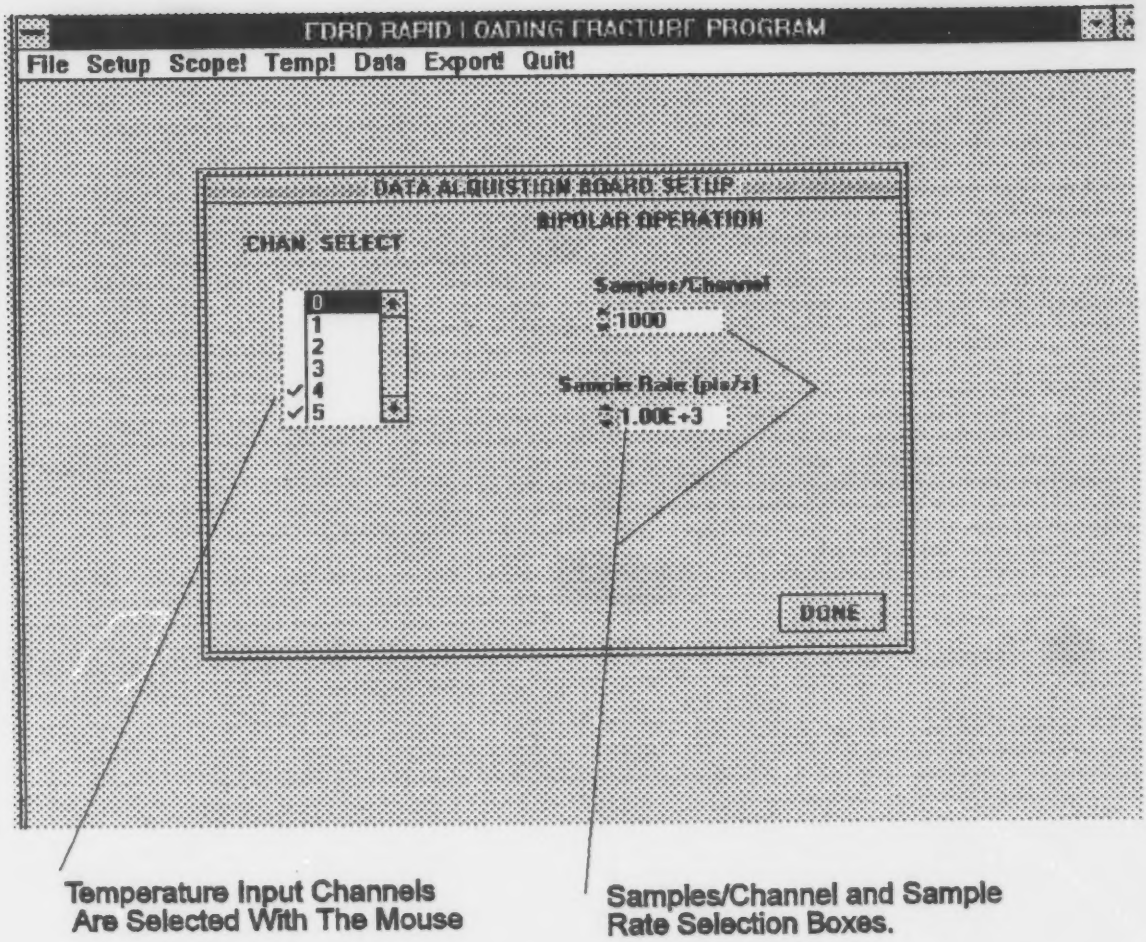

Figure 15.
Temperature Input Setup Panel.

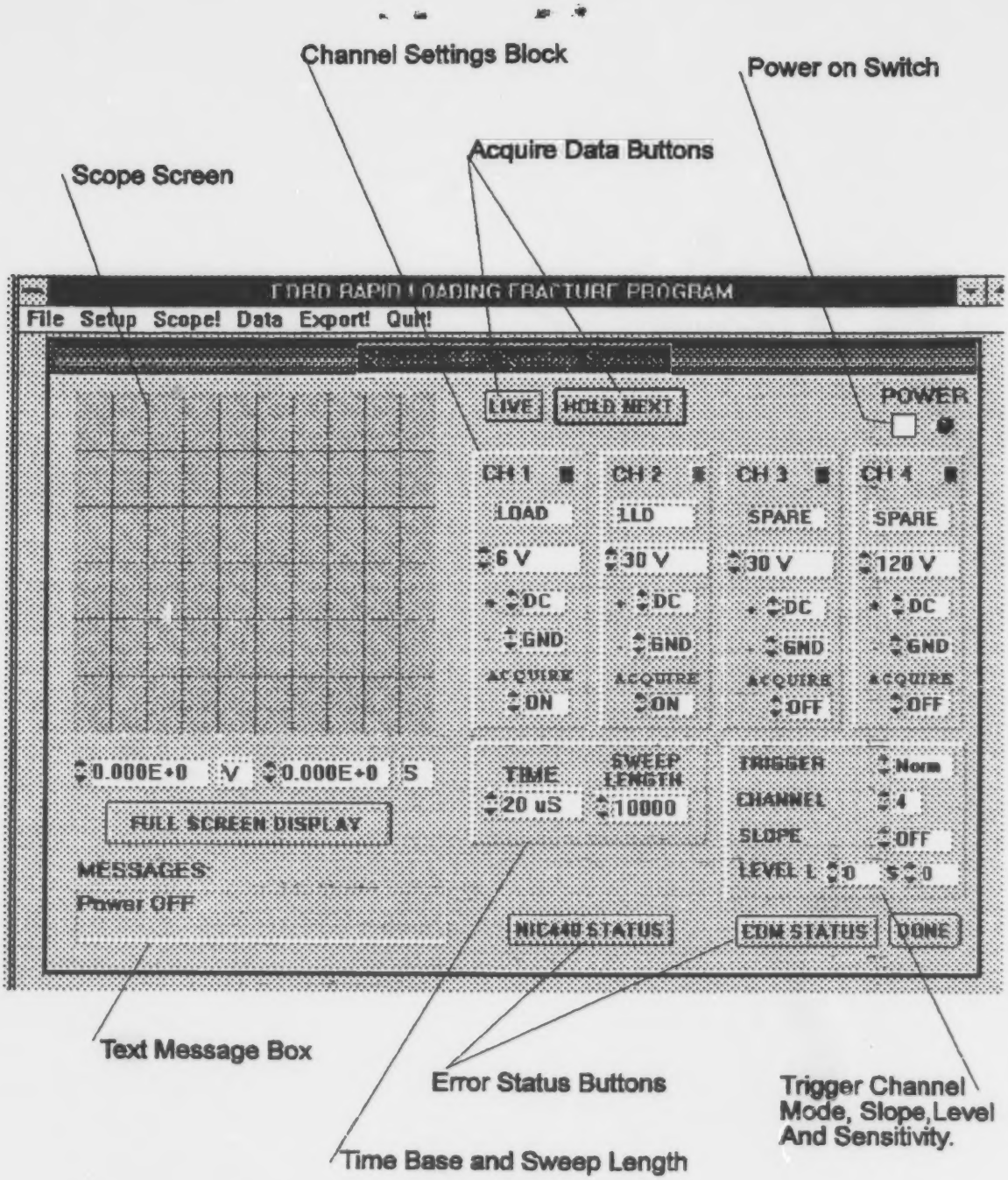

Figure 16.
Scope Panel.

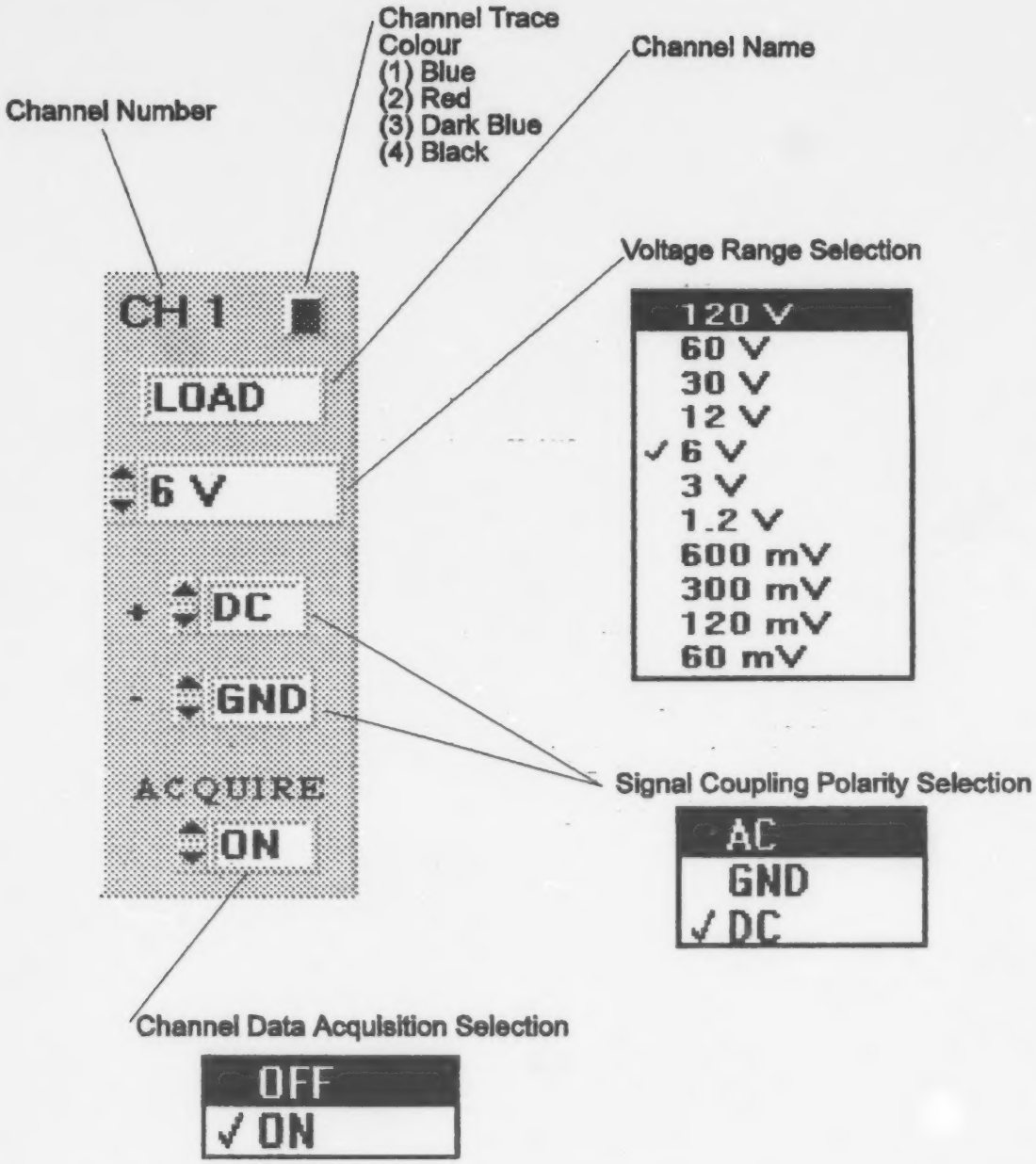

Figure 17.
Typical Scope Channel Settings Block.

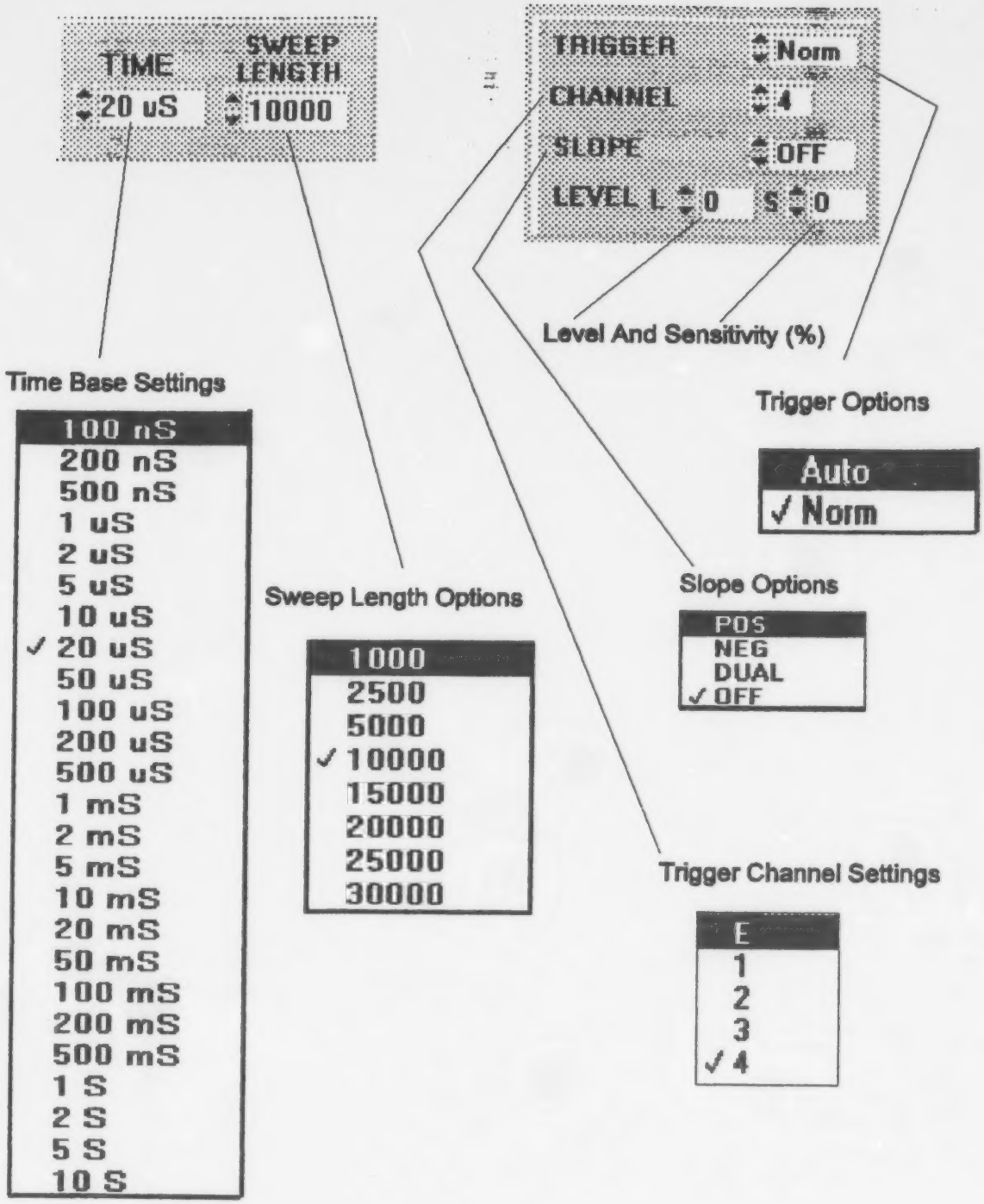

Figure 18.
Scope Time Base and Trigger Options.

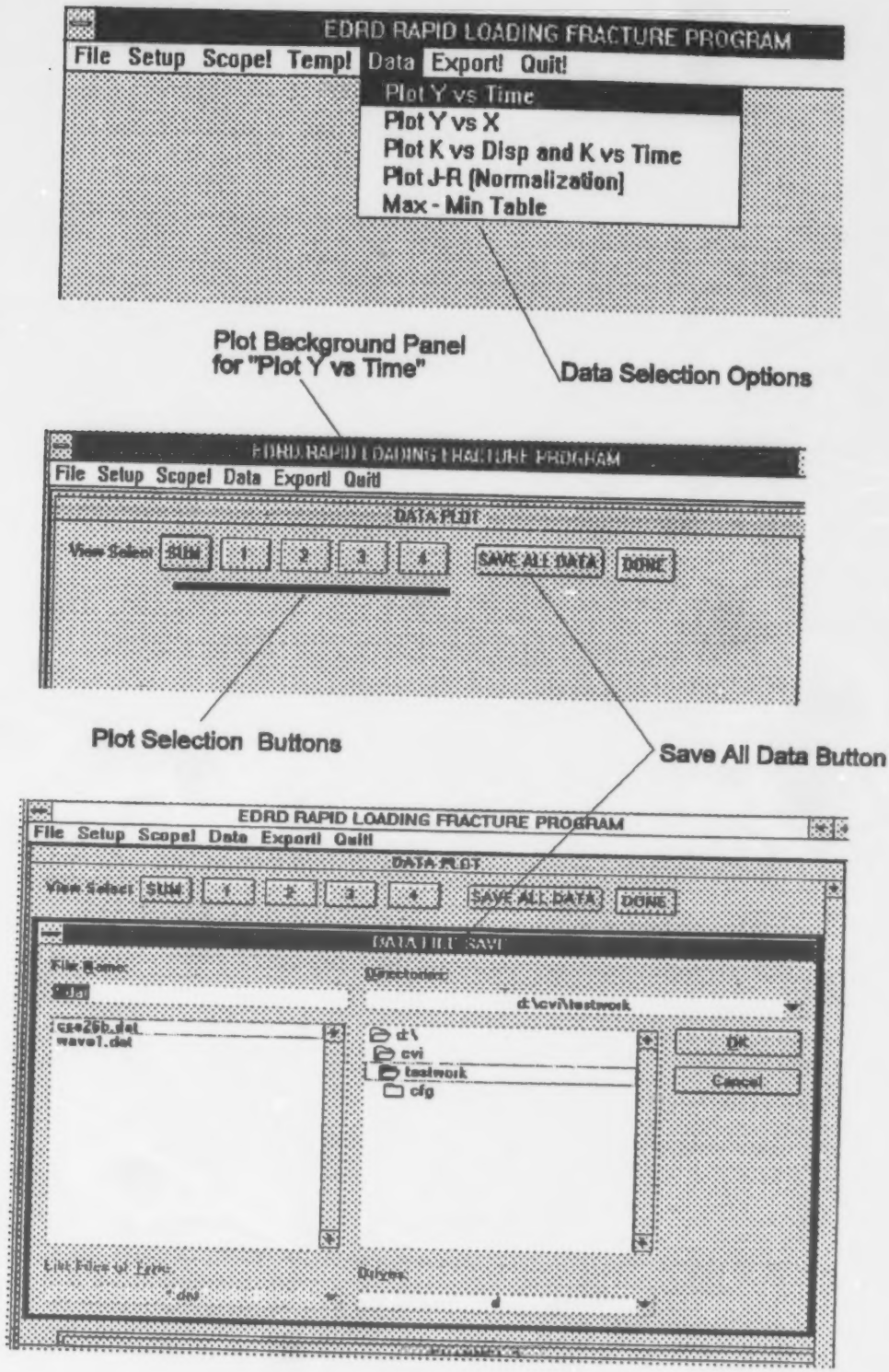

Figure 19.
Data Menu and Plot Background.

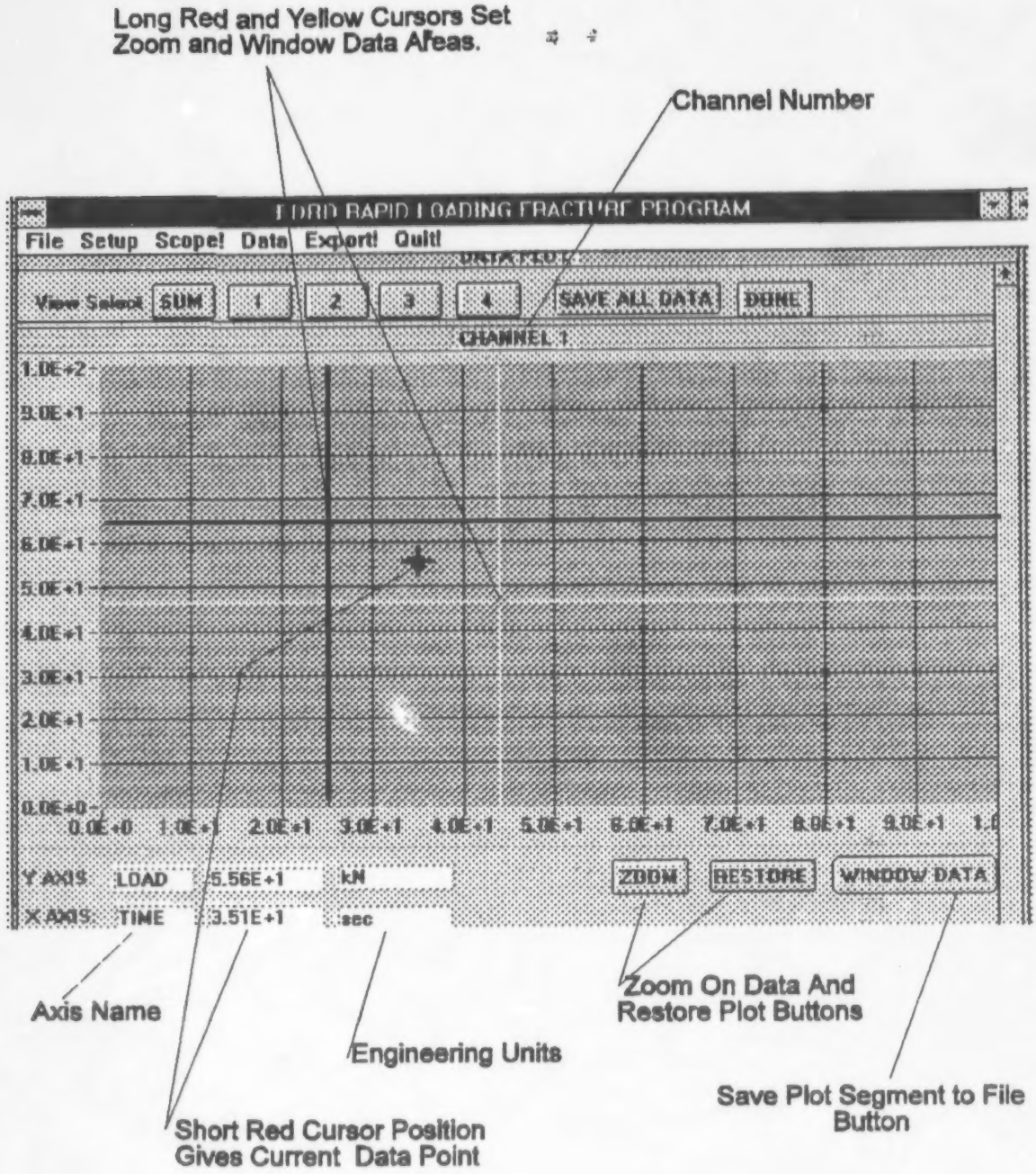

Figure 20.
Channel Plot Illustration.

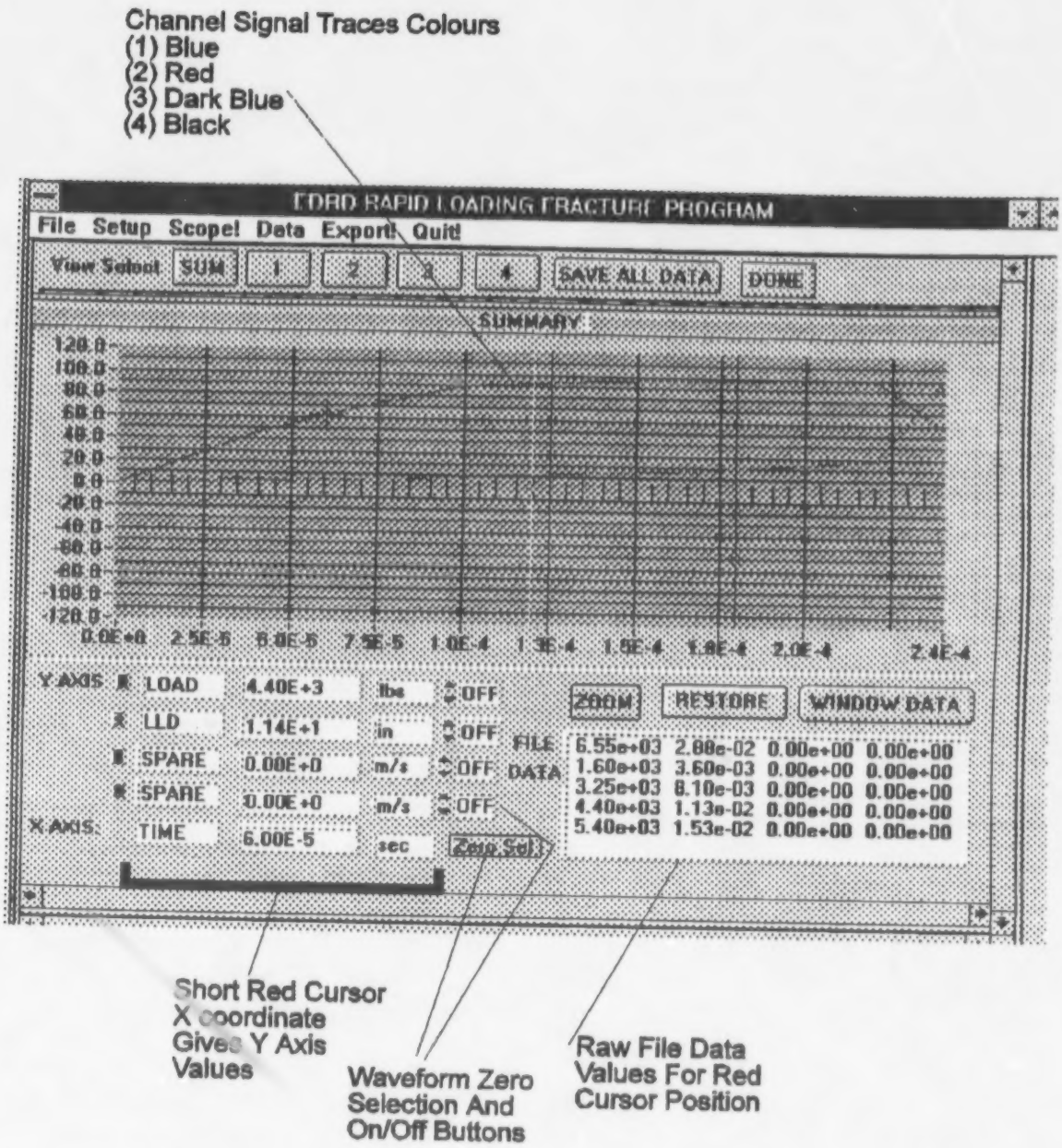

Figure 21.
Summary Plot Features.

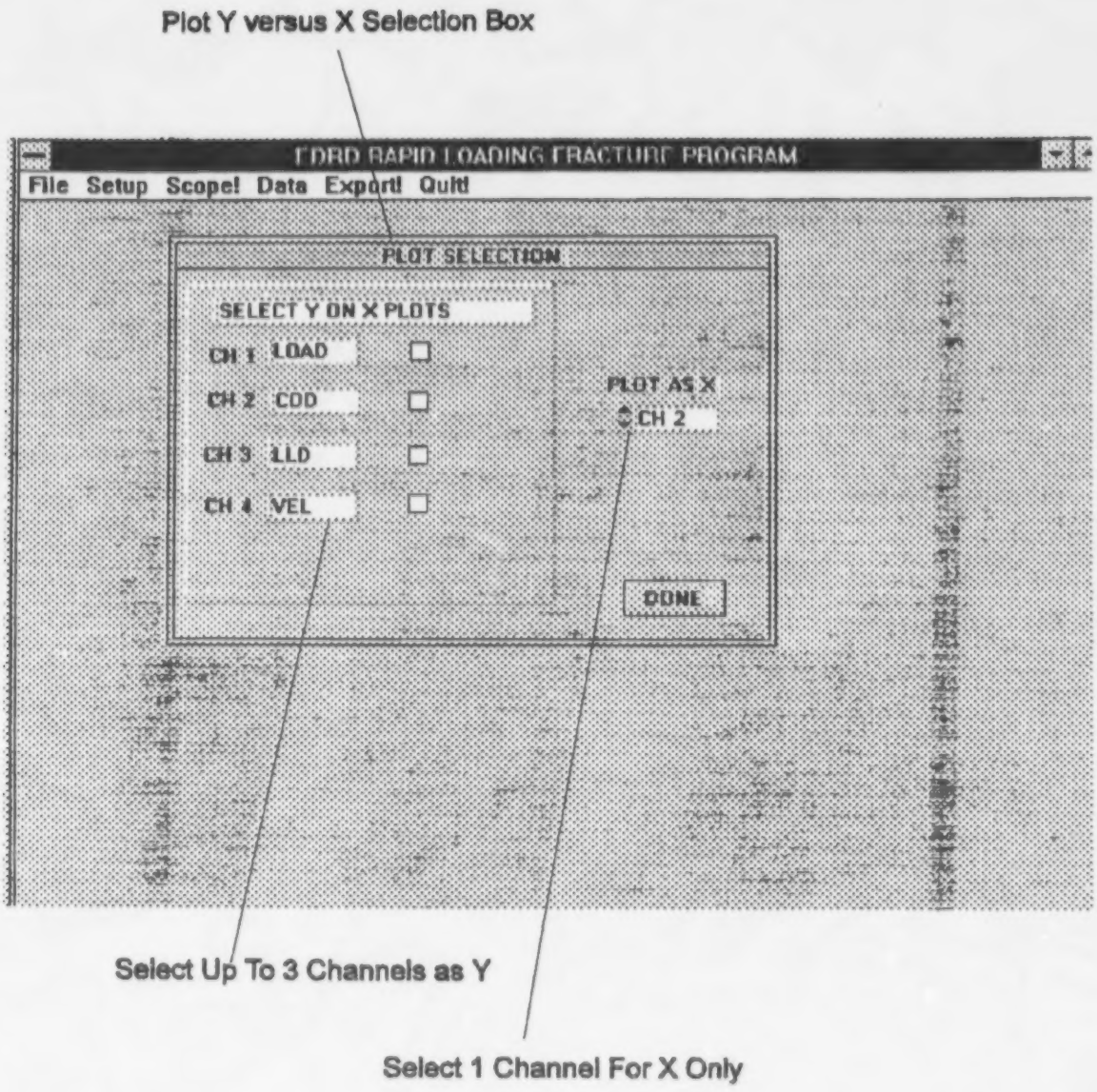

Figure 22.
Typical Plot Y versus X Selection Box.

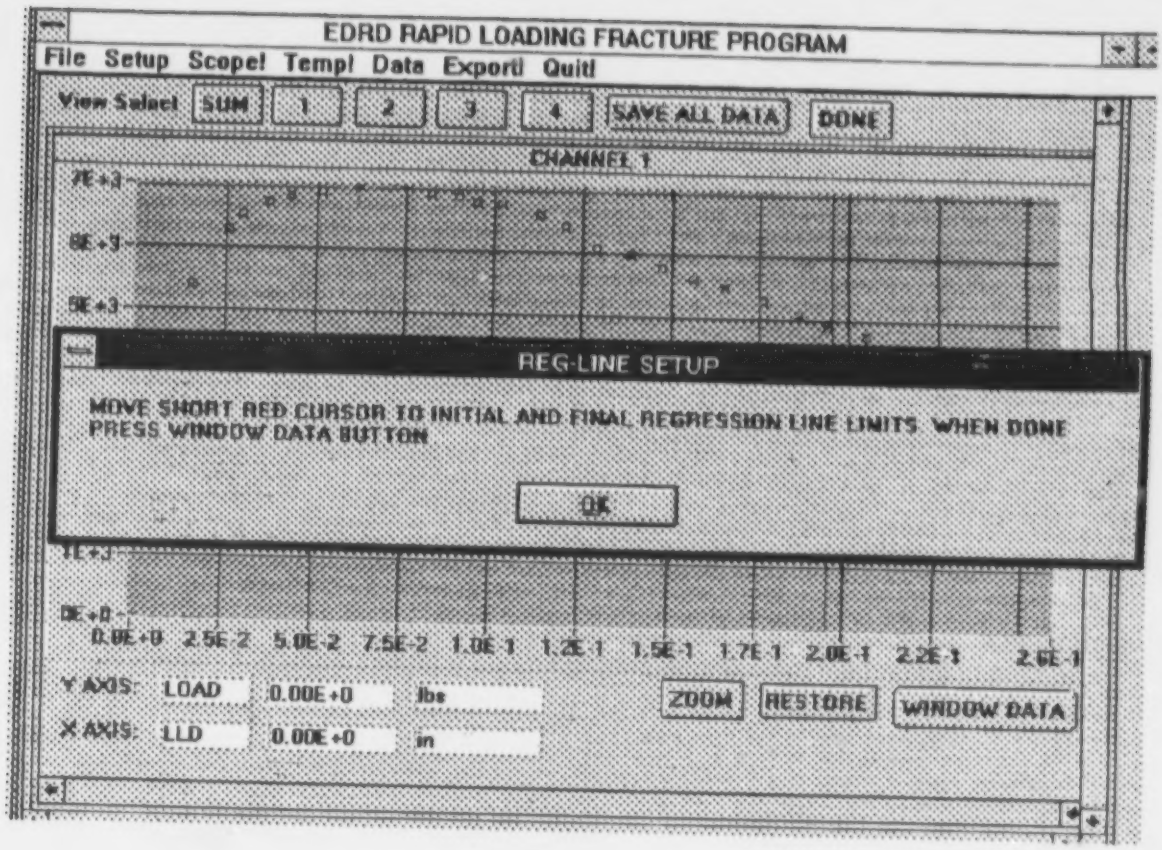

Figure 23.
Regression Line Prompt Panel.

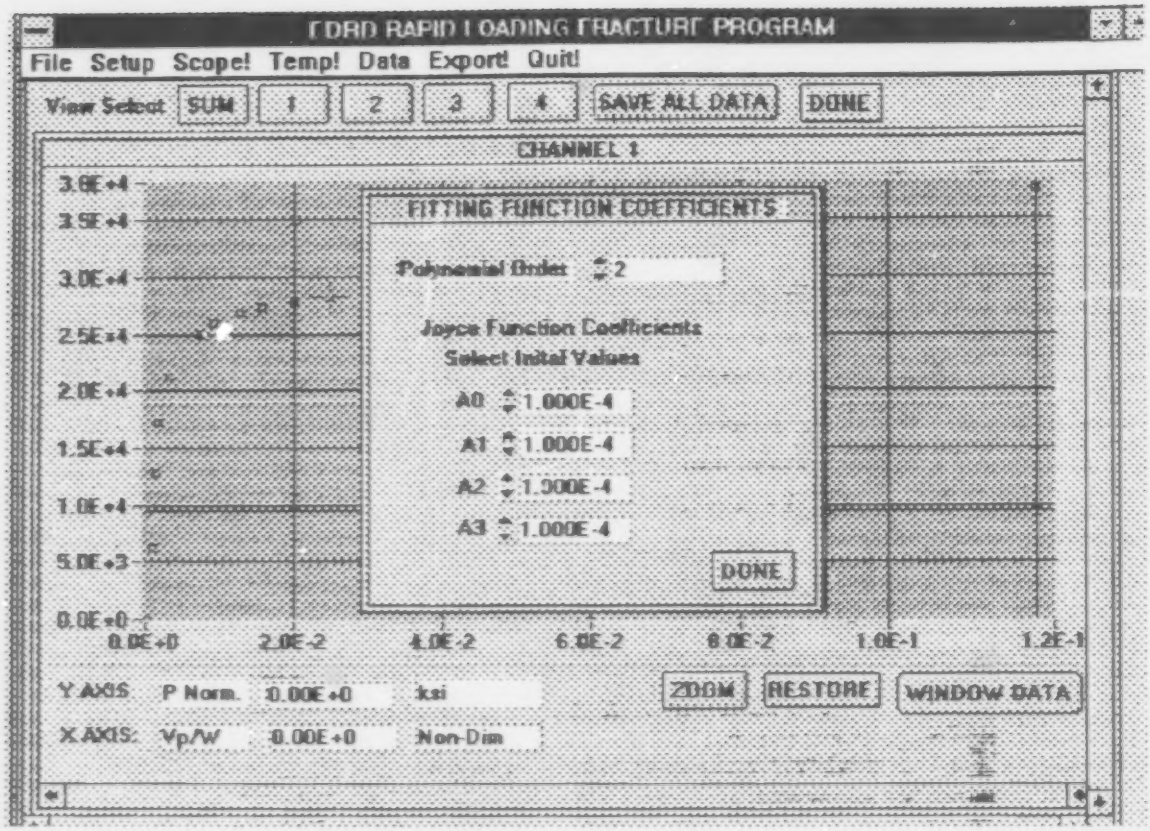

Figure 24.
Polynomial Order and Joyce Function
Coefficient Selection Panel.

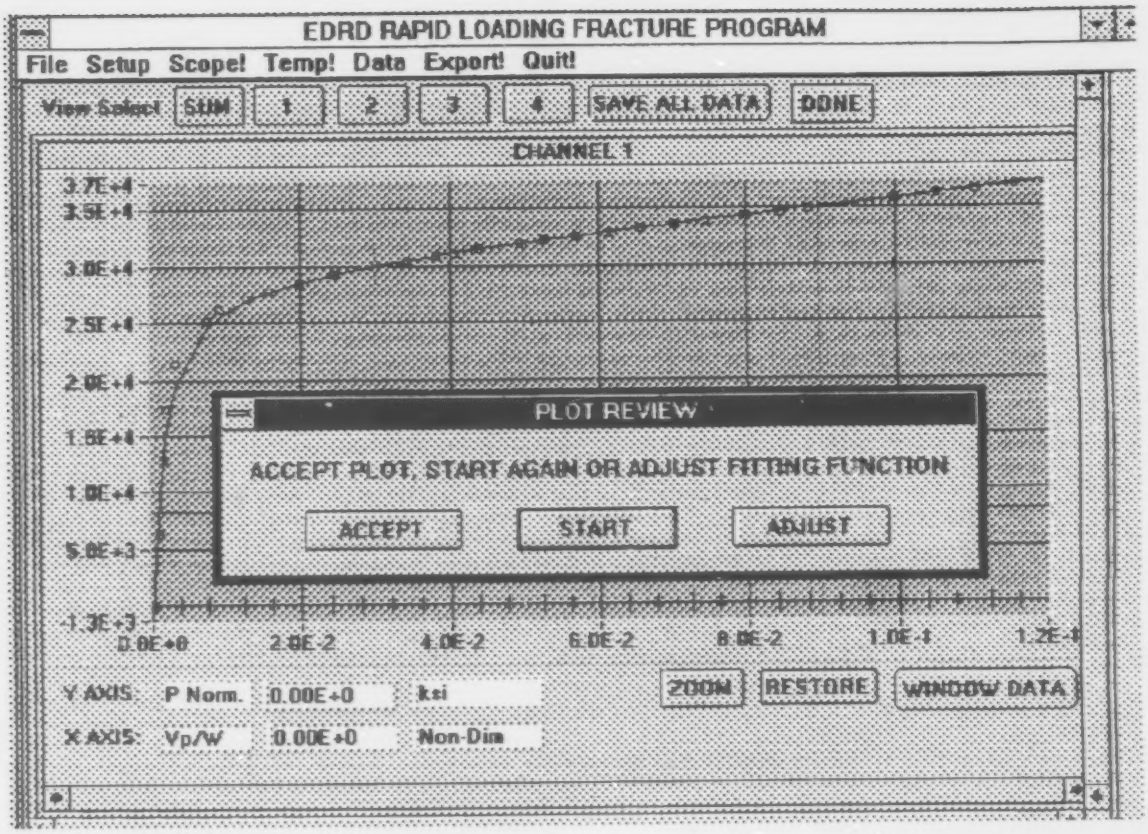

Figure 25.
Typical J-R Normalization Plotting Decision Panel.

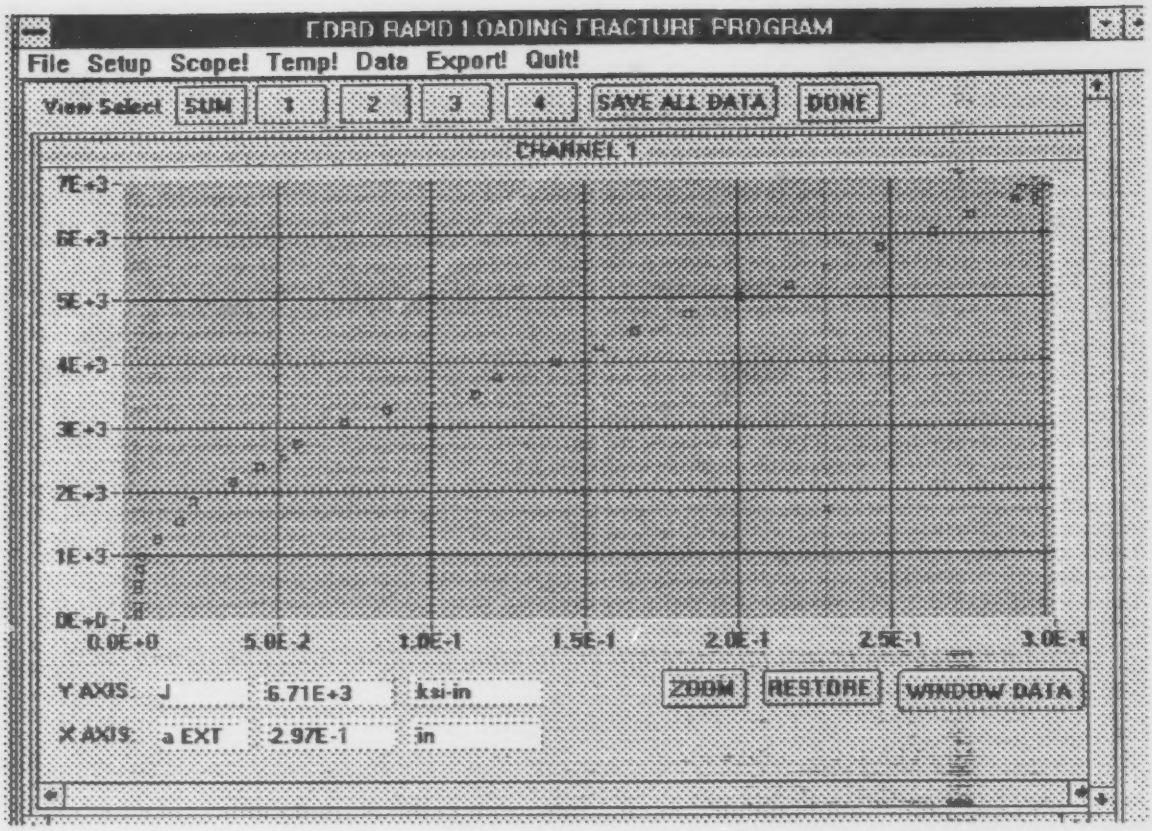

Figure 26.
J-R Data Determined Using The Joyce Function.

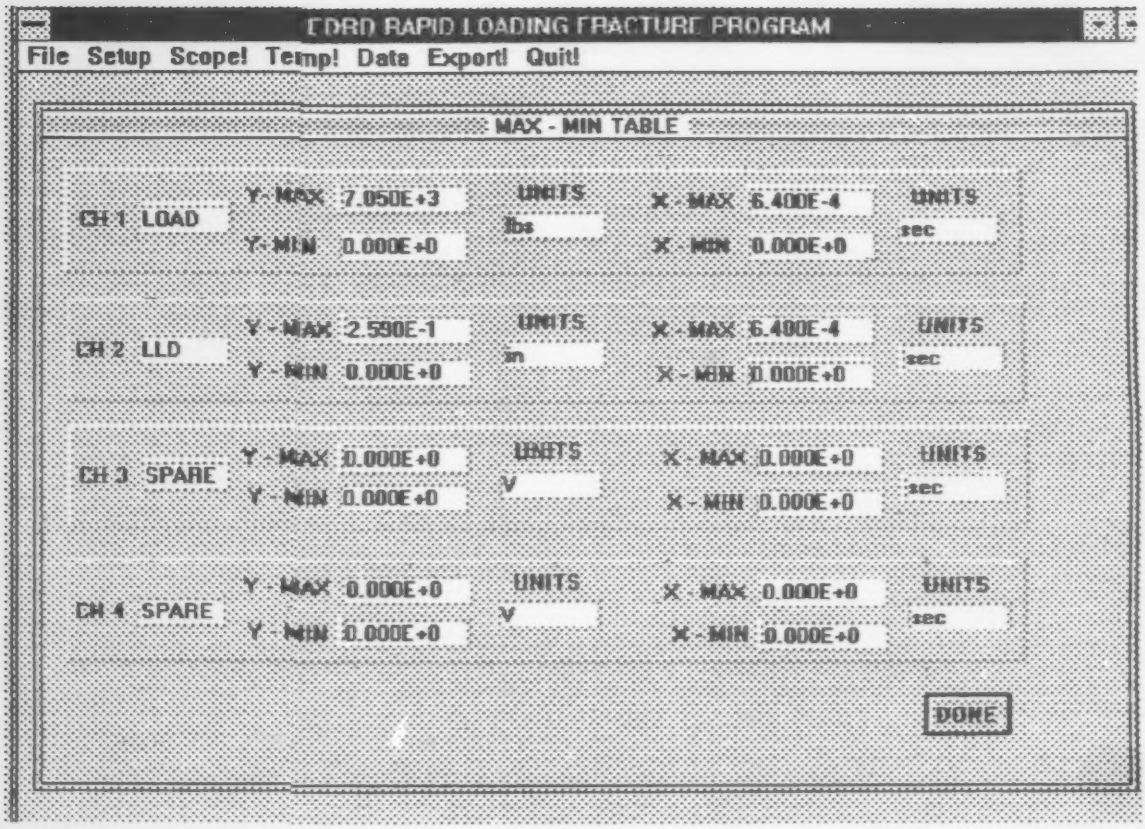

Figure 27.
Max Min Table.

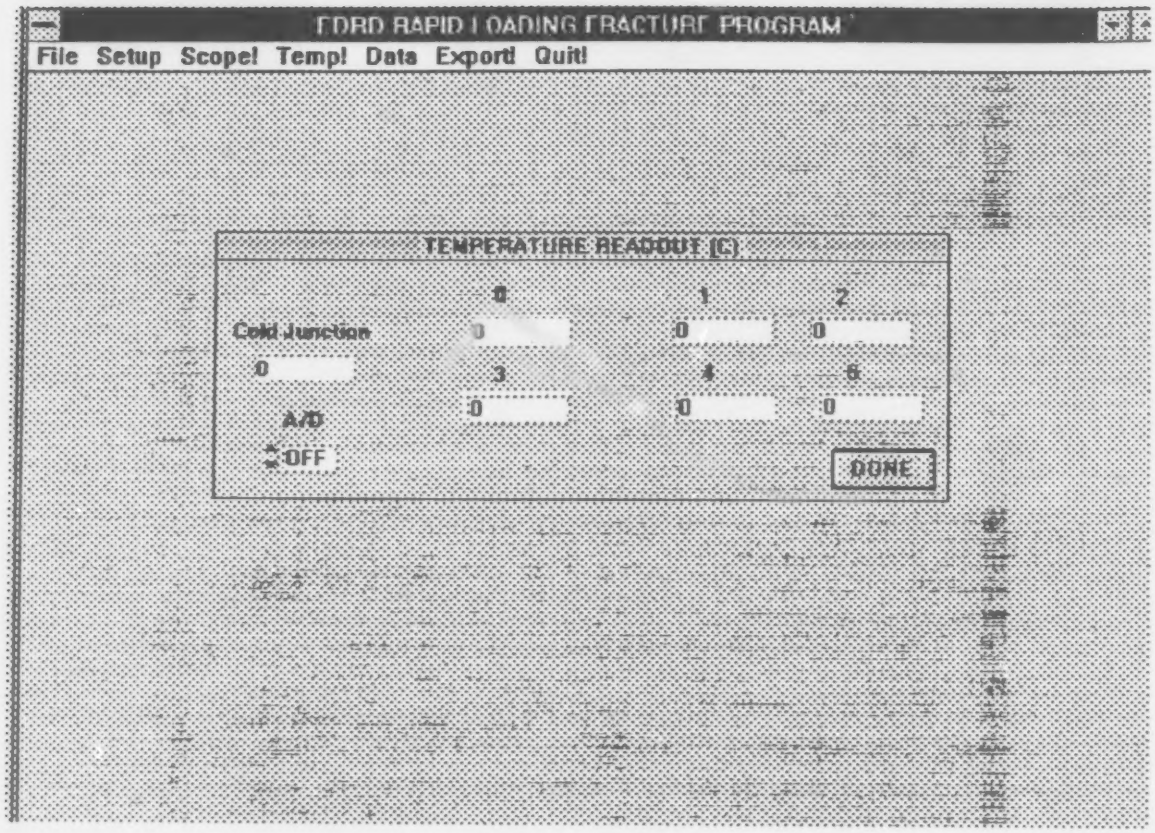

Figure 28.
Temperature Monitor Panel.

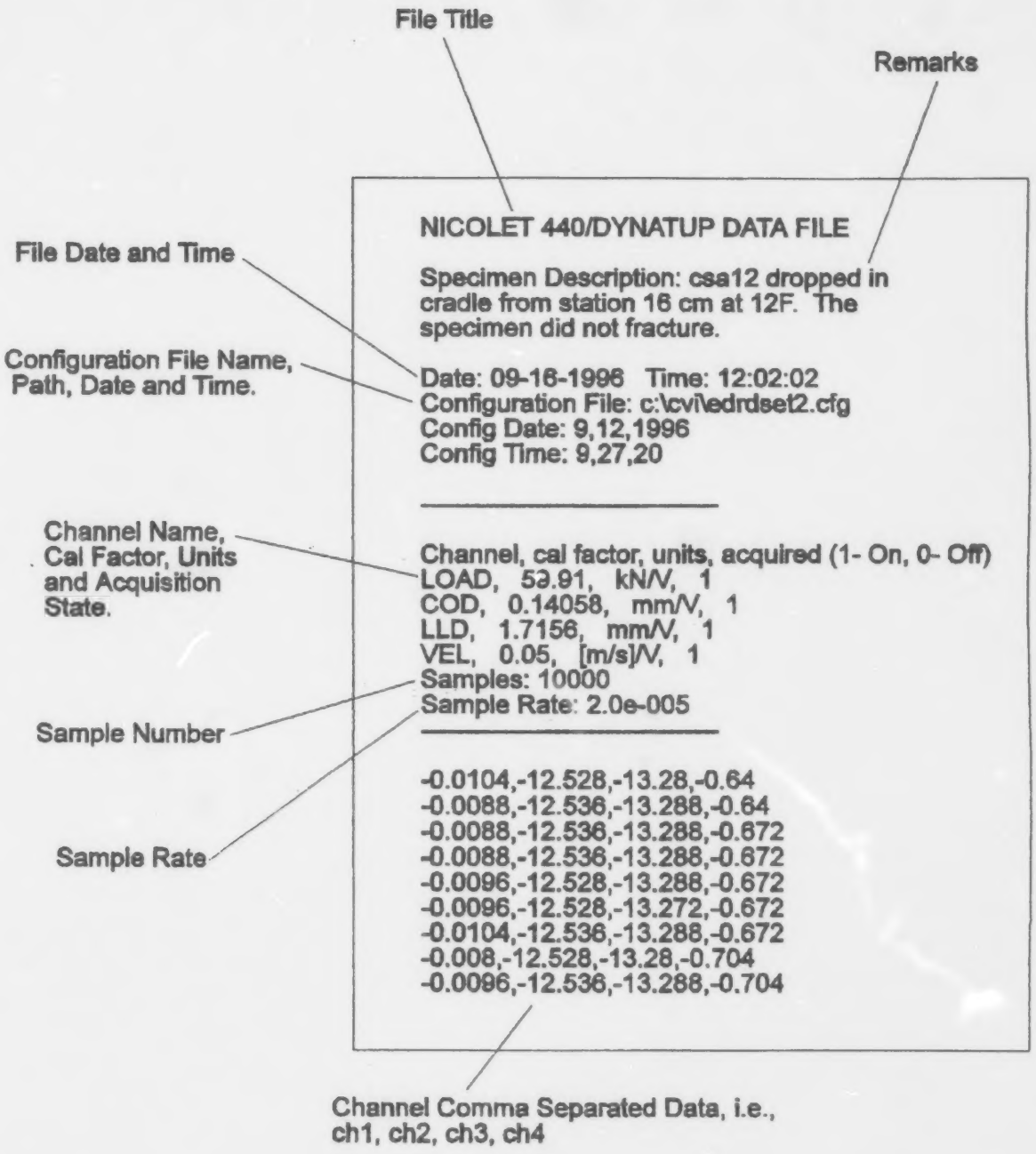

Figure 29.
Export Data File Format.

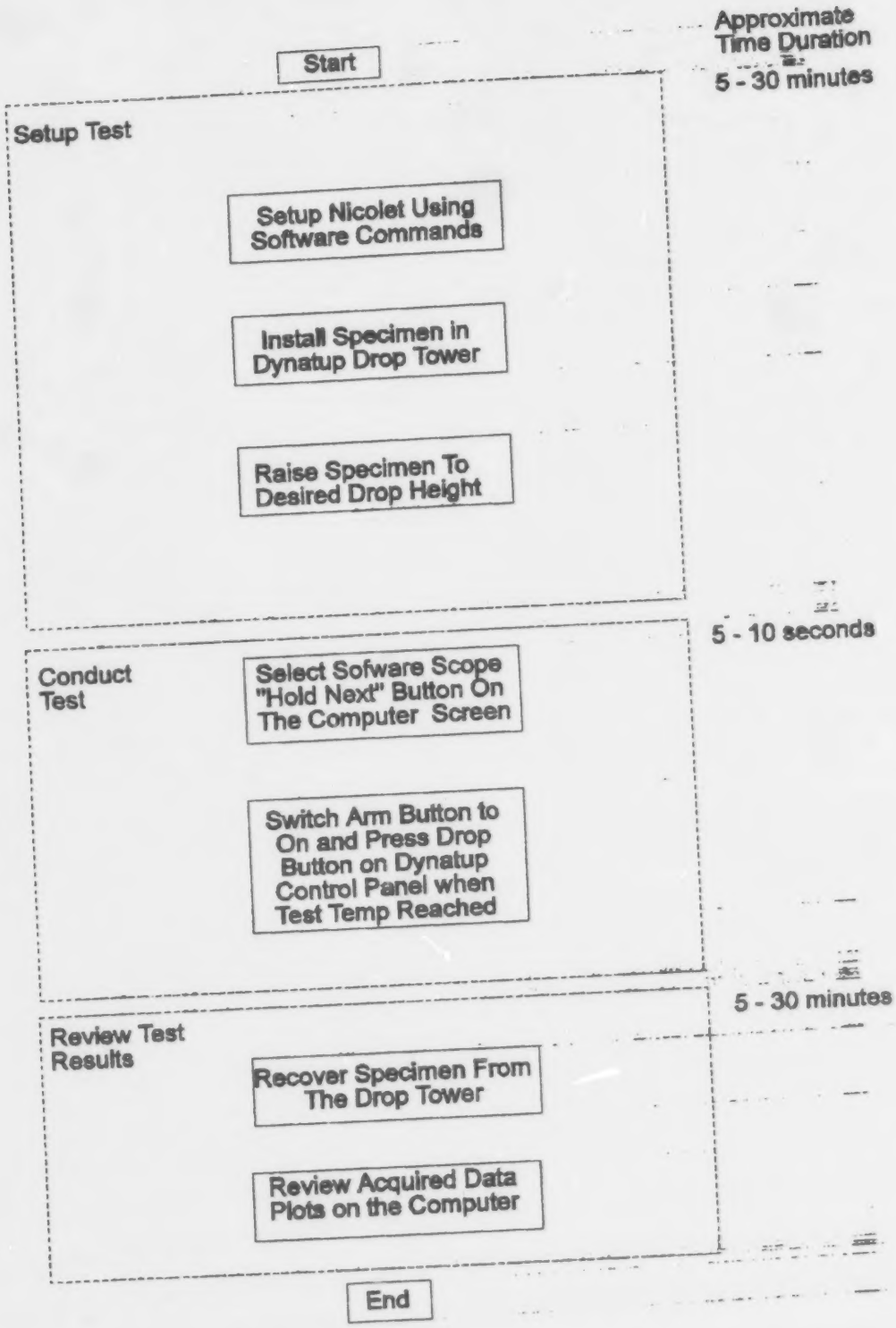
Approximate Time Duration
Start
5 - 30 minutes
Setup Test
Setup Nicolet Using Software Commands
Install Specimen in Dynatup Drop Tower
Raise Specimen To Desired Drop Height
5 - 10 seconds
Conduct Test
Select Sofware Scope "Hold Next" Button On The Computer Screen
Switch Arm Button to On and Press Drop Button on Dynatup Control Panel when Test Temp Reached
5 - 30 minutes
Review Test Results
Recover Specimen From The Drop Tower
Review Acquired Data Plots on the Computer
End

Figure 30.
Ambient Test Procedure.

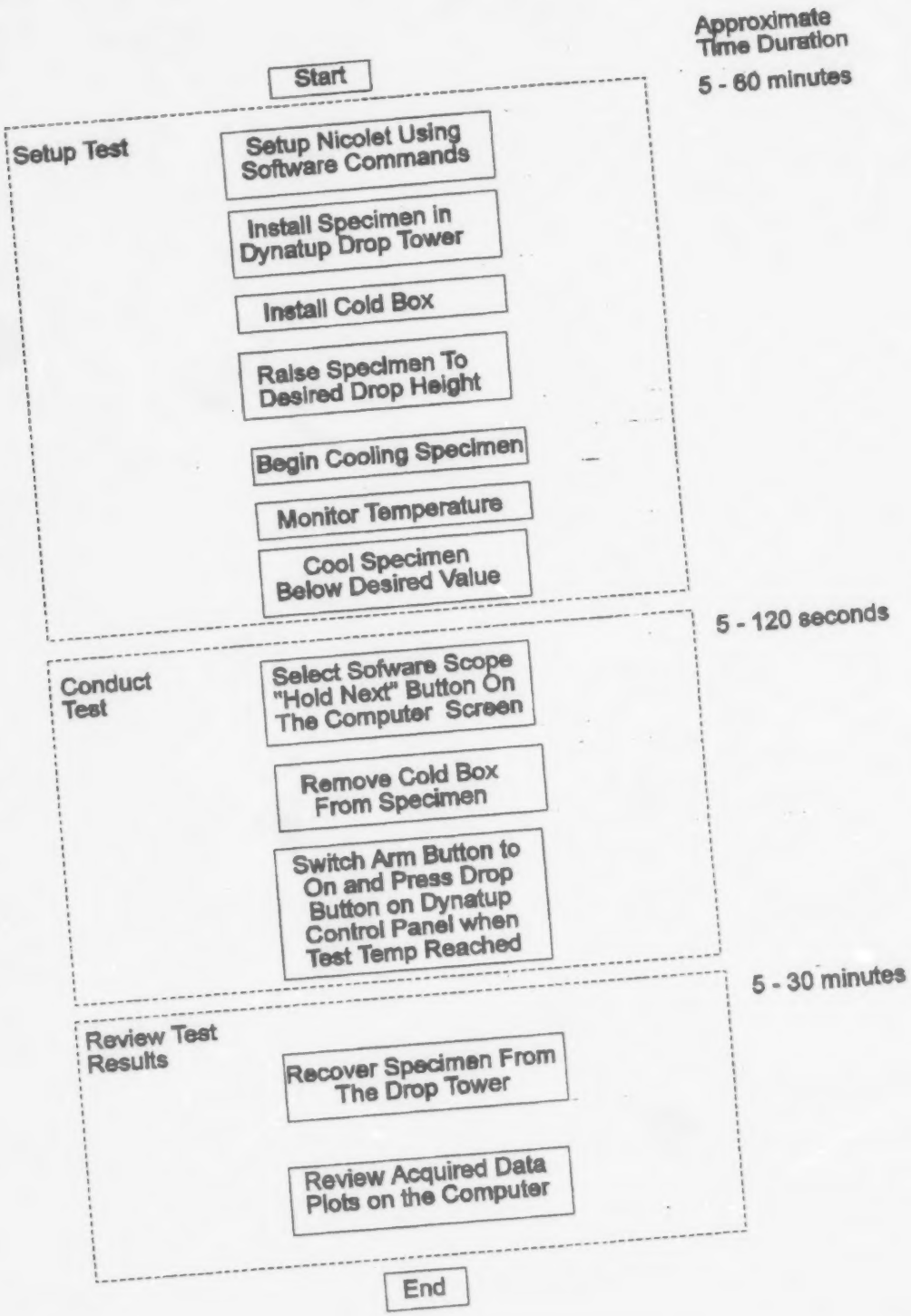
Approximate Time Duration
Start
Setup Test
Setup Nicolet Using Software Commands
Install Specimen in Dynatup Drop Tower
Install Cold Box
Raise Specimen To Desired Drop Height
Begin Cooling Specimen
Monitor Temperature
Cool Specimen Below Desired Value
5 - 60 minutes
Conduct Test
Select Sofware Scope "Hold Next" Button On The Computer Screen
Remove Cold Box From Specimen
Switch Arm Button to On and Press Drop Button on Dynatup Control Panel when Test Temp Reached
5 - 120 seconds
Review Test Results
Recover Specimen From The Drop Tower
Review Acquired Data Plots on the Computer
5 - 30 minutes
End

Figure 31.
Cold Test Procedure - Insitu Specimen

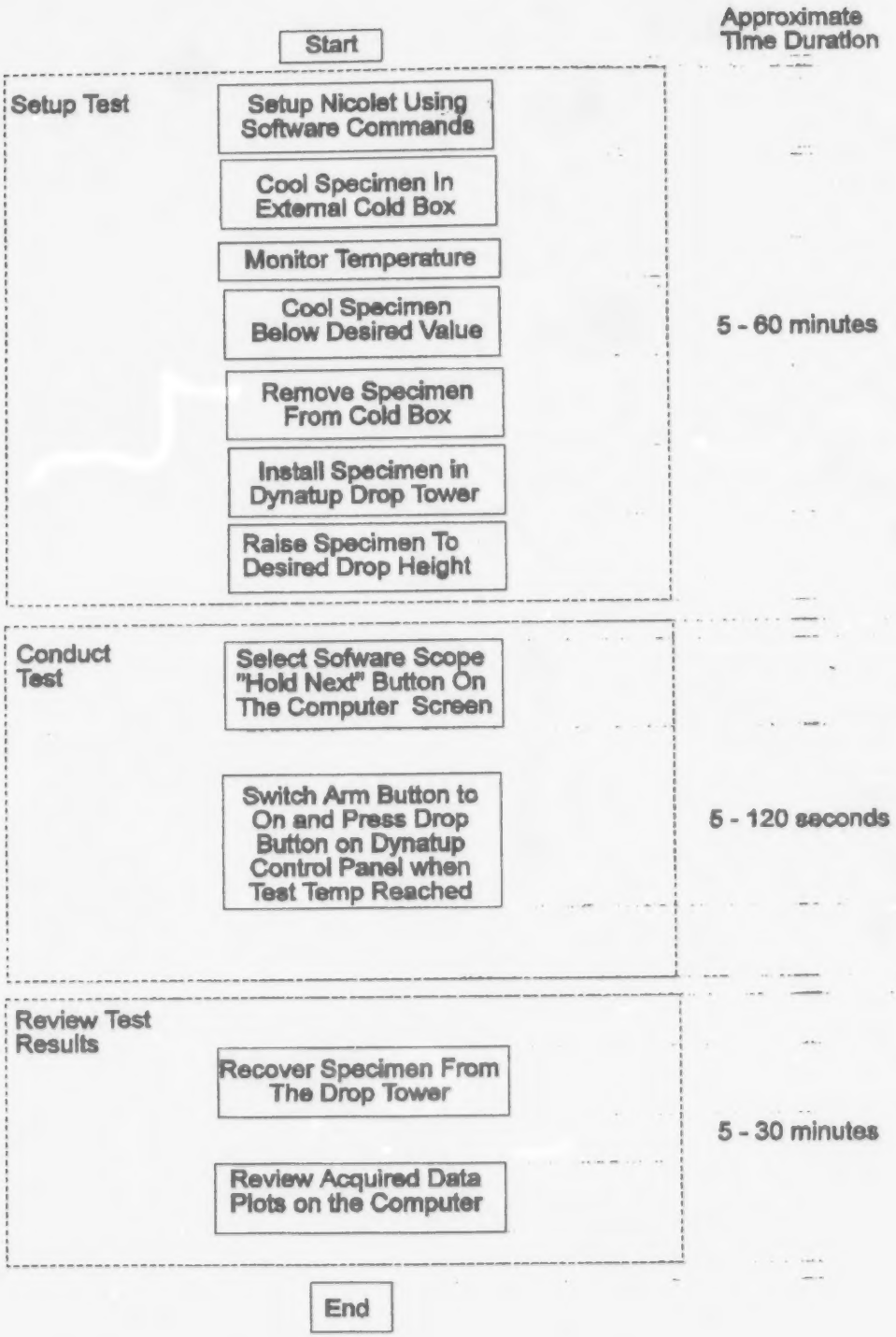
Approximate
Time Duration
Start
Setup Test
Setup Nicolet Using Software Commands
Cool Specimen In External Cold Box
Monitor Temperature
Cool Specimen Below Desired Value
5 - 60 minutes
Remove Specimen From Cold Box
Install Specimen in Dynatup Drop Tower
Raise Specimen To Desired Drop Height
Conduct Test
Select Sofware Scope "Hold Next" Button On The Computer Screen
Switch Arm Button to On and Press Drop Button on Dynatup Control Panel when Test Temp Reached
5 - 120 seconds
Review Test Results
Recover Specimen From The Drop Tower
5 - 30 minutes
Review Acquired Data Plots on the Computer
End

Figure 32.
Cold Test Procedure - External Specimen Cooling.

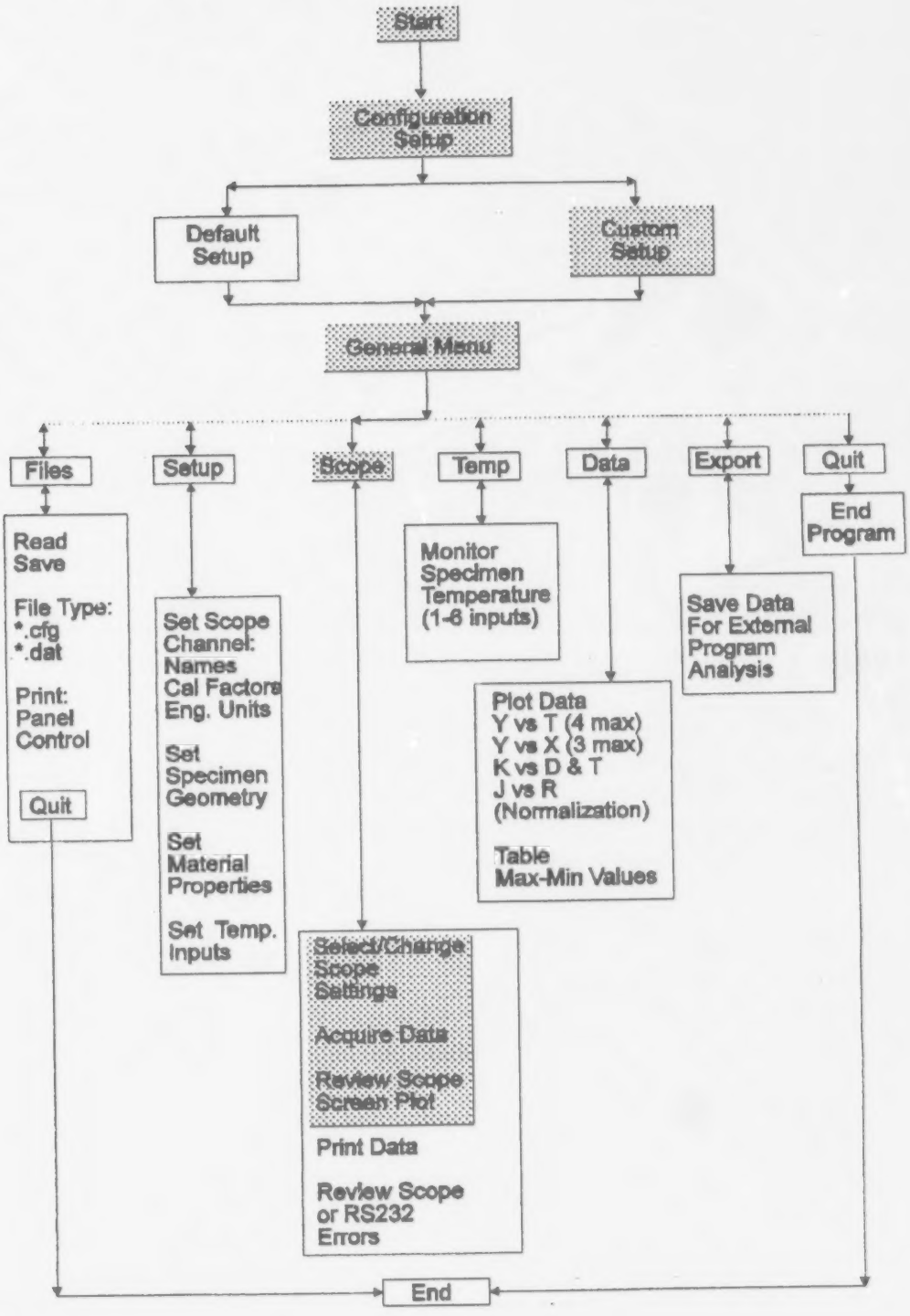

Figure 33.
Scope Setup Procedure Using The Custom Setup.

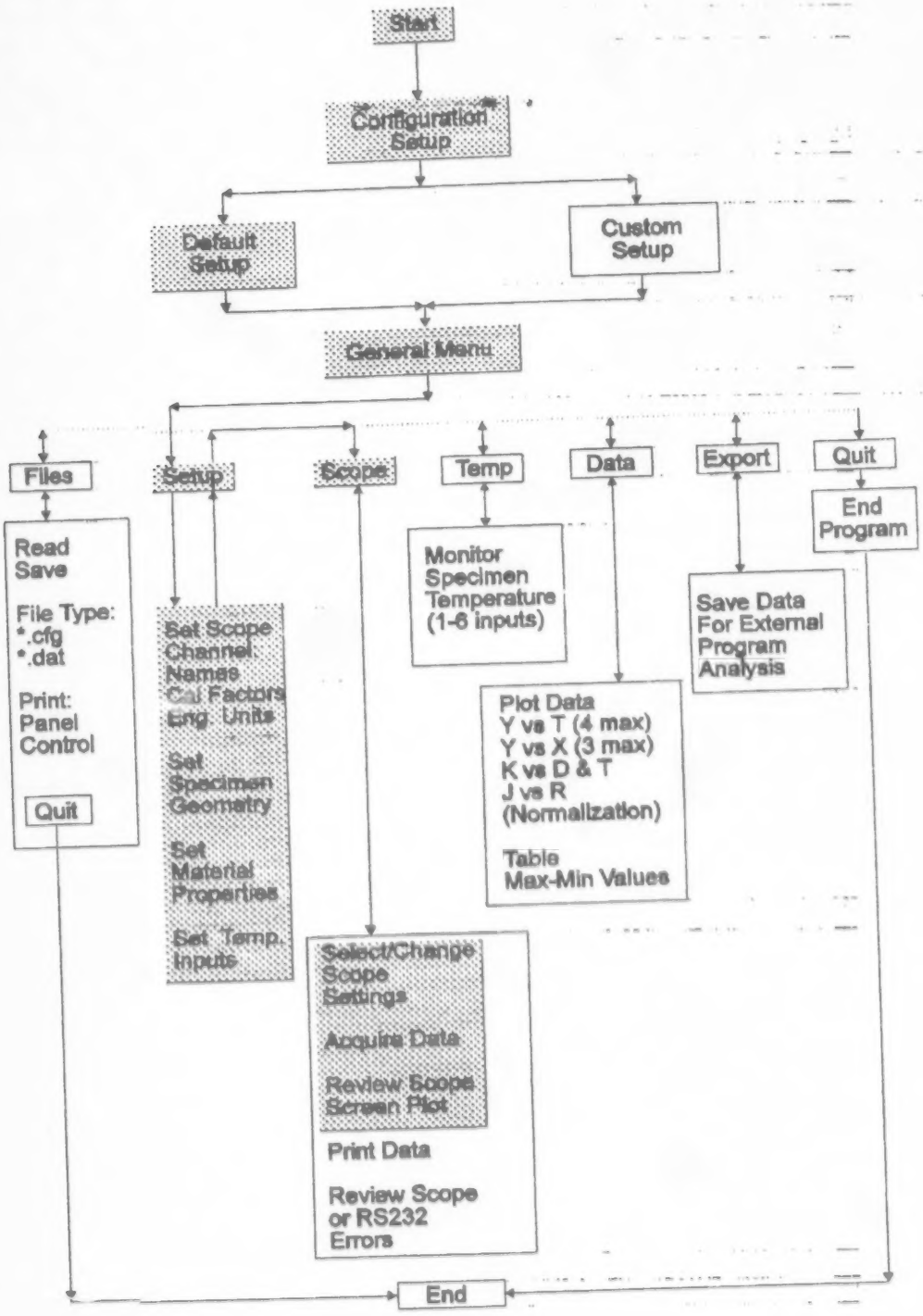

Figure 34.
Scope Setup Procedure Using The Default Setup.

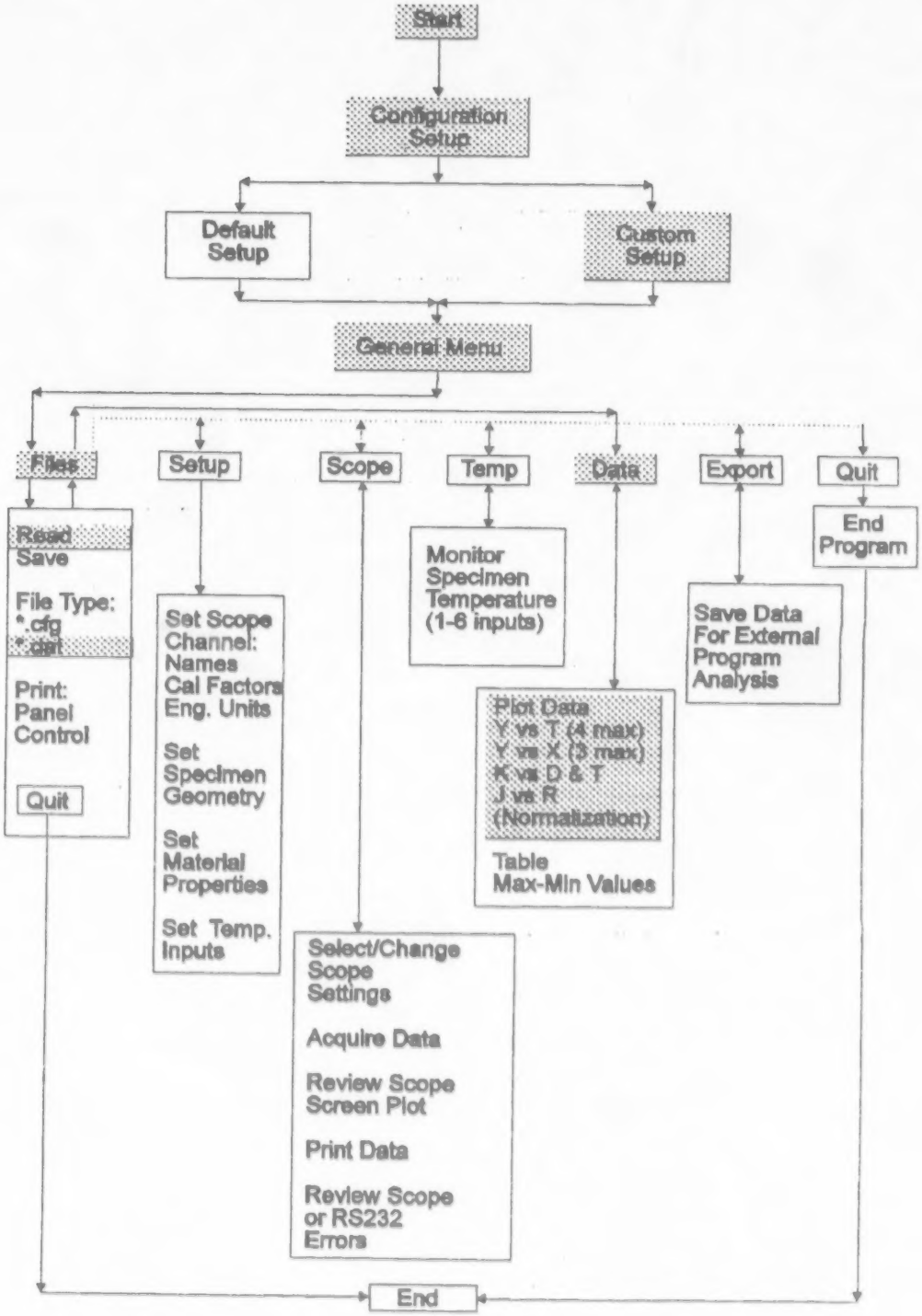

Figure 35.
Plotting Existing Data Using The Custom Setup.

Appendix A

DYNATUP TUP SPECIFICATION

dynatup

General Research Corporation
A GRC Instruments Company

Instrumented Tup Calibration Specifications

Power Supply:	D.C. excitation of 5 volts + .1 volt
Safe Storage Temperature:	-65 to +300 degrees F (-54 to +149C)
Operating Temperature:	-40 to +200 degrees F (-40 to +93C)

NOTE: During impact tests, the tup is usually subjected to high or low temperatures for sufficiently short lengths of time to avoid adverse cooling or heating of strain gages.

Tup output changes with temperature by approximately .3% per degree C. Operating temperature should not significantly vary from calibration temperature.

Compatible with Dynatup Models: 530-I, 730-I, 830-I, 830-SF and 1030-I Data Systems.

The recommended recalibration interval depends on frequency of use. We suggest every 6 months or approximately every 5,000 loadings (impacts). The tup is labeled with the suggested recalibration date.

COMBINED LINEARITY, REPEATABILITY AND HYSTERESIS WITHIN 3% FOR RECOMMENDED LOAD RANGE(S)

MAIN OFFICE: 5383 Hollister Avenue • Santa Barbara, California 93111 USA • (805) 681-6825 • FAX (805) 964-2914
TECHNICAL CENTER: 203 Townsend Drive • Monroeville, Pennsylvania 15146 USA • (412) 735-5339 • FAX (412) 735-5339

An Equal Opportunity Employer

Appendix B

LVT SPECIFICATION

VT-Z Series
Linear Velocity Transducers

Lucas Schaevitz

- **Linearly proportional DC output**
- **Self-generating; no excitation required**
- **Output indicates direction of motion**
- **Frictionless measurement**
- **Rugged construction**

Lucas Schaevitz VT-Z Series linear velocity transducers (LVTs) produce an electrical output directly proportional to the time rate of change of rectilinear displacement. They are rugged self-generating devices that provide a simple and accurate method of measuring the linear velocity of an object as it is displaced from one position to another.

An LVT consists of an enclosed coil assembly and a separable permanent magnet core free to move axially within the coil assembly without mechanical contact. LVTs are generally used for dynamic measurement on mechanical devices or structures, especially where direct determination of linear velocity is desirable. Usually the low mass magnet core is attached to the moving member, while the coil assembly is attached to the fixed member.

An LVT can be mechanically coupled to a suitable LVDT to give independent position and velocity information for stability feedback in servo systems. Other typical applications include structural vibration measurements, seismic instruments, actuator speed controls, and dynamic balancing equipment.

Lucas Schaevitz VT-Z Series LVTs feature frictionless measurement and infinite mechanical life, because there is no physical contact between the magnet core and the bore of the coil assembly. They can measure linear velocity over an extremely wide range. Maximum velocity input, limited only by winding insulation, is at least 1,000 inches per second for most VT-Z models. Minimum velocity is limited only by the noise threshold of the associated instrumentation. Resolution is essentially infinite.

VT-Z Series LVTs are available with linear displacement ranges from 1/2 inch to 20 inches. They normally utilize Alnico-V cores for high sensitivity. For applications requiring extra ruggedness, unbreakable Cunife cores are available, but sensitivity is reduced. (Refer to Sensitivity Chart.) Because the permanent magnet cores have high retentivity, field calibration is unnecessary; each LVT is shipped with an individual calibration record specifying its sensitivity factor.

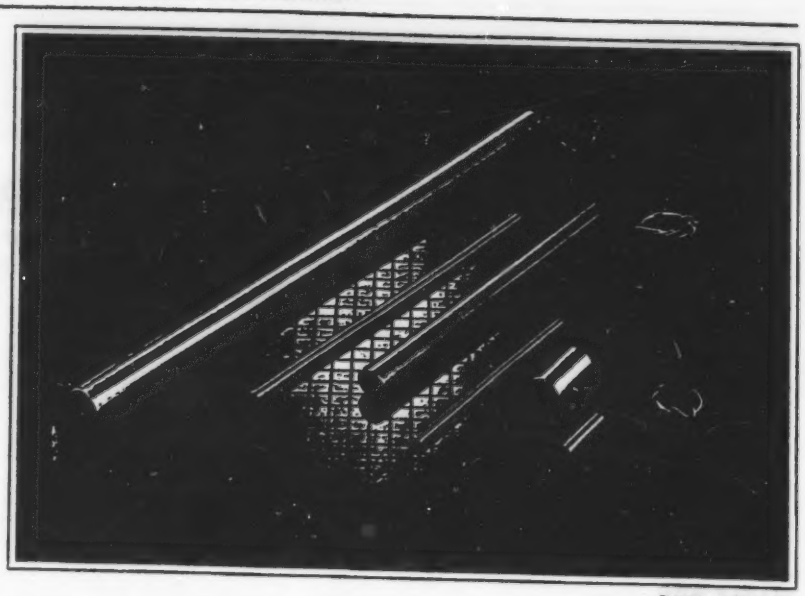

Grid Scale 3/8" x 3/8"

Theory of Operation

A typical linear velocity transducer, Figure 1, utilizes a small cylindrical permanent magnet core of high coercive force enclosed in a nonmagnetic sleeve. This sleeve has internally threaded inserts at each end to facilitate attaching the magnet core to a test member. Two identical coils are wound side-by-side on a coil form that is coaxial with the magnet core.

By Faraday's law of induction, a voltage proportional to the rate of change of magnetic flux is developed in each coil as one pole (end) of the magnet moves axially inward. This voltage depends on the number of turns of wire in the coil per unit length multiplied by the number of lines of force. Because the flux of the permanent magnet is constant, the rate of change of flux in each coil is a linear function of the rate of change of displacement (i.e., velocity) of the magnet core. Therefore, the magnitude of the output voltage is linearly proportional to core velocity.

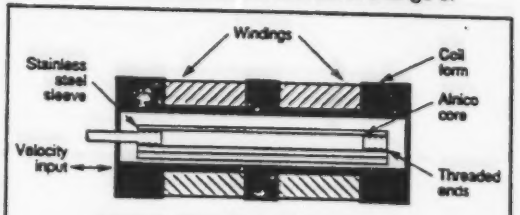

Figure 1. Simplified LVT cross-section

However, if both poles of the magnet core entered a coil, the net voltage in that coil would be zero, because the opposite magnetic poles would produce equal but opposite polarity voltages. To obviate this condition, the two coils are connected in a series-opposing configuration. The resulting output voltage is then the sum of the differential voltages in the two coils. The polarity of the output voltage depends on the direction of core motion and the orientation of the core's magnetic poles.

Sensitivity

	mV DC per in/sec (mm/sec)			
Model	**Alnico-V**		**Cunife**	
3L5 VT-Z	150	(6.0)	60	(2.4)
3L1 VT-Z	120	(4.8)	50	(2.0)
6L1 VT-Z	650	(26.0)	260	(10.4)
6L2 VT-Z	450	(18.0)	180	(7.2)
6L3 VT-Z	500	(20.0)	200	(8.0)
6L4 VT-Z	450	(18.0)	180	(7.2)
7L6 VT-Z	200	(8.0)	80	(3.2)
7L9 VT-Z	140	(5.6)	55	(2.2)
7L10 VT-Z	200	(8.0)	80	(3.2)
7L20 VT-Z	120	(4.8)	50	(2.0)

VT-Z Series Linear Velocity Transducers

Characteristics

Figure 2 shows the output characteristics of an ideal LVT as the core moves through the entire length of the coil at a constant velocity. The figure shows a displacement range over which the devices's output voltage is essentially constant. This is referred to as the "maximum range of linear displacement" or "linear range". Note that this is not the range of velocities over which the LVT is linear, but rather the maximum position increment over which a meaningful velocity measurement can be made.

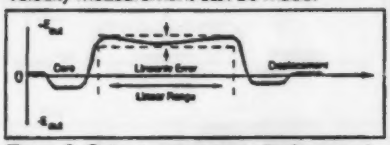

Figure 2. Output versus core displacement.

Sometimes deviations from the constant value occur because of winding variations, magnetic anomalies, and similar phenomena. Deviation of the output for a constant velocity input through the LVT's linear range is properly known as "positional linearity error", but is most commonly referred to as "LVT linearity" and is expressed as a percent of output.

This terminology can cause confusion regarding an LVT's "characteristic linearity error" which quantifies changes in the slope of the transfer function of the LVT. Theorectically, the output of an ideal LVT with an infinite load impedance is perfectly linear, but in practice, there can be some loading effect from the input circuits of the instrumentation connected to an LVT. The effect of the unit's self-inductance may show up as nonlinearity and/or response limitations, particularly at higher velocities.

Because LVTs are normally used as precalibrated devices, the effects of positional linearity error cannot be separated from errors due to output loading. In high accuracy applications, linearity error due to output loading may be minimized by increasing the load impedance. However, when an LVT is used as a feedback element for servo system stabilization, linearity errors may be less significant.

The sensitivity of an LVT is determined at the factory and recorded on a data sheet shipped with the transducer. This calibration is valid for the lifetime of the transducer as long as the magnetic force of the core remains constant. Therefore, the permanent magnet core must be stored and handled in a manner that prevents fracture, physical shock, or demagnetization.

Specifications

Linearity	±1% of output
Temperature Range	-65°F to 200°F (-55°C to 95°C)
Shock Survival	1,000 *g* for 11 milliseconds
Vibration Tolerance	20 *g* up to 2 kHz
Insulation Rating	500 volts peak
Core Material	Standard: Alnico-V; Unbreakable: Cunife
Housing Material	AISI 400 series stainless steel
Lead Wires	28 AWG stranded copper, Teflon-insulated, 12 inches (300 mm) long (nominal)

Specifications by Model

Model Number	Nominal Linear Range in	(mm)	Total Coil Resistance Kohms	Total Coil Inductance Henries	Weight Coil oz	(g)	Core oz	(g)
3L5 VT-Z	0.5	(12.7)	4	0.3	0.70	(20.0)	0.14	(4.0)
3L1 VT-Z	1.0	(25.4)	5	0.2	0.88	(25.0)	0.14	(4.0)
6L1 VT-Z	1.0	(25.4)	20	5.0	2.75	(78.0)	0.39	11.0)
6L2 VT-Z	2.0	(50.8)	15	3.7	4.23	(120.0)	0.49	(14.0)
6L3 VT-Z	3.0	(76.2)	26	6.5	5.29	(150.0)	0.53	(15.0)
6L4 VT-Z	4.0	(101.6)	23	5.5	6.70	(190.0)	0.70	(20.0)
7L6 VT-Z	6.0	(152.4)	2	0.5	11.10	(315.0)	2.29	(65.0)
7L9 VT-Z	9.0	(228.6)	2	0.9	13.57	(385.0)	2.68	(76.0)
7L10 VT-Z	10.0	254.0)	30	0.9	28.43	(750.0)	1.94	(55.0)
7L20 VT-Z	20.0	(508.0)	23	1.6	42.29	(1,200.0)	2.75	(78.0)

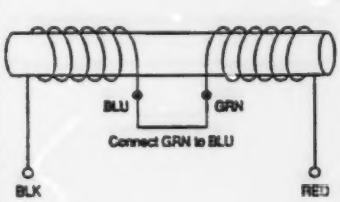

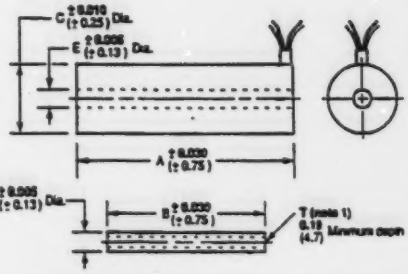

Note 1: Metric threaded cores are available:

Dimensions

Model Number	A in	(mm)	B in	(mm)	C in	(mm)	D in	(mm)	E in	(mm)	Note 1
3L5 VT-Z	3.16	(80.3)	2.40	(61.0)	0.375	(9.5)	0.125	(3.18)	0.14	(3.55)	1-72
3L1 VT-Z	4.22	(107.2)	2.40	(61.0)	0.375	(9.5)	0.125	(3.18)	0.14	(3.55)	1-72
6L1 VT-Z	5.00	(127.0)	3.50	(88.9)	0.625	(15.9)	0.187	(4.75)	0.22	(5.59)	4-40
6L2 VT-Z	7.00	(177.8)	4.50	(114.3)	0.625	(15.9)	0.187	(4.75)	0.22	(5.59)	4-40
6L3 VT-Z	9.00	(228.6)	5.25	(133.4)	0.625	(15.9)	0.187	(4.75)	0.22	(5.59)	4-40
6L4 VT-Z	11.25	(285.8)	6.75	(171.5)	0.625	(15.9)	0.187	(4.75)	0.22	(5.59)	4-40
7L6 VT-Z	15.75	(400.0)	9.25	(235.0)	0.750	(19.0)	0.230	(5.85)	0.31	(7.87)	4-40
7L9 VT-Z	22.75	(577.9)	11.75	(298.5)	0.750	(19.0)	0.230	(5.85)	0.31	(7.87)	4-40
7L10 VT-Z	19.60	(497.8)	7.63	(193.8)	0.750	(19.0)	0.230	(5.85)	0.30	(7.62)	6-40
7L20 VT-Z	34.28	(870.7)	12.00	(304.8)	0.750	(19.0)	0.230	(5.85)	0.30	(7.62)	6-40

The statements, information and data published in this literature are, to the best of our knowledge, accurate, reliable and true. Because Lucas Schaevitz has no control over the use to which others may put these products, we do not guarantee that the same results as those described herein will be obtained. Each user should test under his own conditions to determine the product's suitability for his own particular applications.

Lucas Schaevitz

Technical Bulletin #1101A 5000M-3/90

U.S. Operations
7905 N. Route 130
Pennsauken, NJ 08110-1489
Tel: (609) 662-8000
Fax: (609) 662-6281
Telex: (710) 892-0714

U.K. Operations
543 Ipswich Road
Slough, Berks SL 1 4EG England
Tel: (0753) 37622
Fax: (0753) 823563
Telex: 847818G

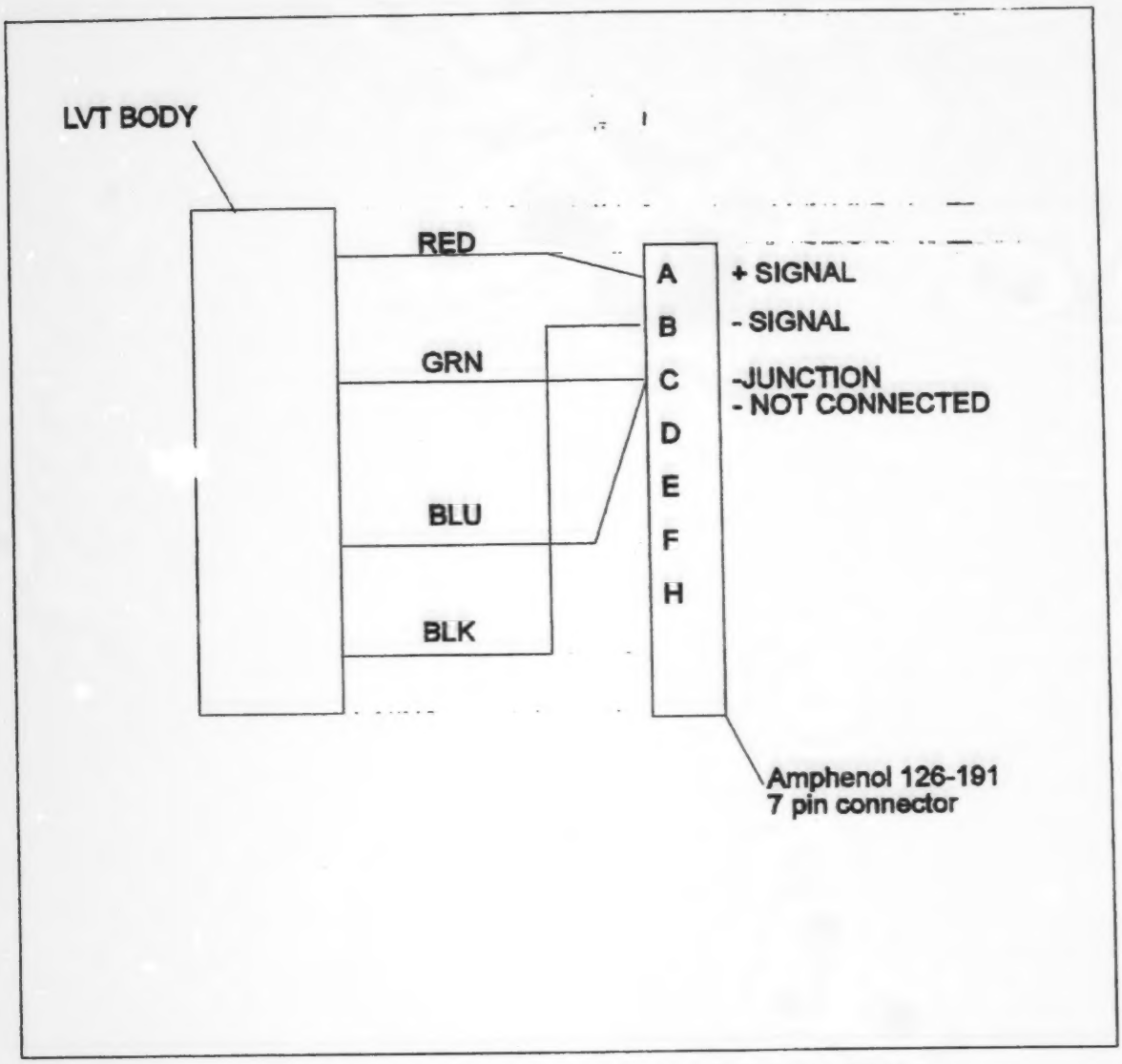

LINEAR VELOCITY TRANSDUCER WIRING DIAGRAM.

LVT SPECIFICATIONS

MANUFACTURER:	LUCAS SHAEVITZ
MODEL:	6L3VT-Z
SERIAL NO.:	7198
CORE:	ALNICO-V
SENSITIVITY:	20 mV/MM/SEC (500mV/IN/SEC)
NOMINAL LINEAR RANGE:	76.2 mm (3.0 IN.)
TOTAL RESISTANCE:	28 kOHMS
TOTAL COIL INDUCTANCE:	6.5 HENRIES
COIL WEIGHT:	150 g
CORE WEIGHT:	15 g

Appendix C

PINOUT/WIRE DESIGNATION FOR THERMOCOUPLE INPUTS

GUI	MIO Connector (preceding page)	Screw Terminal Box	Amphenol Con. (20-27)	Remote Thermocouple Box
CH0	ACH0	3	B	T/C #1 +
	ACH8	4	C	T/C #1 -
CH1	ACH1	5	D	T/C #2 +
	ACH9	6	E	T/C #2 -
CH2	ACH2	7	F	T/C #3 +
	ACH10	8	G	T/C #3 -
CH3	ACH3	9	H	T/C #4 +
	ACH11	10	I	T/C #4 -
CH4	ACH4	11	M	T/C #5 +
	ACH12	12	N	T/C #5 -
CH5	ACH5	13	K	T/C #6 +
	ACH13	14	L	T/C #6 -
CJC Sensor	ACH6 ACH14	15 -U4 16 - 2 (AIGND)	J	CJC Sensor -
AMP offset	ACH7 ACH15	17 - 1 (AIGND) 18 - 1 (AIGND)		
	+5V	35	A	CJC Sensor +

Table C1.
Drop Tower Mounted Remote Thermocouple Junction Box Wire Designation/Pinout.

This appendix describes the connectors on the optional cables for the AT-MIO E Series boards.

Figure B-1 shows the pin assignments for the 50-pin MIO connector. This connector is available when you use the SH6850 or R6850 cable assemblies with the AT-MIO-16E-2, AT-MIO-16E-10, or the AT-MIO-16XE-50. It is also one of the two 50-pin connectors available when you use the R1005050 cable assembly with the AT-MIO-16DE-10 or AT-MIO-64E-3.

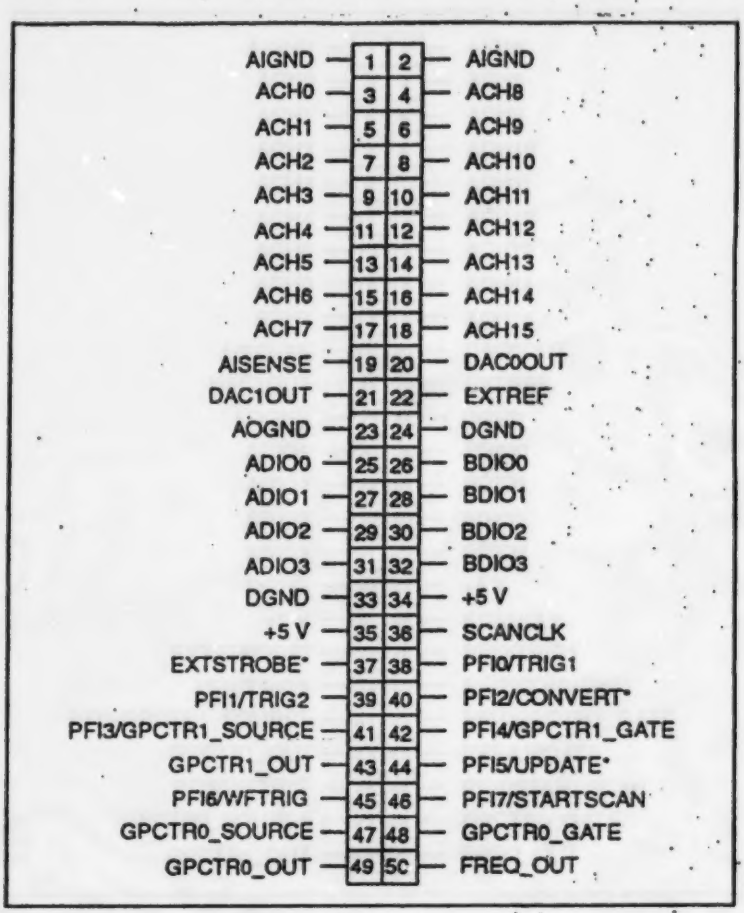
AIGND 1 2 AIGND
ACH0 3 4 ACH8
ACH1 5 6 ACH9
ACH2 7 8 ACH10
ACH3 9 10 ACH11
ACH4 11 12 ACH12
ACH5 13 14 ACH13
ACH6 15 16 ACH14
ACH7 17 18 ACH15
AISENSE 19 20 DAC0OUT
DAC1OUT 21 22 EXTREF
AOGND 23 24 DGND
ADIO0 25 26 BDIO0
ADIO1 27 28 BDIO1
ADIO2 29 30 BDIO2
ADIO3 31 32 BDIO3
DGND 33 34 +5 V
+5 V 35 36 SCANCLK
EXTSTROBE* 37 38 PFI0/TRIG1
PFI1/TRIG2 39 40 PFI2/CONVERT*
PFI3/GPCTR1_SOURCE 41 42 PFI4/GPCTR1_GATE
GPCTR1_OUT 43 44 PFI5/UPDATE*
PFI6/WFTRIG 45 46 PFI7/STARTSCAN
GPCTR0_SOURCE 47 48 GPCTR0_GATE
GPCTR0_OUT 49 50 FREQ_OUT

Figure C1.
Data Acquistion Card Ribbon Cable Pin Designations
(Ref: National Instruments AT-MIO E Series User Manual
October 1994 Edition.)

UNCLASSIFIED
SECURITY CLASSIFICATION OF FORM
(highest classification of Title, Abstract, Keywords)

DOCUMENT CONTROL DATA

(Security classification of title, body of abstract and indexing annotation must be entered when the overall document is classified)

1. ORIGINATOR (the name and address of the organization preparing the document.. Organizations for whom the document was prepared, e.g. Establishment sponsoring a contractor's report, or tasking agency, are entered in section 8.)

Engineering Material Research

2. SECURITY CLASSIFICATION (overall security classification of the document including special warning terms if applicable).

UNCLASSIFIED

3. TITLE (the complete document title as indicated on the title page. Its classification should be indicated by the appropriate abbreviation (S,C,R or U) in parentheses after the title).

Drop Tower Upgrade Project (U) Volume 1 Instrumentation and Data Acquisition System
Volume 2 Operator Manual: Tower and Application Software

4. AUTHORS (Last name, first name, middle initial. If military, show rank, e.g. Doe, Maj. John E.)

D.A. Hull

5. DATE OF PUBLICATION (month and year of publication of document)

April1999

6a. NO .OF PAGES (total containing information Include Annexes, Appendices, etc).

Vol 1 33
Vol 2 30

6b. NO. OF REFS (total cited in document)

Vol1 42 refs
Vol 2 3 refs

7. DESCRIPTIVE NOTES (the category of the document, e.g. technical report, technical note or memorandum. If appropriate, enter the type of report, e.g. interim, progress, summary, annual or final. Give the inclusive dates when a specific reporting period is covered).

CONTRACT REPORT

8. SPONSORING ACTIVITY (the name of the department project office or laboratory sponsoring the research and development. Include address).

Defence Research Establishment Atlantic, PO Box 1012, Dartmouth NS B2Y 3Z7

9a. PROJECT OR GRANT NO. (if appropriate, the applicable research and development project or grant number under which the document was written. Please specify whether project or grant).

9b. CONTRACT NO. (if appropriate, the applicable number under which the document was written).

W7708-4-1386

10a ORIGINATOR'S DOCUMENT NUMBER (the official document number by which the document is identified by the originating activity. This number must be unique to this document.)

DREA CR 1999-034

10b OTHER DOCUMENT NOs. (Any other numbers which may be assigned this document either by the originator or by the sponsor.)

11. DOCUMENT AVAILABILITY (any limitations on further dissemination of the document, other than those imposed by security classification)

(X) Unlimited distribution
( ) Defence departments and defence contractors; further distribution only as approved
( ) Defence departments and Canadian defence contractors; further distribution only as approved
( ) Government departments and agencies; further distribution only as approved
( ) Defence departments; further distribution only as approved
( ) Other (please specify):

12. DOCUMENT ANNOUNCEMENT (any limitation to the bibliographic announcement of this document. This will normally correspond to the Document Availability (11). However, where further distribution (beyond the audience specified in (11) is possible, a wider announcement audience may be selected).

UNCLASSIFIED
SECURITY CLASSIFICATION OF FORM

13. ABSTRACT (a brief and factual summary of the document. It may also appear elsewhere in the body of the document itself. It is highly desirable that the abstract of classified documents be unclassified. Each paragraph of the abstract shall begin with an indication of the security classification of the information in the paragraph (unless the document itself is unclassified) represented as (S), (C), (R), or (U). It is not necessary to include here abstracts in both official languages unless the text is bilingual).

This report describes contract work to upgrade the capabilities of the drop tower at the DREA Dockyard Laboratory (Pacific). There was a need for improved fracture data acquisition and analysis software. In addition elastic-plastic fracture measurements at impact velocities and low temperatures required improved transducer performance.

The contract requirements included a review of high rate testing standards and developments in instrumentation and data acquisition, the development of customized software for routine data acquisition and display, and drop tower modifications to meet specified performance criteria. One of the main requirements was to identify and apply promising methods of measuring crack mouth opening and load line displacement, to increase manageable drop tower velocities for such tests from 2 m.s-1 to 5 m.s-1, and to improve the low temperature capability.

14. KEYWORDS, DESCRIPTORS or IDENTIFIERS (technically meaningful terms or short phrases that characterize a document and could be helpful in cataloguing the document. They should be selected so that no security classification is required. Identifiers, such as equipment model designation, trade name, military project code name, geographic location may also be included. If possible keywords should be selected from a published thesaurus. e.g. Thesaurus of Engineering and Scientific Terms (TEST) and that thesaurus-identified. If it not possible to select indexing terms which are Unclassified, the classification of each should be indicated as with the title).

Drop Tower
Toughness
Instrumentation
Lab Windows

DCD03 2/06/87-M/ DREA mod. 17 Dec 1997